
Electronic Thesis and Dissertation Repository

10-11-2018 12:00 PM

Characterizing the Sensorimotor Properties of a Rapid Visuomotor Reach Movement on Human Upper Limb Muscles

Chao Gu
The University of Western Ontario

Supervisor
Corneil, Brian D
The University of Western Ontario

Graduate Program in Psychology
A thesis submitted in partial fulfillment of the requirements for the degree in Doctor of
Philosophy
© Chao Gu 2018

Follow this and additional works at: <https://ir.lib.uwo.ca/etd>



Part of the [Behavioral Neurobiology Commons](#), and the [Systems Neuroscience Commons](#)

Recommended Citation

Gu, Chao, "Characterizing the Sensorimotor Properties of a Rapid Visuomotor Reach Movement on Human Upper Limb Muscles" (2018). *Electronic Thesis and Dissertation Repository*. 5750.
<https://ir.lib.uwo.ca/etd/5750>

This Dissertation/Thesis is brought to you for free and open access by Scholarship@Western. It has been accepted for inclusion in Electronic Thesis and Dissertation Repository by an authorized administrator of Scholarship@Western. For more information, please contact wlsadmin@uwo.ca.

Abstract

Humans and other primates rely heavily on vision as a primary sensory input to drive our upcoming volitional motor actions. Our motor system makes so many of these visual-to-motor transformations that they become ubiquitous in our daily lives. However, a central question in systems neuroscience is how does the brain perform these transformations?

Reaching movements have been an ideal model for studying volitional motor control in primates. Broadly, these visually-guided reach movements encompass at least three inherent sensorimotor components: an action selection component, a motor execution component, and a motor learning component. A core assumption is that as reach movements become more complex, our motor system requires more cortical processing, which prolongs the time between stimulus onset and reach initiation. Most visually-guided reach movements occur within 200-300 ms after the onset of a visual stimulus.

Recent human behavioural studies have shown that prior to these volitional reach movements, a directionally-tuned neuromuscular response can also be detected on human upper limb muscles within 100 ms after the onset of a novel visual stimulus. In this thesis, I characterized the sensorimotor properties of these visual stimulus-locked responses (*SLR*), under the same framework that has been used to describe volitional motor control.

In Chapter 2, I showed that the SLR is a reflexive motor command generated towards the visual stimulus location regardless of the current task

demands. In Chapter 3, by changing the initial starting hand position and the pre-planned reach trajectory, I showed that like volitional control, the pathway mediating the SLR can rapidly transform the eye-centric visual stimuli into a proper hand-centric motor command. In Chapter 4, I showed that the directional tuning of the SLR can be influenced after motor learning. However unlike volitional control, the SLR is selectively influenced by the implicit, but not explicit, component of motor learning. These three main results from this thesis suggest that despite the reflexive nature of the SLR, the SLR shares some sensorimotor properties that have been classically reserved for volitional motor control.

Keywords

Human; reaching; EMG; visual processing; reference frame; cognitive control; motor learning; action selection; reach trajectory; visuomotor control

Co-Authorship Statement

I was involved in all aspects of the experiments conducted, ranging from experimental design, data collection, data analysis, and the initial draft of the manuscript. **Dr. Brian D. Corneil** supervised and contributed to the experimental design, data interpretation, and manuscript revisions for all chapters. **Dr. Daniel K. Wood** assisted in experimental design and data interpretation in Chapter 2. **Dr. Paul L. Gribble** assisted in experimental design, data interpretation and manuscript revisions for Chapters 2-4. **Dr. J. Andrew Pruszynski** assisted in experimental design, data interpretation, and manuscript revisions for Chapters 3 and 4.

The chapters presented in this dissertation are either already published (Chapters 2 and 3) or have already been submitted (Chapter 4). Wherever possible, please reference the published work:

Chapter 2: Gu C, Wood DK, Gribble PL, Corneil BD (2016) A trial-by-trial window into sensorimotor transformations in the human motor periphery. *J Neurosci* 36:8273-8282.

Chapter 3: Gu C, Pruszynski JA, Gribble PL, Corneil BD (2018) Done in 100ms: path-dependent visuomotor transformation in the human upper limb. *J Neurophysiol* 119:1319-1328.

Chapter 4: Gu C, Pruszynski JA, Gribble PL, Corneil BD (2018) A rapid visuomotor response on the human upper limb is selectively influenced by implicit, but not explicit, motor learning. *bioRxiv* 354381.

Acknowledgments

I would like to first and foremost thank my supervisor, Dr. Brian Corneil, for his support and guidance to allow me to grow not only as a researcher but also as a person. In addition, I would like to thank him for the opportunity to collaborate with other scientists and entrusting me with my own projects. As well as having the opportunities to travel aboard and share my work with scientists from all over the world, I cannot have asked for a better supervisor.

I would like to thank our fantastic collaborators (Drs. Mel Goodale, Paul Gribble, Andrew Pruszynski, and Daniel Wood) at Western that have made the experiments in this thesis possible. I want to thank Dr. Tyler Peel, Darren and the rest of trainees from Dr. Corneil's and Dr. Everling's lab for their friendship in our dark basement office. In addition, I would like to thank Drs. Jeroen Atsma, Pieter Medendorp, and Luc Selen from Donders Institute for making my inviting me to work with them in Nijmegen, the Netherlands.

Finally, I would like to thank my parents and my extended family for their love and support.

Table of Content

Abstract	i
Keywords	ii
Co-Authorship Statement	iii
Acknowledgments	iv
List of Figures	ix
List of Abbreviations	xi
Chapter 1 – General Introduction	1
1.1 Preamble	2
1.1.1 <i>Sensorimotor properties of volitional reach control</i>	3
1.1.2 <i>Rapid visuomotor reach control</i>	8
1.2 Cortical control of volitional reach movements	9
1.2.1 <i>Visual-related responses within the motor cortices</i>	12
1.2.2 <i>Visual-to-motor transformations within the motor cortices</i>	14
1.2.3 <i>Reference frames of visual responses in the motor cortices</i>	16
1.2.4 <i>The role of motor cortices in motor learning</i>	19
1.3 Corrective reach responses	21
1.3.1 <i>Visuomotor properties of rapid corrective responses</i>	23
1.3.2 <i>Possible neural substrates mediating corrective responses</i>	25
1.4 The role of superior colliculus in gaze control	27
1.4.1 <i>Visual-related responses within the SC</i>	29
1.4.2 <i>Sensorimotor transformation within the SCi</i>	31
1.4.3 <i>Express saccades are mediated through the SCi</i>	33
1.5 SCi role in eye-head gaze control	34
1.5.1 <i>Tecto-reticulospinal pathways mediate both eye and head movements</i>	36
1.5.2 <i>Visual stimulus-locked responses on neck muscles</i>	37
1.5.3 <i>Reticular formation contribution to reach control</i>	42
1.6 The role of SCi in reach control	43
1.6.1 <i>Stimulus-locked visual responses on the human upper limb muscles</i>	45
1.7 Thesis motivation and objectives	47
1.7.1 <i>SLR a visual or preparatory motor command?</i>	47
1.7.2 <i>The reference frame of the SLR</i>	49

1.7.3 <i>The influence of implicit and explicit components motor learning on the SLR</i>	49
1.8 References	50
Chapter 2 – A Trial-by-Trial Window into Sensorimotor Transformations in the Human Motor Periphery	68
2.1 Abstract	69
2.2 Introduction	69
2.3 Materials and Methods	72
2.3.1 <i>Apparatus</i>	73
2.3.2 <i>Pro-/Anti-Reach Task</i>	73
2.3.3 <i>Muscle Recordings</i>	74
2.3.4 <i>Data Analysis</i>	75
2.3.5 <i>Receiver-operating characteristic (ROC) analysis</i>	76
2.4 Results	76
2.4.1 <i>The SLR encodes visual stimulus rather than goal location, but is attenuated before correct anti-reaches</i>	78
2.4.2 <i>The SLR generates a transient force towards the visual stimulus for both pro- and anti-reaches</i>	82
2.4.3 <i>Trials with a larger SLR were associated with shorter-RT pro-reaches, but longer-RT anti-reaches</i>	84
2.4.4 <i>Similar SLR magnitudes accompanied erroneous anti-reach trials and correct pro-reach trials</i>	86
2.4.5 <i>Surface EMG recordings can also detect the SLR</i>	88
2.5 Discussion	90
2.5.1 <i>Summary of results</i>	90
2.5.2 <i>Influence of task instruction on visual processing</i>	91
2.5.3 <i>A visual, not goal-directed, nature to the SLR</i>	92
2.5.4 <i>SLR potentially mediated through a reticulospinal pathway</i>	93
2.5.5 <i>Potential sources for task dependent modulation of the SLR</i>	94
2.5.6 <i>SLR as an alternative biomarker for the fast visuomotor response</i>	95
2.6 References	96
Chapter 3 – Done in 100 ms: Path-Dependent Visuomotor Transformation in the Human Upper Limb	103
3.1 Abstract	104
3.2 Introduction	105

3.3 Materials and Methods _____	106
3.3.1 Apparatus and Kinematic Acquisition _____	107
3.3.2 EMG and EOG Acquisition _____	107
3.3.3 Data Analyses _____	108
3.3.4 SLR Detection and Latency Analysis _____	109
3.3.5 Experiment 1: Reference Frame Task _____	111
3.3.6 Experiment 2: Obstacle Task _____	112
3.3.7 Experiment 3: Choice Task _____	113
3.3.8 Experimental Design and Statistical Analysis _____	115
3.4 Results _____	115
3.4.1 The SLR encodes stimulus location relative to hand, not eye, position ____	117
3.4.2 Movement trajectory influences SLR magnitude for reaches to the same visual stimulus _____	120
3.4.3 Initial movement trajectory, not task demands, influences SLR magnitude for curved reaches _____	123
3.4.4 SLR magnitude during Catch Trials were modulated based on the pre- planned movement _____	127
3.5 Discussion _____	129
3.6 References _____	133
Chapter 4 – A rapid visuomotor response on the human upper limb is selectively influenced by implicit motor learning _____	140
4.1 Abstract _____	141
4.2 Introduction _____	141
4.3 Materials and Methods _____	144
4.3.1 Participants and Procedures _____	144
4.3.2 Method Details _____	144
4.3.3 Apparatus and kinematic acquisition _____	145
4.3.4 EMG acquisition _____	146
4.3.5 Experiment 1: Abrupt visuomotor rotation task _____	146
4.3.6 Experiment 2: Gradual visuomotor rotation task _____	147
4.3.7 Experiment 3: Mental visuomotor rotation task _____	148
4.3.8 Data pre-processing _____	149
4.3.9 SLR Detection _____	150
4.3.10 Tuning curve fit _____	151

4.3.11 Statistical Analyses	152
4.3.12 Data and Software Availability	153
4.4 Results	153
4.4.1 Partial adaptation of the SLR during an abrupt 60° CW visuomotor rotation	155
4.4.2 SLR adaptation occurs despite a lack of explicit awareness of a visuomotor rotation	160
4.4.3 Changes in the explicit aiming strategy do not alter the PD of the SLR	164
4.5 Discussion	167
4.5.1 Implicit motor learning drives the partial adaptation of SLR tuning during visuomotor rotations	168
4.5.2 Distinct neural substrates for the implicit and explicit components of motor learning	170
4.5.3 A cerebellar influence on the tectoreticulospinal pathway	172
4.6 References	174
Chapter 5 – General Discussion	181
5.1 Summary of results	182
5.2 Future Directions	187
5.2.1 Neural substrate that mediates the SLR	187
5.2.2 Inter-limb coordination of human rapid visuomotor responses	189
5.2.3 Sensory properties of human rapid visuomotor responses	190
5.3 The role of the rapid visuomotor responses	191
5.4 Reference	193
Appendix A: Documentation of Ethics Approval	200
Curriculum Vitae	201

List of Figures

Figure 1.1: Box model of the visuomotor components of volitional motor control	4
Figure 1.2: Implicit and explicit components of the visuomotor rotation task	7
Figure 1.3: Example of a reach-related neuron within M1	11
Figure 1.4: Neural activity from both M1 and PMd during the delayed reach task	13
Figure 1.5: Neural activity in PPC during the pro-/anti-reach task	15
Figure 1.6: Neural activity from an eye-centric neuron in the PPC	18
Figure 1.7: Rapid corrective responses during ongoing reaching movements	22
Figure 1.8: Properties of the primate superior colliculus	28
Figure 1.9: SCi activity during the pro-/anti-saccade task	32
Figure 1.10: Visuomotor responses in the SCi and on neck muscle activity	35
Figure 1.11: Schematic of the three primary descending motor pathways for reach control	38
Figure 1.12: Neck SLRs during the pro-/anti-saccade task	40
Figure 1.13: SLR on a human upper limb muscle prior to reach movements	46
Figure 1.14: Objectives of this thesis	48
Figure 2.1: Pro-/anti-reach task and behavioural results	71
Figure 2.2: Intramuscular EMG results from an exemplar subject	79
Figure 2.3: EMG activity from seven subjects with a detectable SLR	81
Figure 2.4: Kinetic force profiles offer a crude proxy for EMG activity	83
Figure 2.5: Reversed correlations between SLR and ensuing RT for pro- and anti-reach trials	85
Figure 2.6: SLR magnitudes were similar on pro-reach and erroneous anti-reach trials	88
Figure 2.7: SLRs can be detected with surface EMG recordings	90
Figure 3.1: The SLR generates a motor command toward the visual stimulus in a hand-centric reference frame	116
Figure 3.2: Decreased SLR magnitude for curved compared to straight reaches to the same visual stimulus	121
Figure 3.3: SLR magnitude modulated by pre-planned movement trajectory	125
Figure 3.4: SLR magnitude and RT modulation for Catch Trials based on obstacle shape	128

muscle during visually-guided reaches _____	154
Figure 4.2: Partial adaptation of the SLR tuning during the abrupt visuomotor rotation task _____	156
Figure 4.3: Partial adaptation of the SLR tuning during the gradual visuomotor rotation task _____	161
Figure 4.4: SLR tuning did not adapt during a mental visuomotor rotation task. _____	165
Figure 4.5: An explicit aiming strategy attenuated SLR magnitude and increased RTs. _____	167
Figure 5.1: Summary of results from all experiments. _____	183

List of Abbreviations

~	Approximately
a.u.	Arbitrary units
ANOVA	Analysis of variance
BOLD	Blood-oxygen-level dependent
cm	Centimetre
CW	Clockwise
CCW	Counter-clockwise
°	Degree
Δ	Delta
EMG	Electromyography or Electromyographic
EOG	Electrooculography
<i>F</i>	<i>F</i> Statistics
FEF	Frontal eye field
fMRI	Functional magnetic resonance imaging
>	Greater than
HSD	Honest significant difference
Hz	Hertz
kHz	Kilohertz
<	Less than
LCD	Liquid crystal display
LGN	Lateral geniculate nucleus

μA	Microamps
M1	Primary motor cortex
MOV	Movement
ms	Milliseconds
N	Newton
sec	Seconds
<i>P</i>	Probability value
PD	Preferred Direction
PEC	Pectoralis major muscle
PMd	Dorsal premotor cortex
PPC	Posterior parietal cortex
ROC	Receiver-operating characteristic
RT	Reaction time
SC	Superior Colliculus
SD	Standard deviation
SEM	Standard error of the mean
SLR	Stimulus-locked response
Stim	Stimulus
<i>t</i>	<i>t</i> Statistics

Chapter 1 – General Introduction

1.1 Preamble

From the time that we wake up to the time that we go to sleep, visual information plays a vital role in how we interact with our external environment. Whether it be deciding where to look or grabbing a cup of coffee, we use vision as a primarily sensory modality to guide our upcoming motor actions (Hayhoe, 2017). These visual-to-motor transformations are so ubiquitous in our daily lives that we often take them for granted. Only when we see an individual with extraordinary abilities (such as a professional athlete) or an individual with motor deficits (such as a stroke patient) do we then start to appreciate the sophistication of the human motor system.

One of the fundamental questions within systems neuroscience is how do these visual-to-motor transformations occur within our brain? For example, consider a batter trying to hit a pitch during a baseball game. The batter must incorporate the visual information of the ball with a range of other cognitive factors (i.e. the current score, the tendency of the pitcher, etc.) to decide if they will swing at a pitch. If the batter does decide to swing their bat, the motor system must then execute the appropriate 'volitional' motor commands to try and hit the pitch within a split second.

While a variety of animal models and different types of movements are used to study motor control, here I will primarily focus on how the primate brain generates visually-guided upper limb reach movements. To try and answer this question, previous human behavioural and non-human primate (NHP) neuro-

physiological experiments have primarily studied reach movements that are initiated from a static starting posture and are generated in response to the onset of an external sensory cue (i.e. the onset of a peripheral visual stimulus). A core measurement in these experiments is the reaction time (RT) of a given trial (Luce, 1986), i.e. the time between the onset of the visual stimulus and movement initiation. Typically, visually-guided reach movements to a peripheral visual stimulus occur within 200-300 ms (Welford, 1980). However, these RTs far exceed the minimum conduction time required between the visual input entering the retina and motor commands generated. This additional time delay is inferred to be processing time required to generate a contextually appropriate motor command, as mean RT increases with task complexity (Donders, 1969; Schall, 2003).

1.1.1 Sensorimotor properties of volitional reach control

As a theoretical framework, I will emphasize three inherent sensorimotor components within these visuomotor transformations (**Figure 1.1**). On a given trial, our volitional motor system first selects the motor action (i.e. a **where** component) and then computes the required motor commands (i.e. an **how** component) (Donders, 1969; Wong et al., 2015). During the initial action selection phase, the system selects a desired motor goal by integrating the visual input with the current task demand. Experimentally, both the delayed reach task and the pro-/anti-reach task (Hallett, 1978; Munoz and Everling, 2004; Gail and Andersen, 2006) are examples of how the ensuing motor command can be separated from the visual

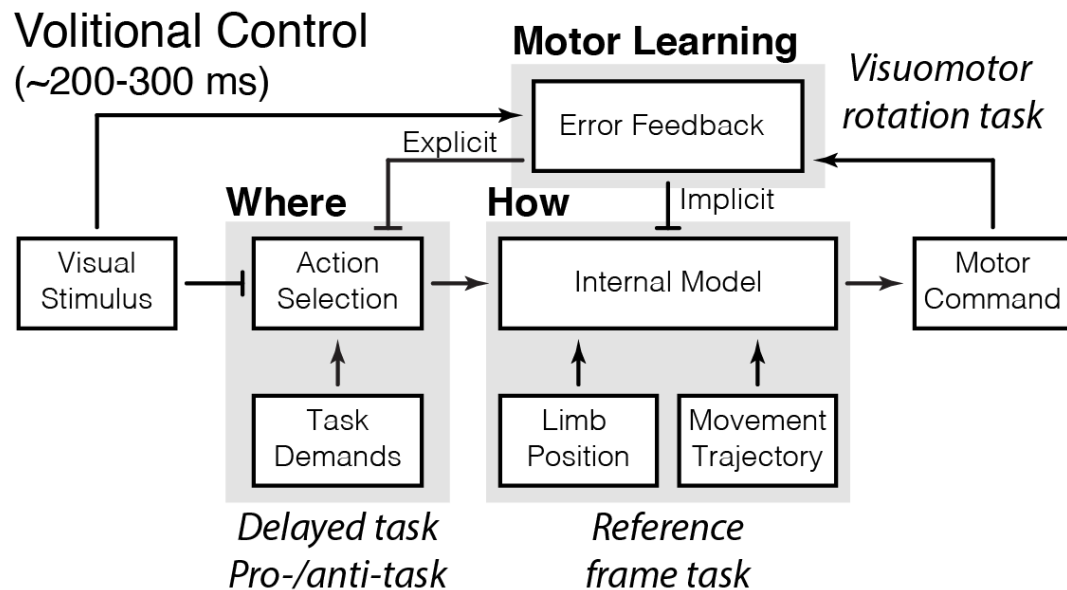


Figure 1.1: Box model of the visuomotor components of volitional motor control

As a theoretical framework, I will separate visually-guided reach movements into three inherent components. (1) **'Where'** component – The motor system must integrate visual inputs with the current task demands to select a desired action. (2) **'How'** component – after the desired action is selected, the motor system must consider both the current body position relative to the goal and plan the movement trajectory to achieve the goal. The system has an internal model of the body to predict the desired motor commands. (3) **'Motor Learning'** component – the system constantly recalibrates its internal model by comparing the predicted and actual motor outcomes.

stimulus. During the delayed reach task, the motor command is temporally dissociated from the visual stimulus by having participants delay their motor command until the onset of a non-spatial go cue (i.e. the offset of the start position). While in the pro-/anti-reach task, the participants generate a motor command either towards (pro-) or in the diametrically opposite direction (anti-reach) of the stimulus location based on the colour of the starting cue. Thus, the exact same peripheral stimulus can elicit two different motor commands based on the current task demand.

Once the motor goal is selected, the system must then consider **how** to execute the motor action to achieve this goal. For the same motor goal, there are multiple different factors that the motor system considers before generating the appropriate motor commands. For example, the brain must transform visual information that enters in an eye-centric reference frame into motor commands that are in a hand-centric reference frame. Note, that while there are different possible hand-centric reference frames (e.g. allocentric, joint-based, and muscle-based), I will use hand-centric as a catch all for term for any reference frame that is independent of the initial eye position. Previous experiments have used the reference frame task to examine how different regions of the brain represent the ensuing motor command. This task systematically alters the participant's initial eye and hand positions to dissociate between the two different reference frames prior to the visually-guided reach movement. Thus, the same eye-centric visual input can elicit different hand-centric motor commands and vice versa. Another way to test this **how** component is by presenting participants with different visual obstacles, so that different movement trajectories are required for reach movements with the same motor goal (Flash and Hogan, 1985; Hocherman and Wise, 1990, 1991; Kaufman et al., 2014). Note, even though I have presented the action selection (**where**) and execute (**how**) in a serial manner, other have proposed that these two components can occur in parallel, see Cisek (2007).

The previous two sensorimotor components have considered how the motor system generates a reach movement, whereas the third **motor learning**

component considers how the motor system recalibrates itself after the motor command is executed. A predominate theory in motor control has suggested that the motor system has an internal model (Wolpert and Miall, 1996; Kawato, 1999). For visually-guided reach movements, this internal model maps visual inputs with its appropriate motor commands. The internal model recalibrates itself by computing an error signal between the actual and predicted sensory consequences of the generated motor command (van Beers, 2009; Herzfeld et al., 2014, 2015). Experimentally, two simple ways to examine and quantify motor learning is by either introducing a novel force during reaches (Shadmehr and Mussa-Ivaldi, 1994) or systematically altering the visuomotor mapping via a visuomotor rotation task (Pine et al., 1996; Krakauer, 2009).

During the visuomotor rotation task (an example of this is shown in **Figure 1.2a**), participants initially perform visually-guided reaches while receiving veridical feedback, in which a visual stimulus, representing hand position (the red dot in **Figure 1.2a**), moves in register with the participant's hand. During the visuomotor rotation, the visual feedback of their hand position is systematically rotated around the start position (45° CW in this example). This creates a mismatch between the predicted location of the participant's hand and the visual feedback of their hand. Thus, for task success the participants must learn to counteract the rotation by reaching 45° CCW relative to the visual stimulus location. When the rotation is applied the participants rapidly learned to counter this rotation (**Figure 1.2b**, decrease in reach error during phase II). The participants then retain the learned

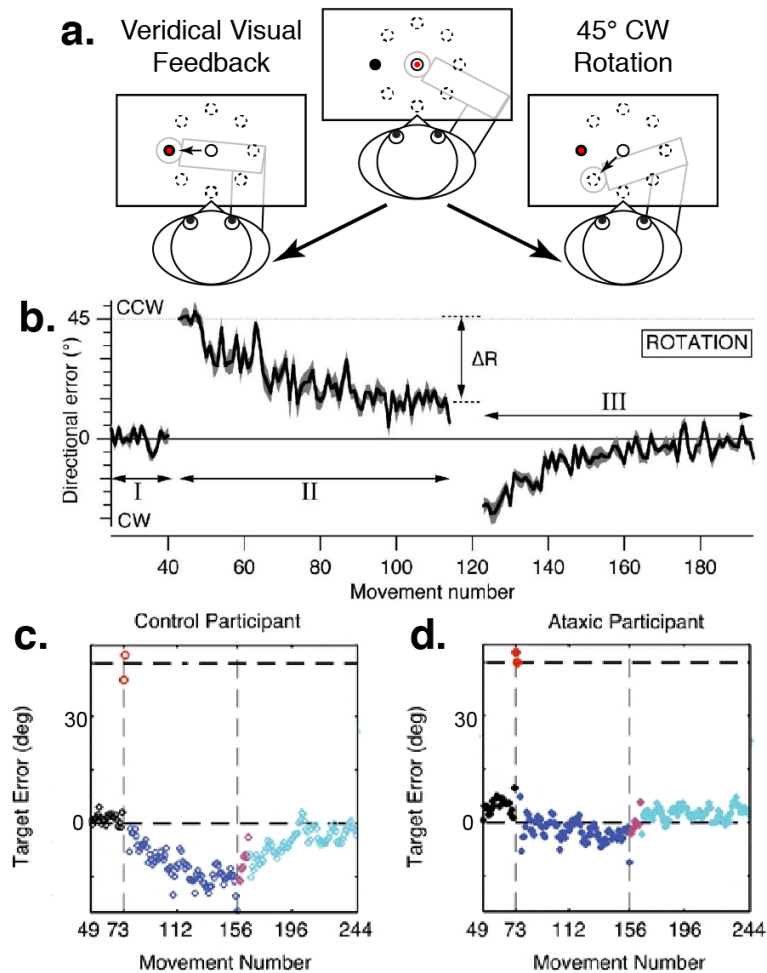


Figure 1.2: Implicit and explicit components of the visuomotor rotation task

(a) Task paradigm for the visuomotor rotation task. Participants perform visually-guided reach movements to eight possible equidistant visual stimulus locations. Prior to and after the visuomotor rotation participants perform reaches with the cursor (red circle) representing the veridical feedback of their hand position. During a 45° CW visuomotor rotation, the cursor is systematically rotated 45° around the start position. (b) Typical learning curve for the visuomotor rotation task. After the 45° CW rotation is induced (II), there is a large 45° CCW reach error. This error gradually decreases as a function of the number of movements in the novel visuomotor mapping. After the rotation is removed (III), there is a large initial aftereffect where the participants generate CW reaches. Modified from Mazzoni and Krakauer, 2006. Reach errors from either a control (c) or cerebellar ataxia patient (d) when they used a cognitive strategy to counteract during a 45° CW visuomotor rotation (between the two vertical dash lines). Modified from Taylor and colleagues, 2004.

visuomotor mapping, as indicated by the prominent aftereffect in the initial few trials after the rotation is removed (**Figure 1.2b**, the reach error flips in the opposite direction during phase III).

Recent behavioural experiments have suggested that motor learning arises from at least two distinct components (Taylor et al., 2014; Huberdeau et al., 2015b; McDougle et al., 2015): an implicit learning component that recalibrates the internal model, which give rise to the prominent and sustained aftereffect (Mazzoni and Krakauer, 2006; Morehead et al., 2017), and an explicit aiming component that helps with the initial rapid learning of the visuomotor rotation (Haith et al., 2015; Huberdeau et al., 2015a). If we go back to the initial batter example, consider when the batter has a new bat. If the new bat is slightly lighter than the old bat, the batter must slowly re-learn the physics of their swing (i.e. implicit learning). To speed up learning, a cognitive (i.e. explicit) strategy that the batter can use to counteract the difference in the weight of the bat is by simply changing the timing of their swing.

1.1.2 Rapid visuomotor reach control

As mentioned earlier, a typical reach movement from a static posture requires 200-300 ms to perform the sensorimotor transformations outlined in the previous section. However, there are instances where reach RTs can approach the minimum conduction time. One specific example is during an ongoing reach movement to a peripheral visual target, a rapid corrective adjustment can occur within 130 ms (Carlton, 1981). There is still a debate about the exact underlying

neural pathway that generates these rapid corrective responses. One methodological challenge in identifying the neural pathway has been that volitional control and online corrective responses are not studied in the same manner, since volitional control is primarily studied when subject start from a static position, whereas online corrective responses are by definition studied during an ongoing reach movement.

Within this thesis, I compared the sensorimotor properties of an alternative rapid visuomotor response that is detectable from a static starting position against the known sensorimotor properties of volitional motor control. These results provide additional support for the notion that a distinct descending motor pathway, which lies in parallel to the well-studied volitional motor control pathway, mediates rapid visuomotor behaviour. Prior to describing this alternative rapid visuomotor response and the experiments conducted in this thesis, I will provide some background on the sensorimotor properties of the neural substrates that mediate volitional motor control, previous behavioural studies of online corrective responses, examples of other types of rapid visuomotor behaviours and the possible neural substrates that mediate them, and finally finish with the objectives of this thesis.

1.2 Cortical control of volitional reach movements

The experiments of David Ferrier (1874) demonstrated that stimulation of the primate cerebral cortex can evoke complex body movements. Since then,

extensive research has investigated the role of the cerebral cortex in the context of visually-guided reach movements. Single cell neurophysiological studies in NHPs have shown that the primary motor (M1), dorsal premotor (PMd), and posterior parietal (PPC) cortices all contain neurons that modulate their firing rates just prior to the onset of reach movements with the animal's contralateral limb (Georgopoulos et al., 1982; Weinrich and Wise, 1982; Taira et al., 1990; Snyder et al., 1998). Additionally, most of these neurons shown directional selectivity, where the reach-related activity is modulated based on the reach direction. For example, **Figure 1.3a** shows a neuron recorded from M1. This neuron preferentially increases and decreases its firing rate across multiple trials prior to the onset of leftward and rightward reach movements, respectively (**Figure 1.3a**). A simple way to quantify the preferred direction (PD) of individual neurons is to assume a sinusoidal relationship between the reach movement direction and the corresponding neural activity around the time of reach onset (**Figure 1.3b**). Similar directional tunings have been observed in human imaging experiments (Fabbri et al., 2010; Haar et al., 2015). However, due to the spatial and temporal limitations of these non-invasive imaging techniques, most of our current knowledge on volitional motor control has still primarily come from both human behavioural experiments and neurophysiological studies in NHPs.

Although these initial reaching experiments have suggested that motor commands are encoded in an extrinsic visual reference frame (Georgopoulos et al., 1982; Georgopoulos, 1988). other studies have shown that M1 activity differed

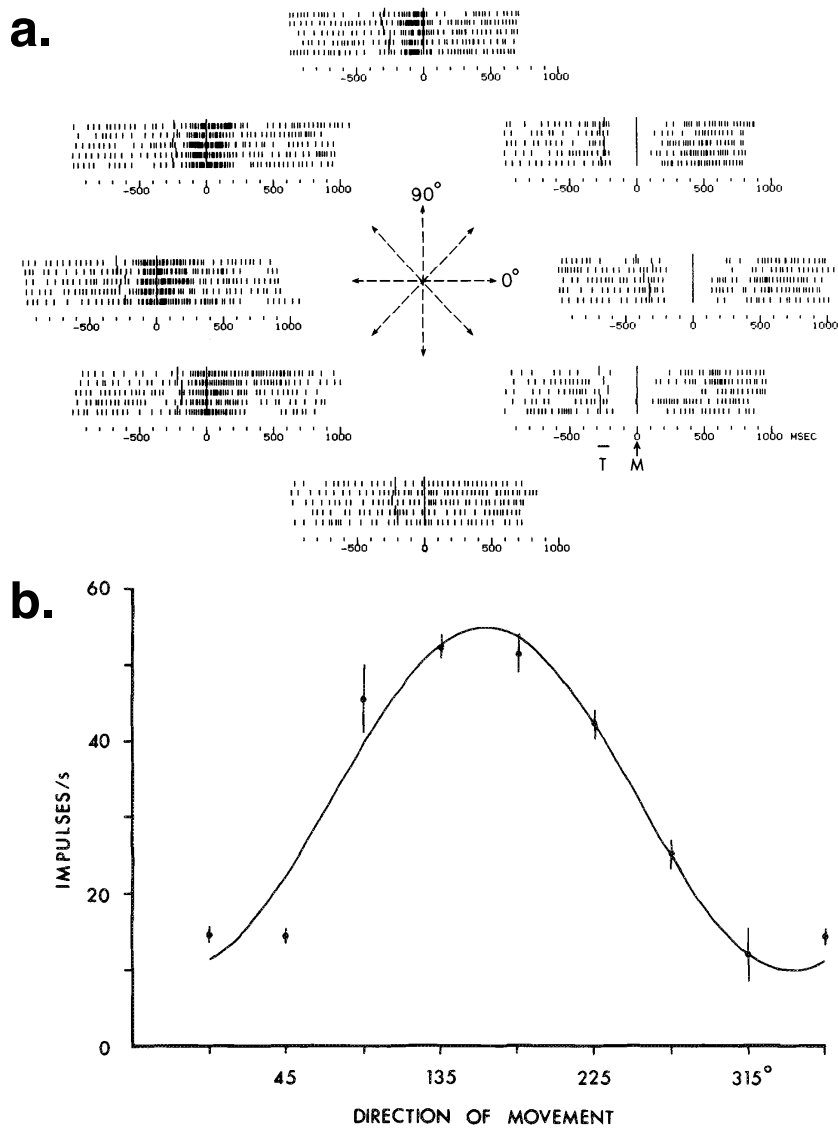


Figure 1.3: Example of a reach-related neuron within M1

(a) Neural activity from during five trials of centre-out visually-guided reaching movements to eight different locations equally spaced around the starting position. Trials are aligned to movement onset (M), with each tick indicating an action potential. (b) The average \pm SEM firing rate of this neurons as function of movement direction; the curve is a fitted sinusoidal function. Modified from Georgopoulos and colleagues, 1982.

for the same external vector-based reach movement if the starting posture of the animal changed (Scott and Kalaska, 1995, 1997; Scott et al., 1997). Furthermore, neural activity in M1, PMd, and PPC are all modulated based on the pre-planned reach movement trajectories (Hocherman and Wise, 1990, 1991; Torres et al., 2013), and neural activity in M1 and PMd are modulated based on the ensuing movement velocity (Churchland et al., 2006). Thus, there are still debates on the exact motor parameters that are encoded within the cortex (Scott, 2003, 2008; Shenoy et al., 2013).

1.2.1 Visual-related responses within the motor cortices

Given that visual information is critical in guiding volitional motor control, how is visual information encoded within the motor cortices? A portion of reach-related neurons within both PMd (Cisek and Kalaska, 2005) and PPC (Snyder et al., 2000) also exhibit visual-related activity that occurs within 100 ms after the onset of a novel visual stimulus. In addition, the overall neural variability (i.e. the consistency of a neuron's firing rate across multiple trials) within both PMd and PPC decreases ~100 ms after visual stimulus onset (Churchland et al., 2010). Although there have been reports of visual-related responses within M1 (Kwan et al., 1981, 1985), the proportion of neurons with visual-related activity is less than that of either PMd or PPC. This can be seen in **Figure 1.4b**, which shows neural activity from both PMd and M1 during a delayed reach task. Each row represents the mean change in firing rate of an individual neuron during the task, with all neurons sorted based on

their PD relative to the stimulus location (black circle). The neural activity is aligned to both the stimulus onset (left) and the go cue (right panels). Note, that neurons within the PMd showed transient visual-related responses after the onset of the visual stimulus. In contrast, both PMd and M1 neurons showed reach-related activity after the go cue, which corresponded with the onset of the reach movements. Neurons within PPC have also shown both visual and reach-related responses (Snyder et al., 2000; Gail and Andersen, 2006).

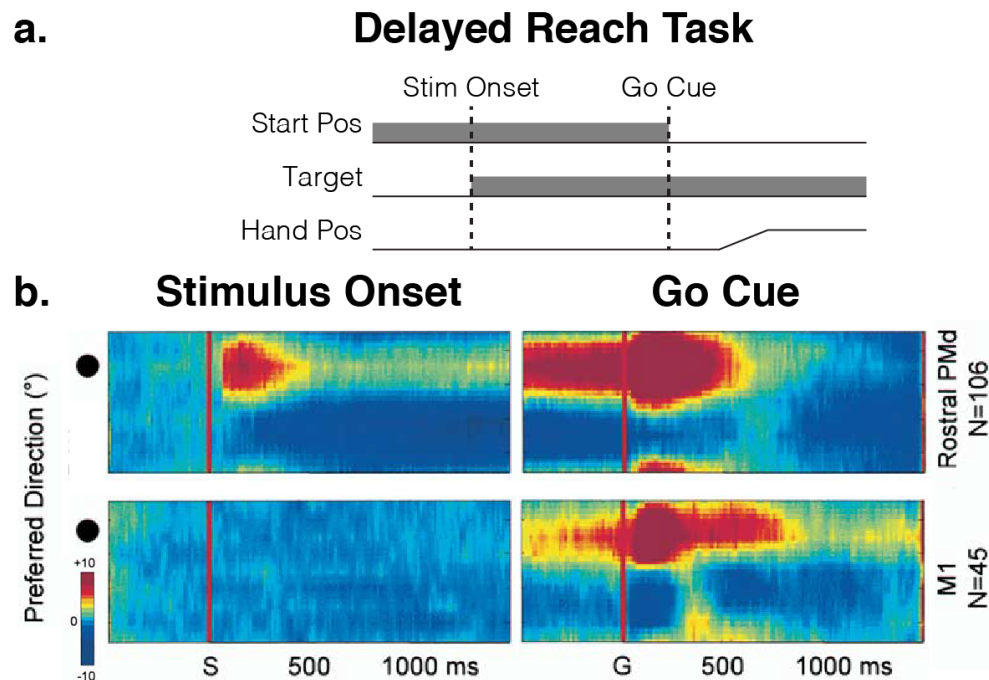


Figure 1.4: Neural activity from both M1 and PMd during the delayed reach task

(a) Timeline of the delayed reach task. Trials start when the hand position enters the start position. Afterwards, a peripheral visual stimulus appears (Stim Onset). The participants withhold their reach movement until the offset of the start position (Go Cue). (b) Neural activity from both PMd (top) and M1 (bottom panels) aligned to both the stimulus onset (left) and go cue (right panels). Each row indicates the change in mean firing rate of a single neuron relative to baseline activity. Neurons are sorted based on their PD, where the rows next to the filled circle indicates neurons with a PD that corresponds to the location of the visual stimulus. Modified from Cisek and Kalaska, 2005.

1.2.2 Visual-to-motor transformations within the motor cortices

A fundamental question from these observations of visual-related activity within both PMd and PPC is how these cortical regions transform these visual signals into the appropriate goal-oriented motor commands (**Figure 1.1**). Previous studies have examined both the PPC (Gail and Andersen, 2006; Gail et al., 2009) and PMd (Westendorff et al., 2010; Klaes et al., 2011) during a memory version of the pro-/anti-reach task (**Figure 1.5b**, top panel). The animals are instructed on the current trial by the colour of the starting position. The stimulus location is then flashed for 200 ms (cue epoch), but the animals withheld their reach movements until the offset of the starting position (memory-epoch). **Figure 1.5b** also shows the firing rate of a neuron from the PPC with a leftward PD during this task. This neuron displays an initial visual-related response after the onset of the leftward stimulus (cue epoch, solid lines) regardless of the task demand. Afterwards during the memory period, the firing rate of this neuron modulated to the appropriate goal-directed direction. The neuron increases and decreases its activity for the leftward (dashed light blue) and rightward (solid blue) reaches directions during anti-reach trials, respectively. This sensory-to-motor transformation can also be seen at a population level. **Figure 1.5c** shows the performance of a decoder that trained on neural data from the pro-reach trials to predict the location of either the visual stimulus or motor goal during anti-reach trials. This decoder initially predicted the visual stimulus location when using neural activity during the cue epoch. The decoder then predicted the motor goal when using neural activity during the

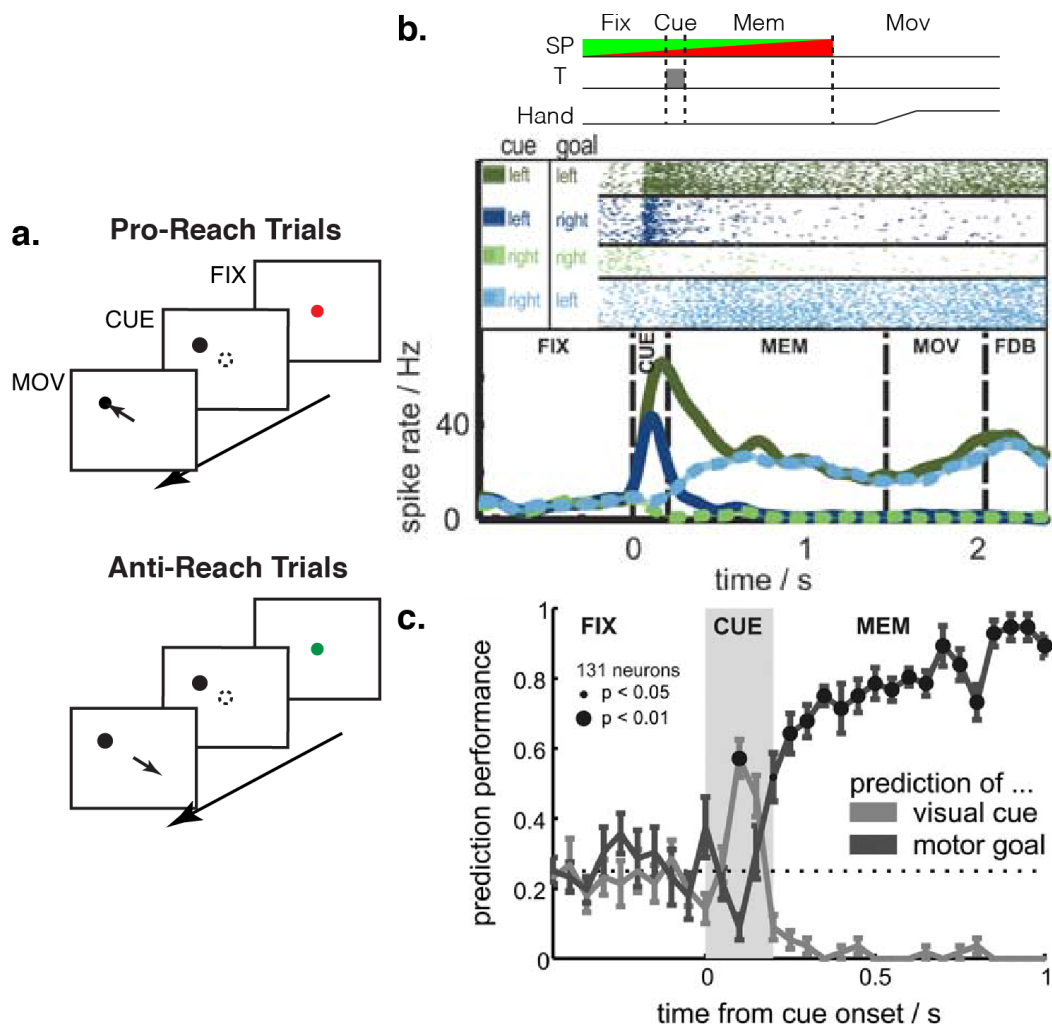


Figure 1.5: Neural activity in PPC during the pro-/anti-reach task

(a) Timeline of the pro-/anti-reach task. Colour of the starting position indicates if the current trial is either a pro- (red, in this case) or anti-reach trial (green). (b) Example of a neuron in the PPC that shows both visual and reach-related activity during a modified memory pro-/anti-reach task (top panel). This neuron preferentially fires for leftward reaches. Upper panel denotes neural activity for individual trials, while lower panel denotes the mean firing rate. Note the initial visual-related responses during the cue epoch for leftward stimuli (solid lines) regardless of the task demands. During the memory epoch, the neuron then encodes the appropriate motor command. (c) Population dynamics of sensory versus motor representation within the PPC. A classifier was trained on pro-reach trials to predict the location of either the motor goal (dark gray) or visual cue (light gray line) relative to the onset the peripheral stimulus. Note, that immediately after cue onset (~200 ms), PPC represents the visual cue location rather than the actual motor goal. The decoder performance flips during the memory period. Modified from Gail and Andersen, 2006.

memory epoch. This temporal change from encoding visual to motor goal in neural activity has also been observed in PMd (Westendorff et al., 2010; Klaes et al., 2011). Thus, these results suggest that the brain reflexively encodes an initial motor response towards the novel visual stimuli and then integrates the visual signal with the current task demand to generate a goal-oriented response.

1.2.3 Reference frames of visual responses in the motor cortices

As mentioned in the preamble, visual information needs to be transformed from an eye-centric visual input into the appropriate hand-centric motor output. This transformation is critical for visually-guided reach movements as patients with lesions to the PPC exhibit optic ataxia (Perenin and Vighetto, 1988; Andersen et al., 2014), which is the inability to perform visually-guided reach movements despite the lack of any primary visual and/or motor-related deficits. These clinical observations suggest that the PPC is a critical node in mediating these sensory to motor transformations.

Studies examining these reference frame transformations have used a reference frame task (**Figure 1.6**), where animals start in different initial eye and hand positions and reach towards a peripheral visual stimulus (Batista et al., 1999; Buneo et al., 2002). They tested three possible reference frames: (1) An eye-centric, i.e. sensory input reference frame, which predicted that the neural activity would be modulated as a function of the reach direction relative to the only the initial eye position, regardless of the hand position. (2) A hand-centric, i.e. motor

output reference frame, which predicted that the neural activity would be modulated as a function of the reach direction relative to only the initial hand position, regardless of the eye position. (3) An intermediate reference frame, which predicted that the neural activity would be modulated as a function of both the initial eye and hand positions.

Figure 1.6 also shows a PPC neuron with an eye-centric reference frame. Note, that the neural activity was largest for downward reach movements of the initial eye positions, regardless of the initial hand position (left panel). In contrast, they found no consistent modulation of this neuron's firing rate when the target was aligned to the initial hand position (right panel). At a population-level, neurons within the PPC primarily encoded reach movement directions in either an eye-centric or an intermediate reference frame (Batista et al., 1999; Cohen and Andersen, 2000; Buneo et al., 2002). Consistent with these neurophysiological studies, eye-centric reference frames in the PPC have also been observed in human imaging studies (Connolly et al., 2003; Medendorp et al., 2003). In contrast, neurons within the PMd primarily encoded reach movement directions in either a hand-centric or intermediate reference frame (Pesaran et al., 2006; Batista et al., 2007). The prevalence of eye-centric encoding within the PPC versus hand-centric encoding within the PMd, suggests that there is a feedforward flow of information from PPC to PMd.

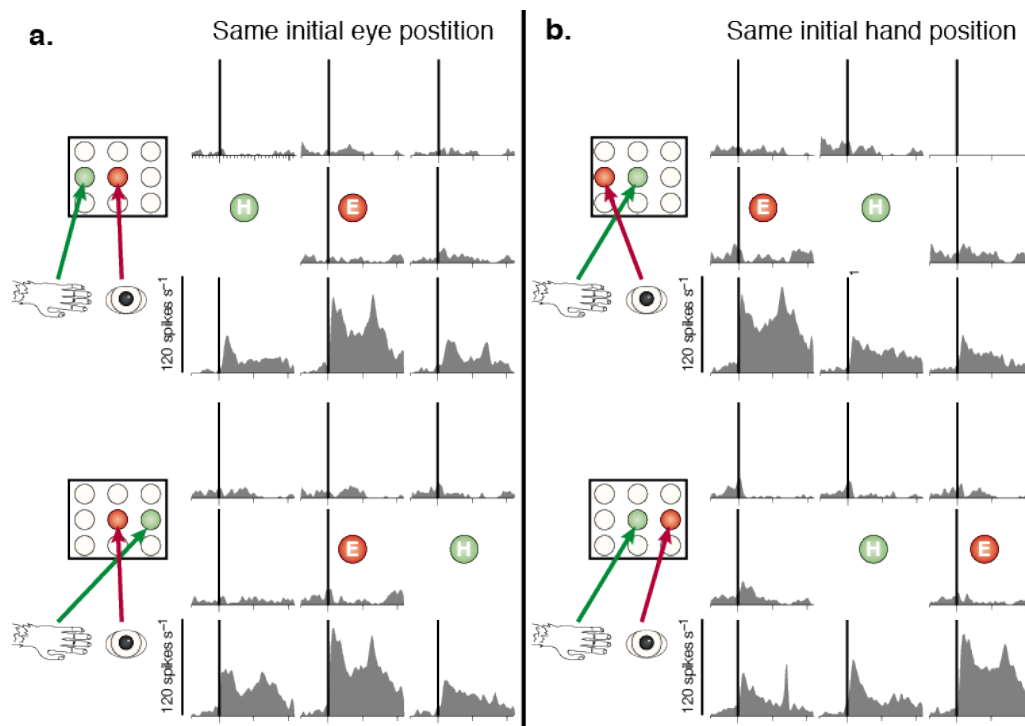


Figure 1.6: Neural activity from an eye-centric neuron in the PPC

The reference task begins by having the participant start at different hand and eye positions. In this case, the animal starts with their hand on the red LED and looks at the green LED. Next, a peripheral stimulus is flashed at one of eight locations, after a delay the monkey reaches to the peripheral stimulus location. Each subpanel, shows the mean firing of this neuron aligned to the onset of the peripheral stimulus (black vertical lines). This is an example of an eye-centric neuron in PPC. Note, the similarities in neural activity when the trials are aligned to the initial eye position (left) but not when aligned to the initial start position (right panels). Modified from Cohen and Andersen, 2002.

1.2.4 The role of motor cortices in motor learning

A predominate theory in motor control is that the brain has an internal model that converts the motor goal into the appropriate motor command (Wolpert and Kawato, 1998; Wolpert et al., 1998a). As we grow and age the motor system is constantly recalibrating its internal model. Classically, motor learning is thought to be mediated via the cerebellum (Miall et al., 1993; Wolpert et al., 1998b; Shadmehr and Krakauer, 2008), as individuals with cerebellar degeneration have difficulties learning a variety of different motor learning tasks (Martin et al., 1996; Smith and Shadmehr, 2005; Izawa et al., 2012; Roemmich et al., 2016). However these individuals are still able to perform the visuomotor rotation task if they are explicitly given the correct cognitive strategy to counteract the rotation (Taylor et al., 2010, **Figure 1.2d**). In contrast, when healthy participants are instructed to use the same cognitive strategy, their task performance slowly declines throughout the experiment, presumably as the internal model implicitly adapting to the novel sensorimotor mapping (Mazzoni and Krakauer, 2006; Taylor et al., 2010, **Figure 1.2c**). This is one piece of evidence that motor learning may be comprised of two distinct learning components (Mazzoni and Krakauer, 2006; Taylor et al., 2014): an implicit learning component that is mediated through the cerebellum and an explicit cognitive strategy that is largely independent of the cerebellum.

Despite the large number of human behavioural experiments studying motor learning, there are only a handful of experiments that have examined M1 and PMd activity during either a force field or a visuomotor rotation task. Paz and

colleagues (2003) found that after NHPs learned a new visuomotor rotation, neurons within M1 modified their firing rates to the new learned movement direction. Similar results have shown that M1 activity altered to match the new motor command generated when different mechanical loads are applied onto the limb (Kalaska et al., 1989; Gribble and Scott, 2002). However, other groups have reported that only a subpopulation of M1 neurons altered their firing rates to the new motor command in similar task (Shen and Alexander, 1997a; Wise et al., 1998; Gandolfo et al., 2000). There are also conflicting reports of whether PMd activity modulated during the visuomotor rotation task, as Shen and Alexander (1997b) found that most neurons within PMd encoded the visual stimulus location, while Wise and colleagues (1998) found a mixture of responses, with some neurons encoding the visual location and others encoding the movement direction. Thus, more neurophysiological studies are required to understand the roles of the motor cortices during motor learning.

To my knowledge, no study has examined the modulation of reach-related neural activity in the PPC during motor learning. However, Steenrod and colleagues (2013) did examine saccade-related activity in the PPC during a saccadic adaptation task. They found that neurons continued to encode the stimulus location rather than the new adapted saccadic endpoint. Similar results have been observed in a previous human imaging study, where the PPC encodes the visual stimulus location during a visuomotor task (Haar et al., 2015). However, a major limitation is the fact that most of the tasks used in these experiments have

elicited both implicit and explicit components of motor learning. Additional studies are required to attribute the changes in neural activity within these motor cortices to either implicit and/or explicit motor learning and to examine the interactions between the motor cortices and the cerebellum.

1.3 Corrective reach responses

As mentioned in the preamble, the additional time required to initiate a volitional reach movement is assumed to arise from the prolonged cortical processing. However, a separate stream of research has shown that RTs for corrective responses during ongoing reach movements can be drastically reduced to within 150 ms of the stimulus onset (Carlton, 1981; Soechting and Lacquaniti, 1983; Fautrelle et al., 2010). Further, these rapid visuomotor responses have also been observed in humans, cats, and NHPs (Perfiliev et al., 2010).

A simple way to evoke these rapid corrective responses is by having participants reach towards a peripheral visual stimulus (**Figure 1.7a**, green circle). On a subset of trials, the visual stimulus will shift either leftward (red) or rightward (blue) shortly after the participants initiate their reach movement. The shift of the visual stimulus location is usually in the perpendicular direction of the ongoing reach movement. Thus, any deviation in the perpendicular direction is taken to be a corrective response. Unlike volitional control, these rapid visuomotor responses can occur without the participant's awareness that the stimulus location

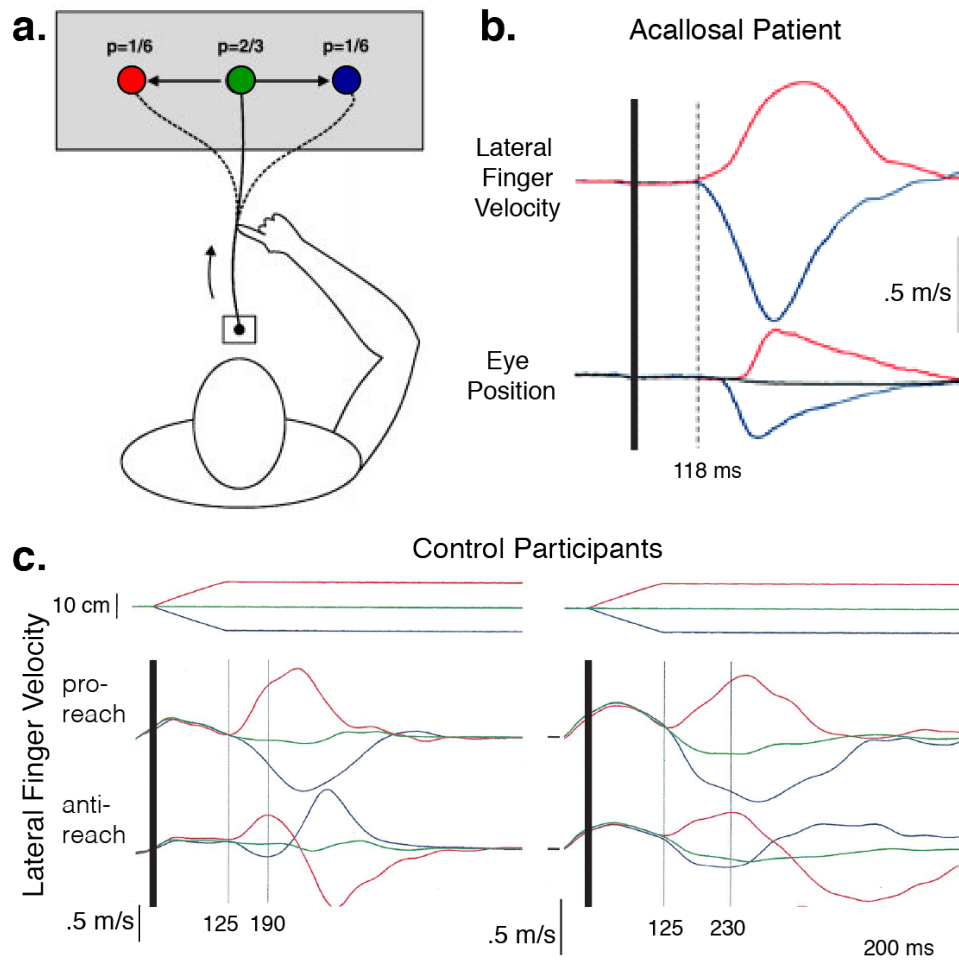


Figure 1.7: Rapid corrective responses during ongoing reaching movements

(a) Top-down view of the experimental paradigm during an online control experiment. Participants are instructed to point towards a visual stimulus (green). On a subset of trials, the stimulus shifted either to the left (red) or right (blue circle) after the onset of the pointing movement. Participants must rapidly adjust their reach movements to the new visual stimulus location. (b) Mean lateral finger velocity (top) and eye position (bottom row) of an acallosal patient during the online correction task aligned to the stimulus shift (thick black line). The dashed line is the average latency of these corrective responses. Modified from Day and Brown, 2001. (c) Mean lateral finger velocity from two different healthy participants during either pro-corrective reaches (top) or anti-corrective reaches (bottom row). The two numbers indicate the average corrective latency and the latency of the intended direction during anti-reach trials. Modified from Day and Lyon, 2000.

has shifted (Goodale et al., 1986). Further, even when participants are fully aware that the stimulus location has shifted, these corrective responses persist when participants are explicitly told not to movement towards the shifted stimulus location (Franklin and Wolpert, 2008). Thus, these rapid corrective responses seem to be a reflexive motor command towards the visual stimulus.

1.3.1 Visuomotor properties of rapid corrective responses

A seminal study from Day and Lyon (2000) further supported this notion. They used the pro-/anti-reach task to demonstrate that these corrective responses are composed of two distinct phases (**Figure 1.7c**). Like other studies, during the pro-reach trials the mean lateral finger velocity start to separate ~120 ms after the stimulus shifted (**Figure 1.7c**, top row). During the anti-reach trials, the initial automatic response occurs at the same latency and direction as the pro-reach trials, i.e. towards the direction of the shifted stimulus. Only after ~200 ms do participants start to generate the correct motor response away from the visual stimulus. The latencies of those contextually appropriate responses are in line with RTs of volitional reach movements initiated from a static posture. This key finding suggests that the initial automatic reflexive responses may be generated from a rapid visuomotor pathway, while the later responses are generated by volitional control.

Another key point from this experiment is that, due to the mass of the upper limb and the inherit motor noise of the initial reach movement, these ‘automatic’

responses are relatively small. **Figure 1.7c** shows the change in lateral velocity. The mean change in lateral position between the leftward and rightward anti-reach trials across their participants was less than 5 mm. Additionally, the magnitude of corrective responses saturates when the stimulus shift is greater than ~ 2 cm (Franklin et al., 2016), while the lateral volitional response scale linearly as a function of the size of the stimulus shift. Thus, a potential functional role of these automatic corrective responses may be to initial a rapid change in the reach direction, but the later volitional control is responsible for generated the more contextually appropriate motor command.

Despite the difference in the pro-/anti-reach task, there are some similarities between corrective responses and volitional control. For example, both the latency and magnitude of the corrective responses are invariant to the eye position at the time of the stimulus shift (Diedrichsen et al., 2004). Thus like volitional control, the pathway mediating corrective responses can rapidly transform the eye-centric visual input into the appropriate motor commands to move towards the shifted visual stimulus location (i.e. hand-centric reference frame).

Further, the magnitude of corrective responses is modulated during both a force field task (Franklin et al., 2012) and a visuomotor rotation task (Telgen et al., 2014; Hayashi et al., 2016). However, there are still some questions that have not been answered. First, even though these responses are modulated during learning, these experiments have not been able to quantify the extent of motor learning (i.e. if these responses fully adapted). Second, these experiments have also not

selectively tested the contributions of implicit and explicit motor learning components on corrective responses.

1.3.2 Possible neural substrates mediating corrective responses

Due to the inconsistencies in task structure, it has been hard to interpret results between different labs. For example, labs use different criteria to trigger the shift in stimulus location. Day and Lyon (2000) used a force plate to detect movement onset, Goodale and colleagues (1986) measured eye position and used the participant's peak saccade velocity, while Oostwoud Wijdenes and colleagues (2011) used fixed time delays between the onset and the shift of the visual stimulus. Further, even the direction of the stimulus shifts varied across labs. While human behavioural experiments have primarily shifted the stimulus perpendicularly along the reach direction (Carlton, 1981; Day and Lyon, 2000; Pisella et al., 2000), the limited number of neurophysiological studies have shifted the stimulus location in the opposite direction of the ongoing reach movement (Archambault et al., 2009, 2011). Thus, these differences have contributed to the ongoing debate about the exact underlying neural substrates mediating these rapid corrective responses. Below, I will briefly detail two possible neural substrates of these corrective responses.

Due to the prominent role of the PPC in the visuomotor transformation during static reaching movements as mentioned above, the PPC has been speculated to also play a role in generating corrective responses. Research

involving individuals with bilateral PPC lesions have reported deficits during online corrective movements (Pisella et al., 2000; Gréa et al., 2002). Similar conclusions have been made in healthy participants by creating 'virtual' lesions to the PPC with transcranial magnetic stimulation (Desmurget et al., 1999). Further, there has been one causal experiment in NHPs that has temporally inactivated PPC while the animals performed corrective movements (Battaglia-Mayer et al., 2013). They found that inactivation of PPC resulted in longer movement times and slower hand velocity. However, these experiments did not specifically examine the reach kinematics during the initial portion of the corrective responses (i.e. < 150 ms after stimulus onset). Thus, it is unclear if these experiments are reporting a deficit for the initial 'automatic' corrective response or a deficit in normal volitional control.

An alternative hypothesis is that online corrective responses are mediated through a subcortical pathway (Day, 2014), rather than the corticospinal pathway that is classically associated with mediating volitional reach movements. One piece of clinical evidence to support this notion comes from an acallosal individual (Day and Brown, 2001). This individual has a complete agenesis of the corpus callosum, which precludes direct communication between the left and right cerebral cortices. As a result, this individual has prolonged RTs for visually-guided reach movements from a static starting posture when the visual stimulus when the visual stimulus was in opposite compared to the same visual hemifield. However, this RT difference was abolished when the individual was making online corrective responses (**Figure 1.7b**). Further, the latency of these corrective responses (~120

ms) was in line with healthy age matched participants. Thus, these results suggest that corrective responses do not require transfer of information between the two cerebral cortices like that of the later volitional control. Day (2014) speculated a subcortical pathway possibly via the superior colliculus (SC), which has been classically associated in visuomotor transformation for gaze control, may play a critical role for mediating these rapid visuomotor reach responses.

1.4 The role of superior colliculus in gaze control

The SC, a midbrain structure, has been an attractive region for studying visuomotor transformations, historically in the context of the oculomotor control (Wurtz and Albano, 1980; Sparks and Mays, 1990; Gandhi and Katnani, 2011). More recently it has been suggested that the SC may also play a role in gross orienting movements to visual stimuli, like during visually-guided reach movements (Corneil and Munoz, 2014).

The SC is composed of seven anatomical layers (May, 2006), which can be grouped into two functional layers (Wurtz and Albano, 1980). The superficial layers of SC (SCs) consist of the top three anatomical layers, while the intermediate and deep layers of SC (SCi) consist of the bottom four anatomical layers. **Figure 1.8a** shows the three functional neuron types that are typically examined within the caudal SC during oculomotor experiments. Visual neurons are primarily found within the SCs and discharge a high frequency visual-related response within ~50

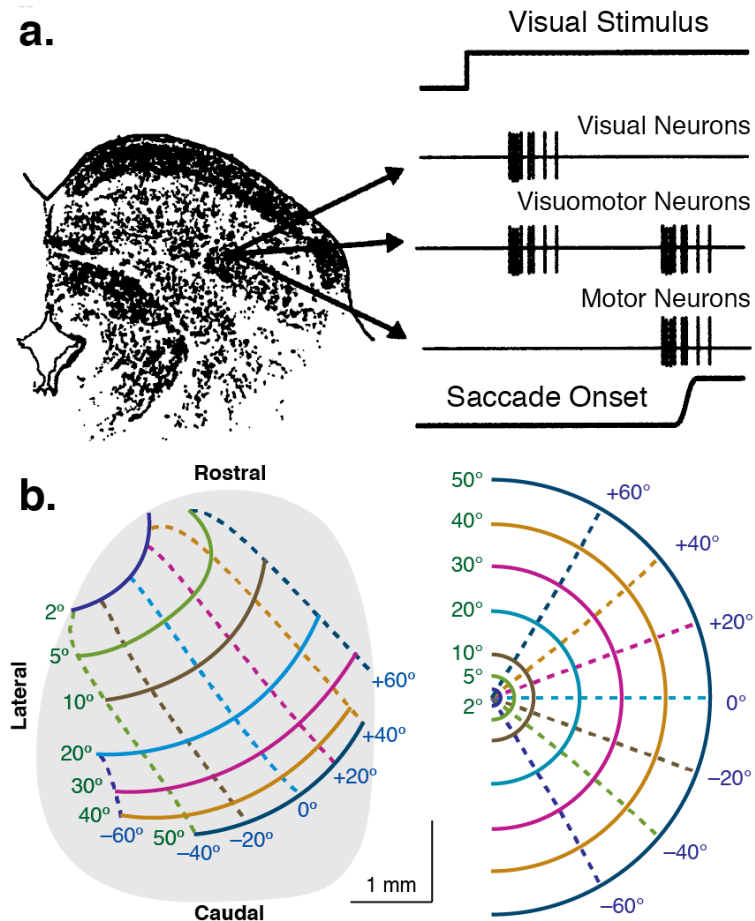


Figure 1.8: Properties of the primate superior colliculus

(a) Coronal view of the SC. The three major types of neurons within the SC during visually-guided saccades: visual neurons that respond to the onset of the visual stimulus, motor neurons that respond prior to the onset of the saccades, and visuomotor neurons that respond to both visual stimulus and saccade onset. Modified from Sparks and colleagues, 2000. (b) Top down view of the left SC. Schematic of the topographic organization of the SC (left) and the corresponding right visual hemifield (right panel). Note the over-representation of the fovea within the rostral SC. Modified from Gandhi and Katnani, 2011.

ms of visual stimulus onset in the neuron's receptive field (Goldberg and Wurtz, 1972a). Visuomotor and motor neurons are found exclusively within the SCi and discharge just prior to onset of a saccade into the neuron's receptive field (Wurtz and Goldberg, 1972).

The SC has a clear retinotopic organization of neural receptive fields that encompass the entire contralateral visual hemifield (Robinson, 1972; Hafed and Chen, 2016). **Figure 1.8b** shows a top-down view of the SC and the corresponding retinotopic mapping. Visual eccentricity is represented along the rostrocaudal axis, with the fovea and the periphery encoded within the rostral and caudal SC, respectively. Visual elevation is represented along the mediolateral axis, with upper and lower visual fields represented in the medial and lateral portions of the SC, respectively. This retinotopic mapping has been replicated in human imaging experiments for both visual stimulus location (Katyal and Ress, 2014) and saccadic eye movements (Savjani et al., 2018).

1.4.1 Visual-related responses within the SC

The initial high frequency visual-related responses in both visual and visuomotor neurons are modulated by different visual stimulus properties. Increasing the contrast of the visual stimulus evokes higher peak firing rates and shorter onset latencies of the initial visual responses (Marino et al., 2012, 2015). Similarly, lower spatial frequency visual stimulus evokes larger and quicker visual responses (Chen et al., 2018). Other cognitive factors such as attention (Goldberg and Wurtz,

1972b; Ignashchenkova et al., 2004; Krauzlis et al., 2013) or different task demands like the pro-/anti-saccade task (Everling et al., 1999) can also selectively influence the magnitude, but not latency, of the initial visual-related activity.

Visual information enters the SC through either direct projections from the retina (retinotectal pathway) or indirect projections from the primary visual cortex (corticotectal pathway) via the lateral geniculate nucleus (LGN) in the dorsal thalamus. The retinotectal pathway, originating from both the contralateral and ipsilateral retinae, projects primarily to the caudal SCs (Hubel et al., 1975) and has very few projections to the rostral SCs (Pollack and Hickey, 1979). In contrast, both foveal and peripheral visual information are relayed into both the SCs and SCi via corticotectal projections (Wilson and Toyne, 1970). Additionally, corticotectal neurons within primary visual cortex are broadly tuned and binocularly driven (Schiller et al., 1976). The visual-related activity within the SCi is dependent on the integrity of the indirect corticotectal pathway, as inactivation of either LGN (Schiller et al., 1979) or primary visual cortex (Schiller et al., 1974) selectively abolishes SCi, but not SCs, visual-related responses. Note, that only inactivation of magnocellular layers of LGN (Schiller et al., 1979), which carries contrast and low spatial frequency visual information, disrupts visual responses in SCi. This result is in line with previous neurophysiological studies that showed the SCi preferentially respond to changes in contrast and low spatial frequency visual stimulus (Marino et al., 2012; Chen et al., 2018).

1.4.2 Sensorimotor transformation within the SCi

Consistent with the retinotopic mapping, neurons within the rostral SCi encode the foveal region and discharge during periods of fixation (Munoz and Wurtz, 1993a). Microstimulation within the rostral SCi causes prolonged fixation (Munoz and Wurtz, 1993b) and ceases any ongoing saccades (Munoz et al., 1996). In contrast, neurons within the caudal SCi discharge just prior to the onset of a saccade into the neuron's specific receptive field (Wurtz and Goldberg, 1972; Munoz and Wurtz, 1995), and microstimulation within the caudal SCi produces non-truncated saccades into the same retinotopic location regardless of the initial eye position (Robinson, 1972; Stanford et al., 1996). Further, prolonged electrical stimulation results in 'staircase' saccades, which consists of consecutive saccadic eye movements of the same size and direction (Robinson, 1972; Stryker and Schiller, 1975). These results suggest that the caudal SCi represents gaze shifts in a retinotopic manner.

Neurophysiological recordings during the pro-/anti-saccade task have shown that two distinct bursts of activity occur within the SCi (**Figure 1.9c**). During anti-saccade trials, relative to the visual stimulus the contralateral SCi will exhibit an initial burst of activity that encodes the visual stimulus location (**Figure 1.9c**, left shaded panel). Afterwards, a second burst of activity occurs in the ipsilateral SCi encoding the correct goal-oriented saccade direction. Compared to pro-saccade trials, the initial visual-related response is attenuated for correct anti-

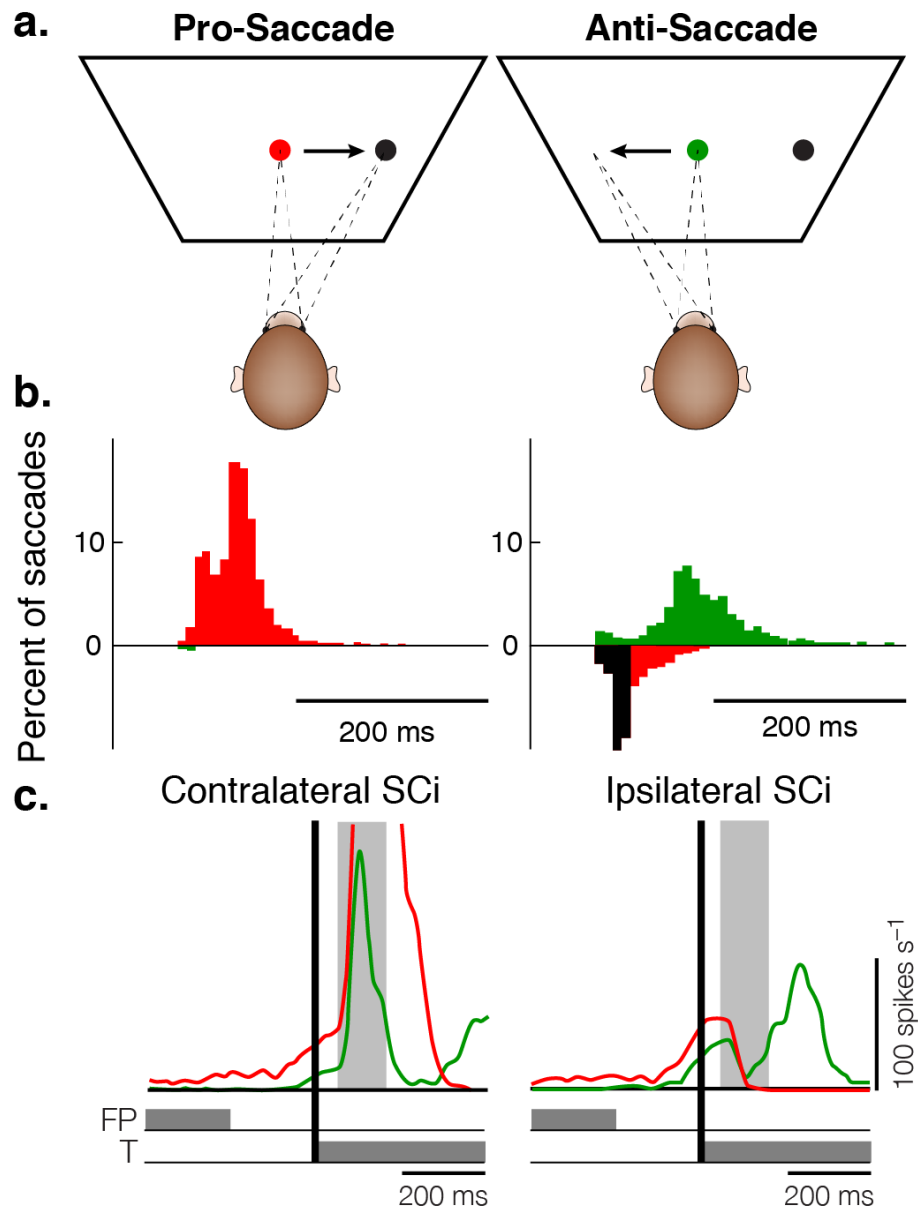


Figure 1.9: SCi activity during the pro-/anti-saccade task

(a) Schematic of the pro-/anti-saccade task for a leftward visual stimulus. (b) Saccadic RT distribution for correct (above) and error (below abscissa) in the pro- and anti-saccade task. The black bar represents express saccade errors during anti-saccade trials. (c) Neural activity within both the contralateral (left) and ipsilateral (right panel) SCi during correct pro- (red) and anti-saccade trials (green traces). The initial visual epoch is represented by the shaded panel. Modified from Munoz and Everling, 2004.

saccade trials (Everling et al., 1999), but not for erroneous anti-saccade trials (Everling et al., 1998). Further, erroneous anti-saccade trials also had higher levels of low-frequency build-up activity within the SCi compared to correct anti-saccade trials (Everling et al., 1998). Thus, these results demonstrate the different stages of the sensorimotor transformation required for generating anti-saccades within the SCi.

1.4.3 Express saccades are mediated through the SCi

Note that during the pro-/anti-saccade task, there are short-latency (RTs < 100 ms) erroneous anti-saccade trials that occurs towards the novel visual stimulus (**Figure 1.9b**, error trials highlighted in black). These reflexive, visually-driven saccades are known as express saccades. Express saccades are also present during pro-saccade trials as they constitute the first peak of the bimodal RT distribution for visually-guided saccades (**Figure 1.9b**), while regular or volitionally generated saccades constitute the second peak of the RT distribution. Express saccades occur within 100 ms after stimulus onset in humans (Fischer and Ramsperger, 1984) and 75 ms in NHPs (Fischer and Boch, 1983). The latencies of express saccades approach the minimum conduction time between visual information entering the retina and the motor commands generated at the eye muscles. Express saccades are mediated through a subcortical pathway via the SCi, as lesions to the SCi permanently abolish express, but not regular, saccades to the contralateral visual hemifield (Schiller et al., 1987).

While the latencies of these express saccades do not change, the task demands can alter the probability of generating an express saccade. For example, express saccade rates increase as the stimulus location becomes more predictable and the overall express saccade rate can increase after a few days of training (Paré and Munoz, 1996). However, despite the changes in the probability of express saccade generation, express saccades show similar kinematics compared to both regular and delayed saccades (Edelman and Keller, 1996), suggesting that both express and regular saccades are generated via the same descending motor command. This interpretation is consistent with previous studies that have examined SCi activity during both express and regular saccades (Edelman and Keller, 1996; Dorris et al., 1997; Sparks et al., 2000). They found that the visual and saccade-related bursts of activity in visuomotor neurons merges into a single burst during express saccades (**Figure 1.10a**).

1.5 SCi role in eye-head gaze control

The previous characterization of SCi has only considered gaze control when the animal's head is fixed. However, gaze shifts normally consist of a coordinated eye-head movement. Under head-unrestrained conditions, both humans and NHPs start to incorporate head movements for horizontal gaze shifts as small as 15° to 20° if the eyes are in the centre of the orbits (Freedman and Sparks, 1997; Stahl, 1999), even though pure eye movements can generate horizontal gaze shifts up to 55° (Guitton and Volle, 1987). Thus, even for smaller gaze shifts, two distinct

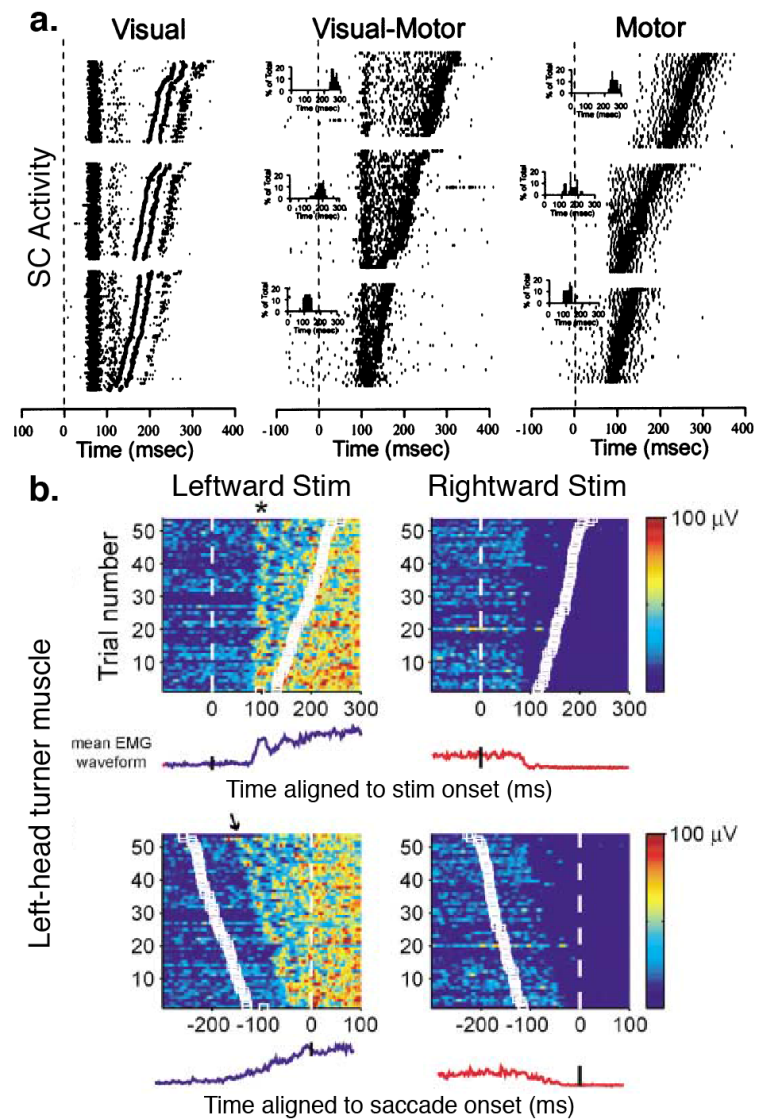


Figure 1.10: Visuomotor responses in the SCi and on neck muscle activity

(a) Visual, visuomotor, and motor neuron activity during visually-guided saccade trials. Individual trials are sorted based on saccadic RTs from longest to shortest (top to bottom). Note that for visuomotor neurons the visual and motor bursts merge during express saccades. Modified from Sparks and colleagues, 2000. (b) Visuomotor activity on a left head turner neck muscle during visually-guided saccades. Trials are segregated by stimulus location. Colour panels show the individual EMG traces and trials are sorted based on saccadic RTs (white squares). Mean EMG activity are plotted below the colour panels. Neck muscle activity is aligned to either the stimulus (top) or saccade onset (bottom). Note the stimulus-locked responses ~ 100 ms after stimulus onset regardless of ensuing RT (* and slanted arrow). Modified from Corneil and colleagues, 2004.

motor commands are generated, one for the eyes and one for the head. Due to the differences between the inertia of the eye and head, the head movement normally occurs in the latter portion of the gaze shift.

Consistent with the previous head-fixed experiments, electrical stimulation of SCi evokes a coordinated eye-head gaze shift during head-unrestrained NHP experiments (Freedman et al., 1996). Further, the evoked gaze shift was of the same size and direction regardless of the animal's initial eye and head positions. However, the eye and head contributions of the gaze shift depended on their initial starting positions. Thus, this last result suggests that the SCi encodes the desired gaze shift, rather than a fixed combination of eye and head movements.

1.5.1 Tecto-reticulospinal pathways mediate both eye and head movements

If the SCi can influence both eye and head movements what is the exact motor pathway that transmit these signals? Skeletal motor control arises from action potentials of lower motoneurons, which reside within the brainstem and the ventral horn of the spinal cord. Eye movements are innervated by cranial nerves, while neck muscles are innervated by both cranial nerves and the upper cervical spinal cord. However, there are very few direct projections from the SCi that terminate within the primate spinal cord (Nudo and Masterton, 1989). The SCi controls both eye and head movements primarily through the reticular formation. The reticulospinal pathway (**Figure 1.11**) projects from the medullary reticular

formation bilaterally to both the ipsi- and contralateral brainstem and spinal cord (Peterson, 1979; Nathan et al., 1996).

Within the reticular formation, the firing rate of neurons in paramedian pontine reticular formation and the rostral interstitial nucleus of medial longitudinal fasciculus encode the horizontal and vertical components of the ensuing saccadic eye movement, respectively (Luschei and Fuchs, 1972; Büttner et al., 1977; Sasaki and Shimazu, 1981). Additionally, disruption of the descending reticulospinal pathway down to the spinal cord manifests in behavioural deficits for both postural control and gross orienting movements (Lawrence and Kuypers, 1968a).

1.5.2 Visual stimulus-locked responses on neck muscles

Even though the head movement occurs in the latter portion of a gaze shift, neuromuscular activity from head turner muscles showed that the neuromuscular command to generate the head movement can precede the eye movement (Zangemeister and Stark, 1982). Further, short-duration or low-current stimulation within the caudal SCi can reliably evoke transient increases in horizontal head turner neck muscles without an overt gaze shift (Corneil et al., 2002), and neck muscle activity also correlated with low-frequency build-up activity within SCi prior to the onset of peripheral visual stimulus (Rezvani and Corneil, 2008). These observations have led to the proposal that there are different thresholds to initiate eye and head movements, with a lower threshold for head movements and a higher threshold for eye movements.

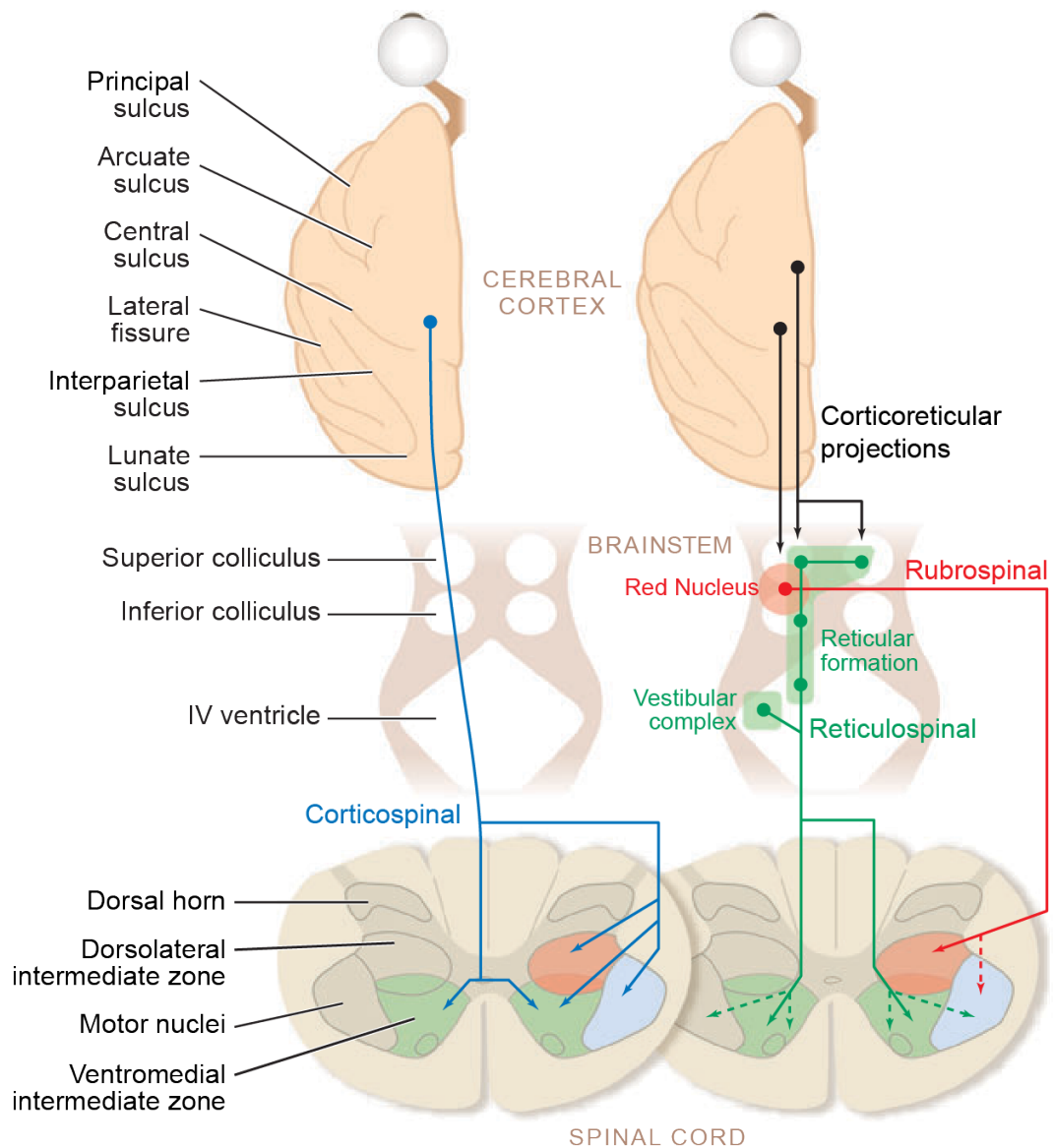


Figure 1.11: Schematic of the three primary descending motor pathways for reach control

The corticospinal pathway (left, blue) originates from the cerebral cortex and terminates primarily in the contralateral spinal cord. There are cortico-motoneuron that projection directly to the motor nuclei. Reticulospinal (green) and rubrospinal (red) pathways originate from the brainstem and project down either bilaterally or contralaterally to the spinal cord, respectively. Modified from Lemon, 2008.

Consistent with this lower threshold for head movements, both the visual and saccade-related responses within the SCi are detectable on horizontal head-turner muscles (Corneil et al., 2004; Goonetilleke et al., 2015). **Figure 1.10b** shows the neuromuscular activity from a leftward head turner neck muscle in a NHP during leftward and rightward visually-guided saccades. Note that the animal was head-fixed, thus no head movements occurred during the experiment. Like the visuomotor neurons within SCi (**Figure 1.10a**), there are distinct waves of activity aligned to both the visual stimulus and saccade onsets. The initial *stimulus-locked responses (SLRs)* occur within 100 ms of visual stimulus onset regardless of the ensuing saccadic RT. The SLRs are directionally-tuned with an increase and decrease in EMG activity for the leftward and rightward stimulus locations, respectively. The directionality of the SLR suggests that it is an orienting response towards the visual stimulus rather than a general freezing response like the startle reflex (Rothwell, 2006). Even though the SLR is time-locked to the visual stimulus onset, the trial-by-trial magnitude of the SLR negatively correlates with the ensuing saccadic RT (Corneil et al., 2004), which is also consistent with previous observation of the visual responses in SCi (Everling et al., 1999; Fecteau and Munoz, 2005).

The SLR also shares similar sensorimotor properties as SCi visuomotor neurons in other oculomotor tasks. For example, Chapman and Corneil (2011) examined the SLRs during the pro-/anti-saccade task (**Figure 1.12a**). They found that the SLR is a reflexive motor command towards the visual stimulus location

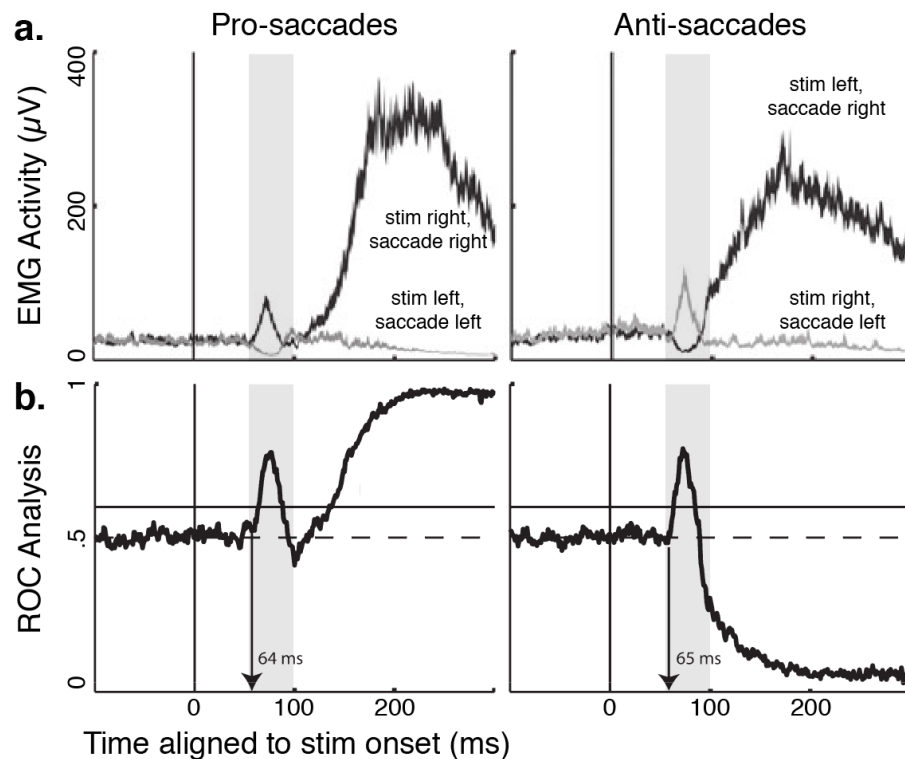


Figure 1.12: Neck SLRs during the pro-/anti-saccade task

(a) Mean EMG activity associated with pro- (left) and anti-saccades (right panel) for a right head turner muscle during rightward (black) and leftward (gray traces) saccades. Note, the flip in mean EMG activity during the anti-saccade trials. (b) Time-series receiver operating characteristic (ROC) analysis relative to stimulus onset. ROC values increased immediately after stim onset for both pro- and anti-saccade trials (shade panel) and they diverged just prior to saccade onset. Modified from Chapman and Corneil, 2011.

and not the ensuing movement direction. Note, that the mean EMG activity traces flipped between the SLR (shaded panel) and the later volitional response during anti-saccade trials (**Figure 1.12a**). This can also be seen with the time-series receiver-operating characteristic (ROC) analysis (Green and Swets, 1966). The ROC value indicates the probability that an ideal observer could discriminate the location of the visual stimulus based solely on the EMG activity at that given time point. A value of 0.5 represents chance, while a value of 1 or 0 represents perfect correct or incorrect discrimination the two trial types. During anti-saccade trials

(**Figure 1.12b**), the ROC value increases to greater than 0.7 at the time of the SLR (i.e. reliably discriminating the visual stimulus location) and then drops towards 0 when the later saccade-related activity occurs (i.e. reliably discriminating the motor direction). Like the visual responses in SCi (Everling et al., 1999), the SLR magnitude attenuated during correct anti-saccade trials (Chapman and Corneil, 2014). These results suggest that the onset of a novel visual stimulus can evoke a reflexive motor command mediated through a tecto-reticulospinal pathway even in a static posture.

The initial reflexive EMG activity on neck muscle towards the visual stimulus during the pro-/anti-saccade task is reminiscent of the 'automatic' response during the pro-/anti-reach corrective response task (Day and Lyon, 2000, **Figure 1.8c**). Could the descending reticulospinal pathway that mediate the neck SLRs also mediate online corrective response? The reticulospinal pathway is also one of the primary descending motor pathways that contribute to reaching movements (Alstermark and Isa, 2012). The other main pathways, the corticospinal pathway (**Figure 1.11**, blue traces), originating from primarily from both M1 and somatosensory cortex (S1), and the rubrospinal pathway (red traces), originating from the magnocellular red nucleus, project almost exclusively onto the contralateral spinal cord. Unlike the reticulospinal pathway, disruption of either the corticospinal or rubrospinal pathways largely disrupted only fine fractionated finger movements (Lawrence and Kuypers, 1968a, 1968b).

1.5.3 Reticular formation contribution to reach control

Based on the original observation of Lawrence and Kuypers (1968a), the reticulospinal pathway is known to play a vital role in both postural control and general orienting movements. The reticular formation receives projections from both M1 and PMd (Kuypers and Lawrence, 1967; Keizer and Kuypers, 1984, 1989; Kably and Drew, 1998). Electrical stimulation within the reticular formation in cats and NHPs evokes short-latency changes in EMG activity across different neck and limb muscles (Drew and Rossignol, 1990a, 1990b; Davidson et al., 2007). Further, the pattern of EMG activity changes based on the phase of locomotion in cats (Drew, 1991), suggesting an integration of the descending motor command with the local spinal inputs. Neurophysiological studies have also suggested that distinct sub-populations of neurons within the reticular formation control for postural and reaching movements (Schepens and Drew, 2004; Schepens et al., 2008). And like cortical areas, these neurons show both preparatory and reach-related activity during upper limb reach movements in both cats (Schepens and Drew, 2006) and primates (Buford and Davidson, 2004). These results all support the notion that the reticulospinal pathway plays a vital role in reach control. However, the role of reticular formation in more complex reaching tasks has not been well studied.

1.6 The role of SCi in reach control

Even though the SCi is generally thought of as a gaze control region, there is evidence for its involvement in reach control. Previous studies have reported reach-related neurons within the SCi (Werner, 1993). These reach-related neurons were intermixed with the canonical oculomotor neurons within the SCi (Werner et al., 1997b). Further, a subset of these reach-related neurons could also be modulated by either a visual stimulus and/or saccadic eye movement (Werner et al., 1997b; Stuphorn et al., 2000) and electrical microstimulation at sites where these reach-related neurons are found evokes saccadic eye movements. These reach-related neurons preferred reach movements with the contralateral arm, although some also did fire during ipsilateral arm movements (Werner et al., 1997a). Consistent with the notion that SCi generating motor commands and receiving efference copies of the change in limb position, these reach-related responses also predictively discharged prior to the onset of upper limb muscle activity (Stuphorn et al., 1999) and low intensity electrical microstimulation ($< 50 \mu\text{A}$) can evoke both contralateral and ipsilateral arm movements in both NHPs (Philipp and Hoffmann, 2014) and cats (Courjon et al., 2004). These reach-related results within the SCi have also been replicated in human imaging experiments, where there is an increase in BOLD activity in SCi during contralateral reach movements (Linzenbold and Himmelbach, 2012).

While reach-related neurons were first observed in the early 90's (Werner, 1993) and it is known that SCi receives corticotectal inputs from multiple different

motor cortices (Fries, 1984, 1985; Distler and Hoffmann, 2015), the role of SCi in the context of reach control has not been well studied. A previous neurophysiological study using the reference frame task has shown that two distinct population of reached-related neurons exist within the SCi and the underlying reticular formation (Stuphorn et al., 2000). There is a group of gaze-dependent, i.e. eye-centric reference frame, reach-related neurons that is located at similar depth (~2 mm from the SC surface) as saccadic-related neurons presumably located within the SCi. A second group of gaze-independent neurons, i.e. hand-centric reference frame, is located below the gaze-dependent neurons (~4 mm) presumably in both the deeper layers of SCi and the underlying reticular formation.

More recently, a pair of studies have examined the role SCi during target selection for reaching movements. Song and McPeck (2015) used a pop-out task in which four stimuli appeared concurrently with one stimulus (i.e. target) having a different isoluminant colour than the other three stimuli (i.e. distractors). NHPs maintained fixation throughout the trial and had to reach towards the target stimulus location without making any eye movements. They found neurons within the SCi had greater sustained activity when the target was in its receptive field compared to distractor. Some of the neurons were also selectively activated during reach trials but not during a delay saccade task, suggesting that these neurons are reach-specific. However, unlike the reach-related neurons mentioned earlier these reach selective neurons did not show a burst of activity with the onset of the reach

movement. Further, inactivation of SCi caused a reach selection deficit into the corresponding receptive field (Song et al., 2011). Despite the deficit in reach selection, the animals' reach velocity and endpoint error did not change during inactivation. However, they did not examine the role of the SCi during online corrective responses.

1.6.1 Stimulus-locked visual responses on the human upper limb muscles

As mentioned earlier, a portion of the reach-related neurons also display visual-related activity (Werner et al., 1997b; Stuphorn et al., 2000) and visuomotor activity can be detected on neck muscles (Corneil et al., 2004; Goonetilleke et al., 2015). Can these visual-related responses from the SCi also be detected on upper limb muscles? Two previous studies have shown SLRs on human upper limb muscles prior to visually-guided reach movements from a static posture (Pruszynski et al., 2010; Wood et al., 2015). **Figure 1.13** shows an example of the SLR on the right pectoralis major (PEC) muscle from a representative participant (Wood et al., 2015). This participant performed intermixed visually-guided (**Figure 1.13b**) and delayed (**Figure 1.13c**) leftward (filled) and rightward (opened) reach trials. There is an increase and decrease in right PEC muscle recruitment associated with the initiation of leftward and rightward reach movement (~200 ms after stimulus onset in **Figure 1.13b**). However, prior to this volitional recruitment, a SLR can be detected within ~100 ms after the stimulus onset for both visually-guided and

delayed trials. The recruitment profile of the SLR mirrors that of the later ‘volitional’ response, with an increase and decrease responses for leftward and rightward stimulus locations, respectively.

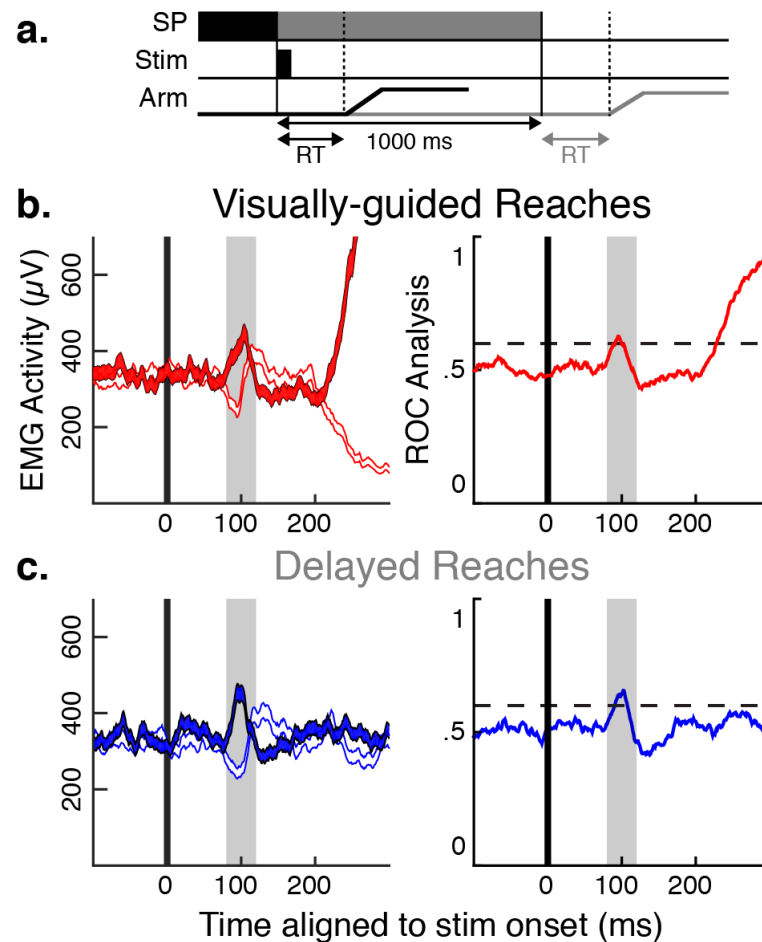


Figure 1.13: SLR on a human upper limb muscle prior to reach movements

(a) Task paradigm. Participants performed intermixed leftward and rightward visually-guided (black) and delayed reach trials (gray). (b) Right PEC muscle activity during leftward (filled) and rightward (opened) visually-guided reach trials. The shaded panel indicates the SLR that occurred ~ 100 ms after stimulus onset. Right panel shows the corresponding time-series ROC analysis. (c) Same layout as (b), but for delayed reaches. Note that the SLRs persist even when the ensuing reach movements are withheld for at least 1 sec. Data from Wood and colleagues, 2015.

1.7 Thesis motivation and objectives

The two previous studies of the SLRs on the human upper limbs have speculated that a common rapid visuomotor system generates both the SLRs and rapid corrective responses via the SCi. If true, this would allow for an alternative method to study the underlying neural substrates of the corrective reach responses. One advantage of examining these SLRs, rather than corrective responses, is the ability to temporally dissociate the SLR from muscle recruitment arising from volitional control. Another advantage is the fact that the SLR can be evoked from a static posture, thus allowing for a direct comparison with the known sensorimotor properties of volitional control from previous neurophysiological studies.

The hypothesis of my thesis is that the SLR on the human upper limb muscles is mediated by the same neural substrates as online corrective responses. Thus, within this thesis, I compared the sensorimotor properties of SLRs on upper limb muscles with the known properties of the corrective responses. To do this, I used the same theoretical framework that I have laid out for 'volitional' control.

Figure 1.14 shows the three main objectives of thesis.

1.7.1 SLR a visual or preparatory motor command?

Wood and colleagues (2015) demonstrated that the SLR persisted even when the ensuing volitional reach movement is temporarily withheld. While Wood and colleagues suggested that the upper limb SLR is a visual-related response that

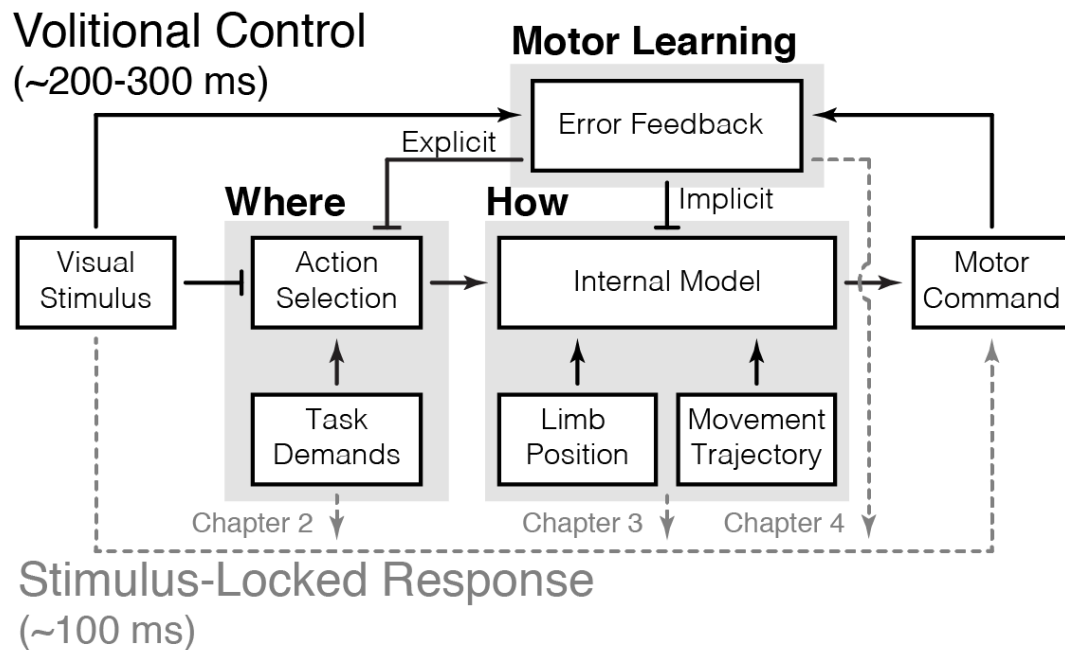


Figure 1.14: Objectives of this thesis

In Chapter 2, I will quantify the ‘**where**’ component by altering the task demand (i.e. pro-/anti-reach task). In Chapter 3, I will quantify the ‘**how**’ component by changing the participant’s initial limb position (i.e. reference frame task) and movement trajectory (i.e. obstacle task). Finally in Chapter 4, I will quantify the ‘**motor learning**’ component by systematically change the sensorimotor mapping (i.e. visuomotor rotation task).

leaks out to the periphery, an alternative explanation is that the SLR is a preparatory goal-oriented motor response. **Chapter 2** examines if the SLR on upper limb muscles is either a visual or a preparatory response. To do this, I have participants perform a pro-/anti-reach task into and out of the preferred direction of the SLR. This distinction is vital as previous studies have shown that the SCi (Everling et al., 1999; Edelman and Goldberg, 2001), neck muscle SLRs (Chapman and Corneil, 2011, 2014), and corrective responses (Day and Lyon, 2000) all reflexively encoded the visual stimulus location regardless of the ensuing goal-direct motor response. Thus, if the same pathway mediates the SLR on the

upper limb muscles, then the SLR should still encode the stimulus location during anti-reach trials.

1.7.2 The reference frame of the SLR

As mentioned earlier, corrective responses integrated the visual and underlying hand trajectory to generate the appropriate hand-centric motor command towards the shifted visual stimulus location. **Chapter 3** comprises of three different experiments to test if the pathway mediating the SLR can also perform this visual-to-motor transformation. In the first experiment, I use the reference frame task (**Figure 1.6**) to examine the underlying reference frame of the SLR. In the second and third experiments, I examine if the pathway mediating the SLR can account for the pre-planned reach trajectory. To do this, I have participants making different movement trajectories to the same visual stimulus location. Based on my hypothesis, I predict that like online corrective response the SLR will also encode a hand-centric motor command that also accounts for the pre-planned reach trajectory.

1.7.3 The influence of implicit and explicit components motor learning on the SLR

Finally, **Chapter 4** examines whether the SLR is altered by motor learning. Pruszynski and colleagues (2010) showed that similar to neurons within motor

cortices (**Figure 1.3**), the directional tuning of the SLR can also be quantified with a sinusoidal fit. I quantify the shift in the PD of the SLR during three different variations of the motor rotation tasks (**Figure 1.2a**). Because motor learning is thought to be comprised of two distinct motor learning components, I try to dissociate the role of implicit and explicit motor learning on the SLR. The first experiment employs an abrupt visuomotor rotation that has been shown to engage in both implicit and explicit motor learning (Taylor et al., 2014; Bond and Taylor, 2015). The second experiment minimizes the explicit aiming strategy by using a gradual visuomotor rotation task, where the participants are not consciously aware of a change in the underlying sensorimotor mapping (Galea et al., 2010; Honda et al., 2012). The third and final experiment uses a mental visuomotor rotation task (Mazzoni and Krakauer, 2006). This task eliminates implicit motor learning and purely relies on participants to change their explicit aiming strategy. If like corrective reach responses, the PD of the SLR will systematically change during at least one of these three motor learning experiments.

1.8 References

- Alstermark B, Isa T (2012) Circuits for skilled reaching and grasping. *Annu Rev Neurosci* 35:559–578.
- Andersen RA, Andersen KN, Hwang EJ, Hauschild M (2014) Optic ataxia: from Balint's syndrome to the parietal reach region. *Neuron* 81:967–983.

- Archambault PS, Caminiti R, Battaglia-Mayer A (2009) Cortical mechanisms for online control of hand movement trajectory: The role of the posterior parietal cortex. *Cereb Cortex* 19:2848–2864.
- Archambault PS, Ferrari-Toniolo S, Battaglia-Mayer A (2011) Online Control of Hand Trajectory and Evolution of Motor Intention in the Parietofrontal System. *J Neurosci* 31:742–752.
- Batista AP, Buneo CA, Snyder LH, Andersen RA (1999) Reach plans in eye-centered coordinates. *Science* 285:257–260.
- Batista AP, Santhanam G, Yu BM, Ryu SI, Afshar A, Shenoy K V (2007) Reference frames for reach planning in macaque dorsal premotor cortex. *J Neurophysiol* 98:966–983.
- Battaglia-Mayer A, Ferrari-Toniolo S, Visco-Comandini F, Archambault PS, Saberi-Moghadam S, Caminiti R (2013) Impairment of online control of hand and eye movements in a monkey model of optic ataxia. *Cereb Cortex* 23:2644–2656.
- Bond KM, Taylor JA (2015) Flexible explicit but rigid implicit learning in a visuomotor adaptation task. *J Neurophysiol* 113:3836–3849.
- Buford JA, Davidson AG (2004) Movement-related and preparatory activity in the reticulospinal system of the monkey. *Exp Brain Res* 159:284–300.
- Buneo CA, Jarvis MR, Batista AP, Andersen RA (2002) Direct visuomotor transformations for reaching. *Nature* 416:632–636.
- Büttner U, Büttner-Ennever JA, Henn V (1977) Vertical eye movement related unit activity in the rostral mesencephalic reticular formation of the alert monkey. *Brain Res* 130:239–252.
- Carlton LG (1981) Processing visual feedback information for movement control. *J Exp Psychol Hum Percept Perform* 7:1019–1030.
- Chapman BB, Corneil BD (2011) Neuromuscular recruitment related to stimulus presentation and task instruction during the anti-saccade task. *Eur J Neurosci* 33:349–360.

- Chapman BB, Corneil BD (2014) Short-duration stimulation of the supplementary eye fields perturbs anti-saccade performance while potentiating contralateral head orienting. *Eur J Neurosci* 39:295–307.
- Chen C-Y, Sonnenberg L, Weller S, Witschel T, Hafed ZM (2018) Spatial frequency sensitivity in macaque midbrain. *Nat Commun* 9:2852.
- Churchland MM et al. (2010) Stimulus onset quenches neural variability: a widespread cortical phenomenon. *Nat Neurosci* 13:369–378.
- Churchland MM, Santhanam G, Shenoy K V (2006) Preparatory activity in premotor and motor cortex reflects the speed of the upcoming reach. *J Neurophysiol* 96:3130–3146.
- Cisek P (2007) Cortical mechanisms of action selection: the affordance competition hypothesis. *Philos Trans R Soc Lond B Biol Sci* 362:1585–1599.
- Cisek P, Kalaska JF (2005) Neural Correlates of Reaching Decisions in Dorsal Premotor Cortex: Specification of Multiple Direction Choices and Final Selection of Action. *Neuron* 45:801–814.
- Cohen YE, Andersen RA (2000) Reaches to sounds encoded in an eye-centered reference frame. *Neuron* 27:647–652.
- Connolly JD, Andersen RA, Goodale MA (2003) FMRI evidence for a “parietal reach region” in the human brain. *Exp Brain Res* 153:140–145.
- Corneil BD, Munoz DP (2014) Overt Responses during Covert Orienting. *Neuron* 82:1230–1243.
- Corneil BD, Olivier E, Munoz DP (2002) Neck muscle responses to stimulation of monkey superior colliculus. I. Topography and manipulation of stimulation parameters. *J Neurophysiol* 88:1980–1999.
- Corneil BD, Olivier E, Munoz DP (2004) Visual responses on neck muscles reveal selective gating that prevents express saccades. *Neuron* 42:831–841.
- Courjon JH, Olivier E, Pelisson D (2004) Direct evidence for the contribution of the superior colliculus in the control of visually guided reaching movements in the cat. *J Physiol* 556:675–681.

- Davidson AG, Schieber MH, Buford JA (2007) Bilateral spike-triggered average effects in arm and shoulder muscles from the monkey pontomedullary reticular formation. *J Neurosci* 27:8053–8058.
- Day BL (2014) Subcortical visuomotor control of human limb movement. *Adv Exp Med Biol* 826:55–68.
- Day BL, Brown P (2001) Evidence for subcortical involvement in the visual control of human reaching. *Brain* 124:1832–1840.
- Day BL, Lyon IN (2000) Voluntary modification of automatic arm movements evoked by motion of a visual target. *Exp Brain Res* 130:159–168.
- Desmurget M, Epstein CM, Turner RS, Prablanc C, Alexander GE, Grafton ST (1999) Role of the posterior parietal cortex in updating reaching movements to a visual target. *Nat Neurosci* 2:563–567.
- Diedrichsen J, Nambisan R, Kennerley SW, Ivry RB (2004) Independent on-line control of the two hands during bimanual reaching. *Eur J Neurosci* 19:1643–1652.
- Distler C, Hoffmann K-P (2015) Direct projections from the dorsal premotor cortex to the superior colliculus in the macaque (*macaca mulatta*). *J Comp Neurol* 523:2390–2408.
- Donders FC (1969) On the speed of mental processes. *Acta Psychol (Amst)* 30:412–431.
- Dorris MC, Paré M, Munoz DP (1997) Neuronal activity in monkey superior colliculus related to the initiation of saccadic eye movements. *J Neurosci* 17:8566–8579.
- Drew T (1991) Functional organization within the medullary reticular formation of the intact unanesthetized cat. III. Microstimulation during locomotion. *J Neurophysiol* 66.
- Drew T, Rossignol S (1990a) Functional organization within the medullary reticular formation of intact unanesthetized cat. II. Electromyographic activity evoked by microstimulation. *J Neurophysiol* 64:782–795.

- Drew T, Rossignol S (1990b) Functional organization within the medullary reticular formation of intact unanesthetized cat. I. Movements evoked by microstimulation. *J Neurophysiol* 64:767–781.
- Edelman JA, Goldberg ME (2001) Dependence of saccade-related activity in the primate superior colliculus on visual target presence. *J Neurophysiol* 86:676–691.
- Edelman JA, Keller EL (1996) Activity of visuomotor burst neurons in the superior colliculus accompanying express saccades. *J Neurophysiol* 76:908–926.
- Everling S, Dorris MC, Klein RM, Munoz DP (1999) Role of primate superior colliculus in preparation and execution of anti-saccades and pro-saccades. *J Neurosci* 19:2740–2754.
- Everling S, Dorris MC, Munoz DP (1998) Reflex suppression in the anti-saccade task is dependent on prestimulus neural processes. *J Neurophysiol* 80:1584–1589.
- Fabbri S, Caramazza A, Lingnau A (2010) Tuning Curves for Movement Direction in the Human Visuomotor System. *J Neurosci* 30:13488–13498.
- Fautrelle L, Prablanc C, Berret B, Ballay Y, Bonnetblanc F (2010) Pointing to double-step visual stimuli from a standing position: very short latency (express) corrections are observed in upper and lower limbs and may not require cortical involvement. *Neuroscience* 169:697–705.
- Fecteau JH, Munoz DP (2005) Correlates of capture of attention and inhibition of return across stages of visual processing. *J Cogn Neurosci* 17:1714–1727.
- Ferrier D (1874) Experiments on the Brain of Monkeys. *Proc R Soc Lond* 23:409–432.
- Fischer B, Boch R (1983) Saccadic eye movements after extremely short reaction times in the monkey. *Brain Res* 260:21–26.
- Fischer B, Ramsperger E (1984) Human express saccades: extremely short reaction times of goal directed eye movements. *Exp Brain Res* 57:191–195.

- Flash T, Hogan N (1985) The coordination of arm movements: an experimentally confirmed mathematical model. *J Neurosci* 5:1688–1703.
- Franklin DW, Reichenbach A, Franklin S, Diedrichsen J (2016) Temporal Evolution of Spatial Computations for Visuomotor Control. *J Neurosci* 36:2329–2341.
- Franklin DW, Wolpert DM (2008) Specificity of reflex adaptation for task-relevant variability. *J Neurosci* 28:14165–14175.
- Franklin S, Wolpert DM, Franklin DW (2012) Visuomotor feedback gains upregulate during the learning of novel dynamics. *J Neurophysiol* 108:467–478.
- Freedman EG, Sparks DL (1997) Eye-head coordination during head-unrestrained gaze shifts in rhesus monkeys. *J Neurophysiol* 77:2328–2348.
- Freedman EG, Stanford TR, Sparks DL (1996) Combined eye-head gaze shifts produced by electrical stimulation of the superior colliculus in rhesus monkeys. *J Neurophysiol* 76:927–952.
- Fries W (1984) Cortical projections to the superior colliculus in the macaque monkey: a retrograde study using horseradish peroxidase. *J Comp Neurol* 230:55–76.
- Fries W (1985) Inputs from motor and premotor cortex to the superior colliculus of the macaque monkey. *Behav Brain Sci*.
- Gail A, Andersen RA (2006) Neural dynamics in monkey parietal reach region reflect context-specific sensorimotor transformations. *J Neurosci* 26:9376–9384.
- Gail A, Klaes C, Westendorff S (2009) Implementation of spatial transformation rules for goal-directed reaching via gain modulation in monkey parietal and premotor cortex. *J Neurosci* 29:9490–9499.
- Galea JM, Sami SA, Albert NB, Miall RC (2010) Secondary tasks impair adaptation to step- and gradual-visual displacements. *Exp Brain Res* 202:473–484.
- Gandhi NJ, Katnani HA (2011) Motor functions of the superior colliculus. *Annu Rev Neurosci* 34:205–231.

- Gandolfo F, Li C-SR, Benda BJ, Schioppa CP, Bizzi E (2000) Cortical correlates of learning in monkeys adapting to a new dynamical environment. *Proc Natl Acad Sci* 97:2259–2263.
- Georgopoulos AP (1988) Spatial coding of visually guided arm movements in primate motor cortex. *Can J Physiol Pharmacol* 66:518–526.
- Georgopoulos AP, Kalaska JF, Caminiti R, Massey JT (1982) On the relations between the direction of two-dimensional arm movements and cell discharge in primate motor cortex. *J Neurosci* 2:1527–1537.
- Goldberg ME, Wurtz RH (1972a) Activity of superior colliculus in behaving monkey. I. Visual receptive fields of single neurons. *J Neurophysiol* 35:542–559.
- Goldberg ME, Wurtz RH (1972b) Activity of superior colliculus in behaving monkey. II. Effect of attention on neuronal responses. *J Neurophysiol* 35:560–574.
- Goodale MA, Pelisson D, Prablanc C (1986) Large adjustments in visually guided reaching do not depend on vision of the hand or perception of target displacement. *Nature* 320:748–750.
- Goonetilleke SC, Katz L, Wood DK, Gu C, Huk AC, Corneil BD (2015) Cross-species comparison of anticipatory and stimulus-driven neck muscle activity well before saccadic gaze shifts in humans and nonhuman primates. *J Neurophysiol* 114:902–913.
- Gréa H, Pisella L, Rossetti Y, Desmurget M, Tilikete C, Grafton S, Prablanc C, Vighetto A (2002) A lesion of the posterior parietal cortex disrupts on-line adjustments during aiming movements. *Neuropsychologia* 40:2471–2480.
- Green DM, Swets JA (1966) *Signal detection theory and psychophysics*. Oxford England: John Wiley.
- Gribble PL, Scott SH (2002) Overlap of internal models in motor cortex for mechanical loads during reaching. *Nature* 417:938–941.
- Guitton D, Volle M (1987) Gaze control in humans: eye-head coordination during orienting movements to targets within and beyond the oculomotor range. *J Neurophysiol* 58:427–459.

- Haar S, Donchin O, Dinstein I (2015) Dissociating visual and motor directional selectivity using visuomotor adaptation. *J Neurosci* 35:6813–6821.
- Hafed ZM, Chen C-Y (2016) Sharper, Stronger, Faster Upper Visual Field Representation in Primate Superior Colliculus. *Curr Biol* 26:1647–1658.
- Haith AM, Huberdeau DM, Krakauer JW (2015) The Influence of Movement Preparation Time on the Expression of Visuomotor Learning and Savings. *J Neurosci* 35:5109–5117.
- Hallett PE (1978) Primary and secondary saccades to goals defined by instructions. *Vision Res* 18:1279–1296.
- Hayashi T, Yokoi A, Hirashima M, Nozaki D (2016) Visuomotor Map Determines How Visually Guided Reaching Movements are Corrected Within and Across Trials. *eNeuro* 3.
- Hayhoe MM (2017) Vision and Action. *Annu Rev Vis Sci* 3:389–413.
- Herzfeld DJ, Kojima Y, Soetedjo R, Shadmehr R (2015) Encoding of action by the Purkinje cells of the cerebellum. *Nature* 526:439–442.
- Herzfeld DJ, Vaswani PA, Marko MK, Shadmehr R (2014) A memory of errors in sensorimotor learning. *Science* 345:1349–1353.
- Hocherman S, Wise SP (1990) Trajectory-selective neuronal activity in the motor cortex of rhesus monkeys (*Macaca mulatta*). *Behav Neurosci* 104:495–499.
- Hocherman S, Wise SP (1991) Effects of hand movement path on motor cortical activity in awake, behaving rhesus monkeys. *Exp Brain Res* 83:285–302.
- Honda T, Hirashima M, Nozaki D (2012) Adaptation to visual feedback delay influences visuomotor learning. *PLoS One* 7:e37900.
- Hubel DH, LeVay S, Wiesel TN (1975) Mode of termination of retinotectal fibers in macaque monkey: An autoradiographic study. *Brain Res* 96:25–40.
- Huberdeau DM, Haith AM, Krakauer JW (2015a) Formation of a long-term memory for visuomotor adaptation following only a few trials of practice. *J Neurophysiol* 114:969–977.

- Huberdeau DM, Krakauer JW, Haith AM (2015b) Dual-process decomposition in human sensorimotor adaptation. *Curr Opin Neurobiol* 33:71–77.
- Ignashchenkova A, Dicke PW, Haarmeier T, Thier P (2004) Neuron-specific contribution of the superior colliculus to overt and covert shifts of attention. *Nat Neurosci* 7:56–64.
- Izawa J, Criscimagna-Hemminger SE, Shadmehr R (2012) Cerebellar contributions to reach adaptation and learning sensory consequences of action. *J Neurosci* 32:4230–4239.
- Kably B, Drew T (1998) Corticoreticular pathways in the cat. I. Projection patterns and collaterization. *J Neurophysiol* 80:389–405.
- Kalaska JF, Cohen D a, Hyde ML, Prud'homme M (1989) A comparison of movement direction-related versus load direction-related activity in primate motor cortex, using a two-dimensional reaching task. *J Neurosci* 9:2080–2102.
- Katyal S, Ress D (2014) Endogenous Attention Signals Evoked by Threshold Contrast Detection in Human Superior Colliculus. *J Neurosci* 34:892–900.
- Kaufman MT, Churchland MM, Ryu SI, Shenoy K V (2014) Cortical activity in the null space: permitting preparation without movement. *Nat Neurosci* 17:440–448.
- Kawato M (1999) Internal models for motor control and trajectory planning. *Curr Opin Neurobiol* 9:718–727.
- Keizer K, Kuypers HG (1984) Distribution of corticospinal neurons with collaterals to lower brain stem reticular formation in cat. *Exp Brain Res* 54:107–120.
- Keizer K, Kuypers HG (1989) Distribution of corticospinal neurons with collaterals to the lower brain stem reticular formation in monkey (*Macaca fascicularis*). *Exp Brain Res* 74:311–318.
- Klaes C, Westendorff S, Chakrabarti S, Gail A (2011) Choosing Goals, Not Rules: Deciding among Rule-Based Action Plans. *Neuron* 70:536–548.

- Krakauer JW (2009) Motor learning and consolidation: the case of visuomotor rotation. *Adv Exp Med Biol* 629:405–421.
- Krauzlis RJ, Lovejoy LP, Zénon A (2013) Superior colliculus and visual spatial attention. *Annu Rev Neurosci* 36:165–182.
- Kuypers HG, Lawrence DG (1967) Cortical projections to the red nucleus and the brain stem in the Rhesus monkey. *Brain Res* 4:151–188.
- Kwan HC, MacKay WA, Murphy JT, Wong YC (1981) Distribution of responses to visual cues for movement in precentral cortex of awake primates. *Neurosci Lett* 24:123–128.
- Kwan HC, MacKay WA, Murphy JT, Wong YC (1985) Properties of visual cue responses in primate precentral cortex. *Brain Res* 343:24–35.
- Lawrence DG, Kuypers HG (1968a) The functional organization of the motor system in the monkey. II. The effects of lesions of the descending brain-stem pathways. *Brain* 91:15–36.
- Lawrence DG, Kuypers HG (1968b) The functional organization of the motor system in the monkey. I. The effects of bilateral pyramidal lesions. *Brain* 91:1–14.
- Linzenbold W, Himmelbach M (2012) Signals from the deep: reach-related activity in the human superior colliculus. *J Neurosci* 32:13881–13888.
- Luce RD (1986) *Their Role in Inferring Elementary Mental Organization*. New York: Oxford University Press.
- Luschei ES, Fuchs AF (1972) Activity of brain stem neurons during eye movements of alert monkeys. *J Neurophysiol* 35:445–461.
- Marino RA, Levy R, Boehnke SE, White BJ, Itti L, Munoz DP (2012) Linking visual response properties in the superior colliculus to saccade behavior. *Eur J Neurosci* 35:1738–1752.
- Marino RA, Levy R, Munoz DP (2015) Linking express saccade occurrence to stimulus properties and sensorimotor integration in the superior colliculus. *J Neurophysiol* 114:879–892.

- Martin TA, Keating JG, Goodkin HP, Bastian AJ, Thach WT (1996) Throwing while looking through prisms. I. Focal olivocerebellar lesions impair adaptation. *Brain* 119 (Pt 4:1183–1198.
- May PJ (2006) The mammalian superior colliculus: laminar structure and connections. *Prog Brain Res* 151:321–378.
- Mazzoni P, Krakauer JW (2006) An implicit plan overrides an explicit strategy during visuomotor adaptation. *J Neurosci* 26:3642–3645.
- McDougle SD, Bond KM, Taylor JA (2015) Explicit and Implicit Processes Constitute the Fast and Slow Processes of Sensorimotor Learning. *J Neurosci* 35:9568–9579.
- Medendorp WP, Goltz HC, Vilis T, Crawford JD (2003) Gaze-centered updating of visual space in human parietal cortex. *J Neurosci* 23:6209–6214.
- Miall RC, Weir DJ, Wolpert DM, Stein JF (1993) Is the Cerebellum a Smith Predictor? *J Mot Behav* 25:203–216.
- Morehead JR, Taylor JA, Parvin D, Ivry RB (2017) Characteristics of Implicit Sensorimotor Adaptation Revealed by Task-irrelevant Clamped Feedback. *J Cogn Neurosci* 25:1–14.
- Munoz DP, Everling S (2004) Look away: the anti-saccade task and the voluntary control of eye movement. *Nat Rev Neurosci* 5:218–228.
- Munoz DP, Waitzman DM, Wurtz RH (1996) Activity of neurons in monkey superior colliculus during interrupted saccades. *J Neurophysiol* 75:2562–2580.
- Munoz DP, Wurtz RH (1993a) Fixation cells in monkey superior colliculus. I. Characteristics of cell discharge. *J Neurophysiol* 70:559–575.
- Munoz DP, Wurtz RH (1993b) Fixation cells in monkey superior colliculus. II. Reversible activation and deactivation. *J Neurophysiol* 70:576–589.
- Munoz DP, Wurtz RH (1995) Saccade-related activity in monkey superior colliculus. I. Characteristics of burst and buildup cells. *J Neurophysiol* 73:2313–2333.
- Nathan PW, Smith M, Deacon P (1996) Vestibulospinal, reticulospinal and descending propriospinal nerve fibres in man. *Brain* 119 (Pt 6:1809–1833.

- Nudo RJ, Masterton RB (1989) Descending pathways to the spinal cord: II. Quantitative study of the tectospinal tract in 23 mammals. *J Comp Neurol* 286:96–119.
- Oostwoud Wijdenes L, Brenner E, Smeets JBJ (2011) Fast and fine-tuned corrections when the target of a hand movement is displaced. *Exp Brain Res* 214:453–462.
- Paré M, Munoz DP (1996) Saccadic reaction time in the monkey: advanced preparation of oculomotor programs is primarily responsible for express saccade occurrence. *J Neurophysiol* 76:3666–3681.
- Paz R, Boraud T, Natan C, Bergman H, Vaadia E (2003) Preparatory activity in motor cortex reflects learning of local visuomotor skills. *Nat Neurosci* 6:882–890.
- Perenin MT, Vighetto A (1988) Optic ataxia: a specific disruption in visuomotor mechanisms. I. Different aspects of the deficit in reaching for objects. *Brain* 111 (Pt 3:643–674.
- Perfiliev S, Isa T, Johnels B, Steg G, Wessberg J (2010) Reflexive limb selection and control of reach direction to moving targets in cats, monkeys, and humans. *J Neurophysiol* 104:2423–2432.
- Pesaran B, Nelson MJ, Andersen RA (2006) Dorsal premotor neurons encode the relative position of the hand, eye, and goal during reach planning. *Neuron* 51:125–134.
- Peterson BW (1979) Reticulospinal projections to spinal motor nuclei. *Annu Rev Physiol*.
- Philipp R, Hoffmann KP (2014) Arm movements induced by electrical microstimulation in the superior colliculus of the macaque monkey. *J Neurosci* 34:3350–3363.
- Pine ZM, Krakauer JW, Gordon J, Ghez C (1996) Learning of scaling factors and reference axes for reaching movements. *Neuroreport* 7:2357–2361.

- Pisella L, Gréa H, Tilikete C, Vighetto A, Desmurget M, Rode G, Boisson D, Rossetti Y (2000) An “automatic pilot” for the hand in human posterior parietal cortex: toward reinterpreting optic ataxia. *Nat Neurosci* 3:729–736.
- Pollack JG, Hickey TL (1979) The distribution of retino-collicular axon terminals in rhesus monkey. *J Comp Neurol* 185:587–602.
- Pruszynski JA, King GL, Boisse L, Scott SH, Flanagan JR, Munoz DP (2010) Stimulus-locked responses on human arm muscles reveal a rapid neural pathway linking visual input to arm motor output. *Eur J Neurosci* 32:1049–1057.
- Rezvani S, Corneil BD (2008) Recruitment of a head-turning synergy by low-frequency activity in the primate superior colliculus. *J Neurophysiol* 100:397–411.
- Robinson DA (1972) Eye movements evoked by collicular stimulation in the alert monkey. *Vision Res* 12:1795–1808.
- Roemmich RT et al. (2016) Seeing the Errors You Feel Enhances Locomotor Performance but Not Learning. *Curr Biol* 26:2707–2716.
- Rothwell JC (2006) The startle reflex, voluntary movement, and the reticulospinal tract. *Suppl Clin Neurophysiol* 58:223–231.
- Sasaki S, Shimazu H (1981) Reticulovestibular organization participating in generation of horizontal fast eye movement. *Ann N Y Acad Sci* 374:130–143.
- Savjani RR, Katyal S, Halfen E, Kim JH, Ress D (2018) Polar-angle representation of saccadic eye movements in human superior colliculus. *Neuroimage* 171:199–208.
- Schall JD (2003) Neural correlates of decision processes: neural and mental chronometry. *Curr Opin Neurobiol* 13:182–186.
- Schepens B, Drew T (2006) Descending signals from the pontomedullary reticular formation are bilateral, asymmetric, and gated during reaching movements in the cat. *J Neurophysiol* 96:2229–2252.

- Schepens B, Stapley P, Drew T (2008) Neurons in the pontomedullary reticular formation signal posture and movement both as an integrated behavior and independently. *J Neurophysiol* 100:2235–2253.
- Schepens BB, Drew T (2004) Independent and convergent signals from the pontomedullary reticular formation contribute to the control of posture and movement during reaching in the cat. *J Neurophysiol* 92:2217–2238.
- Schiller PH, Finlay BL, Volman SF (1976) Quantitative studies of single-cell properties in monkey striate cortex. II. Orientation specificity and ocular dominance. *J Neurophysiol* 39:1320–1333.
- Schiller PH, Malpeli JG, Schein SJ (1979) Composition of geniculostriate input to superior colliculus of the rhesus monkey. *J Neurophysiol* 42:1124–33.
- Schiller PH, Sandell JH, Maunsell JH (1987) The effect of frontal eye field and superior colliculus lesions on saccadic latencies in the rhesus monkey. *J Neurophysiol* 57:1033–1049.
- Schiller PH, Stryker M, Cynader M, Berman N (1974) Response characteristics of single cells in the monkey superior colliculus following ablation or cooling of visual cortex. *J Neurophysiol* 37:181–94.
- Scott SH (2003) The role of primary motor cortex in goal-directed movements: insights from neurophysiological studies on non-human primates. *Curr Opin Neurobiol* 13:671–677.
- Scott SH (2008) Inconvenient truths about neural processing in primary motor cortex. *J Physiol* 586:1217–1224.
- Scott SH, Kalaska JF (1995) Changes in motor cortex activity during reaching movements with similar hand paths but different arm postures. *J Neurophysiol* 73:2563–2567.
- Scott SH, Kalaska JF (1997) Reaching movements with similar hand paths but different arm orientations. I. Activity of individual cells in motor cortex. *J Neurophysiol* 77:826–852.

- Scott SH, Sergio LE, Kalaska JF (1997) Reaching movements with similar hand paths but different arm orientations. II. Activity of individual cells in dorsal premotor cortex and parietal area 5. *J Neurophysiol* 78:2413–2426.
- Shadmehr R, Krakauer JW (2008) A computational neuroanatomy for motor control. *Exp Brain Res* 185:359–381.
- Shadmehr R, Mussa-Ivaldi FA (1994) Adaptive representation of dynamics during learning of a motor task. *J Neurosci* 14:3208–3224.
- Shen L, Alexander GE (1997a) Neural correlates of a spatial sensory-to-motor transformation in primary motor cortex. *J Neurophysiol* 77:1171–1194.
- Shen L, Alexander GE (1997b) Preferential representation of instructed target location versus limb trajectory in dorsal premotor area. *J Neurophysiol* 77:1195–1212.
- Shenoy K V, Sahani M, Churchland MM (2013) Cortical Control of Arm Movements: A Dynamical Systems Perspective. *Annu Rev Neurosci* 36:337–359.
- Smith MA, Shadmehr R (2005) Intact Ability to Learn Internal Models of Arm Dynamics in Huntington's Disease But Not Cerebellar Degeneration. *J Neurophysiol* 93:2809–2821.
- Snyder LH, Batista AP, Andersen RA (1998) Change in motor plan, without a change in the spatial locus of attention, modulates activity in posterior parietal cortex. *J Neurophysiol* 79:2814–2819.
- Snyder LH, Batista AP, Andersen RA (2000) Saccade-related activity in the parietal reach region. *J Neurophysiol* 83:1099–1102.
- Soechting JF, Lacquaniti F (1983) Modification of trajectory of a pointing movement in response to a change in target location. *J Neurophysiol* 49:548–564.
- Song J-HH, McPeck RM (2015) Neural correlates of target selection for reaching movements in superior colliculus. *J Neurophysiol* 113:1414–1422.

- Song J-HH, Rafal RD, McPeck RM (2011) Deficits in reach target selection during inactivation of the midbrain superior colliculus. *Proc Natl Acad Sci* 108:E1433-40.
- Sparks D, Rohrer WH, Zhang Y (2000) The role of the superior colliculus in saccade initiation: A study of express saccades and the gap effect. *Vision Res* 40:2763–2777.
- Sparks DL, Mays LE (1990) Signal Transformations Required for the Generation of Saccadic Eye Movements. *Annu Rev Neurosci* 13:309–336.
- Stahl JS (1999) Amplitude of human head movements associated with horizontal saccades. *Exp Brain Res* 126:41–54.
- Stanford TR, Freedman EG, Sparks DL (1996) Site and parameters of microstimulation: evidence for independent effects on the properties of saccades evoked from the primate superior colliculus. *J Neurophysiol* 76:3360–3381.
- Steenrod SC, Phillips MH, Goldberg ME (2013) The lateral intraparietal area codes the location of saccade targets and not the dimension of the saccades that will be made to acquire them. *J Neurophysiol* 109:2596–2605.
- Stryker MP, Schiller PH (1975) Eye and head movements evoked by electrical stimulation of monkey superior colliculus. *Exp Brain Res* 23:103–112.
- Stuphorn V, Bauswein E, Hoffmann KP (2000) Neurons in the primate superior colliculus coding for arm movements in gaze-related coordinates. *J Neurophysiol* 83:1283–1299.
- Stuphorn V, Hoffmann KP, Miller LE (1999) Correlation of primate superior colliculus and reticular formation discharge with proximal limb muscle activity. *J Neurophysiol* 81:1978–1982.
- Taira M, Mine S, Georgopoulos AP, Murata A, Sakata H (1990) Parietal cortex neurons of the monkey related to the visual guidance of hand movement. *Exp Brain Res* 83:29–36.
- Taylor JA, Klemfuss NM, Ivry RB (2010) An explicit strategy prevails when the cerebellum fails to compute movement errors. *The Cerebellum* 9:580–586.

- Taylor JA, Krakauer JW, Ivry RB (2014) Explicit and implicit contributions to learning in a sensorimotor adaptation task. *J Neurosci* 34:3023–3032.
- Telgen S, Parvin D, Diedrichsen J (2014) Mirror reversal and visual rotation are learned and consolidated via separate mechanisms: recalibrating or learning de novo? *J Neurosci* 34:13768–13779.
- Torres EB, Quiñan Quiroga R, Cui H, Buneo CA (2013) Neural correlates of learning and trajectory planning in the posterior parietal cortex. *Front Integr Neurosci* 7:39.
- van Beers RJ (2009) Motor learning is optimally tuned to the properties of motor noise. *Neuron* 63:406–417.
- Weinrich M, Wise SP (1982) The premotor cortex of the monkey. *J Neurosci* 2:1329–1345.
- Welford AT (1980) Choice reaction time: basis concepts. In: *Reaction times* (Welford AT, ed), pp 73–128. New York, NY: Academic Press.
- Werner W (1993) Neurons in the primate superior colliculus are active before and during arm movements to visual targets. *Eur J Neurosci* 5:335–340.
- Werner W, Dannenberg S, Hoffmann KP (1997a) Arm-movement-related neurons in the primate superior colliculus and underlying reticular formation: comparison of neuronal activity with EMGs of muscles of the shoulder, arm and trunk during reaching. *Exp Brain Res* 115:191–205.
- Werner W, Hoffmann KP, Dannenberg S (1997b) Anatomical distribution of arm-movement-related neurons in the primate superior colliculus and underlying reticular formation in comparison with visual and saccadic cells. *Exp Brain Res* 115:206–216.
- Westendorff S, Klaes C, Gail A (2010) The cortical timeline for deciding on reach motor goals. *J Neurosci* 30:5426–5436.
- Wilson ME, Toyne MJ (1970) Retino-tectal and cortico-tectal projections in *Macaca mulatta*. *Brain Res* 24:395–406.

- Wise SP, Moody SL, Blomstrom KJ, Mitz AR (1998) Changes in motor cortical activity during visuomotor adaptation. *Exp Brain Res* 121:285–299.
- Wolpert DM, Goodbody SJ, Husain M (1998a) Maintaining internal representations: the role of the human superior parietal lobe. *Nat Neurosci* 1:529–533.
- Wolpert DM, Kawato M (1998) Multiple paried forward and inverse models for motor control. *Neural Networks* 11:1317–1329.
- Wolpert DM, Miall RC (1996) Forward Models for Physiological Motor Control. *Neural Netw* 9:1265–1279.
- Wolpert DM, Miall RC, Kawato M (1998b) Internal models in the cerebellum. *Trends Cogn Sci* 2:338–347.
- Wong AL, Haith AM, Krakauer JW (2015) Motor Planning. *Neurosci* 21:385–398.
- Wood DK, Gu C, Corneil BD, Gribble PL, Goodale MA (2015) Transient visual responses reset the phase of low-frequency oscillations in the skeletomotor periphery. *Eur J Neurosci* 42:1919–1932.
- Wurtz RH, Albano JE (1980) Visual-motor function of the primate superior colliculus. *Annu Rev Neurosci* 3:189–226.
- Wurtz RH, Goldberg ME (1972) Activity of superior colliculus in behaving monkey. III. Cells discharging before eye movements. *J Neurophysiol* 35:575–586.
- Zangemeister WH, Stark L (1982) Gaze latency: Variable interactions of head and eye latency. *Exp Neurol* 75:389–406.

Chapter 2 – A Trial-by-Trial Window into Sensorimotor Transformations in the Human Motor Periphery

Chao Gu (顾超)^{1,3}, Daniel K. Wood⁵, Paul L. Gribble¹⁻³, and Brian D. Corneil¹⁻⁴

Departments of ¹Psychology and ²Physiology & Pharmacology, University of Western Ontario, London, Ontario, Canada N6A 5B7

³Brain and Mind Institute and ⁴Robarts Research Institute, University of Western Ontario, London, Ontario, Canada N6A 5B7

⁵Department of Neurobiology, Northwestern University, Evanston, Illinois 60208

Keywords: cognitive control, human, reaching, visual processing

Gu C, Wood DK, Gribble PL, Corneil BD (2016) A trial-by-trial window into sensorimotor transformations in the human motor periphery. *J Neurosci* 36:8273-8282.

2.1 Abstract

The appearance of a novel visual stimulus generates a rapid stimulus-locked response (SLR) in the motor periphery within 100 ms of stimulus onset. Here, we recorded SLRs from an upper limb muscle while humans reached toward (pro-reach) or away (anti-reach) from a visual stimulus. The SLR on anti-reaches encoded the location of the visual stimulus rather than the movement goal. Further, SLR magnitude was attenuated when subjects reached away from rather than toward the visual stimulus. Remarkably, SLR magnitudes also correlated with reaction times on both pro-reaches and anti-reaches, but did so in opposite ways: larger SLRs preceded shorter-latency pro-reaches but longer latency anti-reaches. Although converging evidence suggests that the SLR is relayed via a tecto-reticulospinal pathway, our results show that task-related signals modulate visual signals feeding into this pathway. The SLR therefore provides a trial-by-trial window into how visual information is integrated with cognitive control in humans.

2.2 Introduction

The reaction time (RT) for almost all visually-guided movements far exceed the minimum conduction time between sensory input and motor output, allowing time for deliberation and strategic action (Luce, 1986; Posner, 1986; Carpenter and Williams, 1995; Schall, 2003). Such behavioural flexibility is captured in tasks where subjects are instructed to move away rather than towards a visual stimulus

(Hallett, 1978; Georgopoulos et al., 1989). Successful performance in these tasks requires cognitive control to: (i) consolidate the instruction, (ii) process stimulus location, and (iii) transform stimulus location into the appropriate motor command. The neural substrates of this sensorimotor transformation has been particularly well-studied in the oculomotor system of non-human primates (Munoz and Everling, 2004), showing for example that trial-by-trial representations of the visual stimulus are attenuated in many oculomotor regions by prior instruction to prepare for an anti-saccade, i.e. looking diametrically away from the visual stimulus (Everling et al., 1999; Gottlieb and Goldberg, 1999; Everling and Munoz, 2000). Such trial-by-trial resolution has simply not been available in humans, hence increases in average RT and error rate on anti-saccade trials have been traditional behavioural biomarkers used to assess cognitive control in healthy and clinical populations (Chan et al., 2005; Antoniades et al., 2013; Luna et al., 2015).

Recent works show that the strong transient response sweeping throughout the brain following visual stimulus onset (Wurtz and Goldberg, 1972; Schmolesky et al., 1998; Churchland et al., 2010) culminate in a short-latency stimulus-locked response (SLR) on both neck (Goonetilleke et al., 2015) and upper limb muscles in humans (Pruszynski et al., 2010; Wood et al., 2015). Based on the latency of the SLR (within 100 ms after stimulus onset) and its temporal separation from the larger wave of muscle recruitment associated with voluntary movement, we and others have speculated that the SLR is conveyed via a reticulospinal rather than a corticospinal pathway (Pruszynski et al., 2010; Wood et al., 2015), and may

therefore share the same circuitry as that generating the fast visuomotor response during corrections of on-going reaching movements (Carlton, 1981; Goodale et al., 1986; Day and Brown, 2001). However previous reports of the SLR had subjects reach toward a visual stimulus immediately or after an instructed delay. In doing so, these studies could not dissociate whether the SLR encoded the visual stimulus or arose as a preparatory response for the ensuing movement. Such dissociation is vital, as it begins to shed light on the underlying neural substrates of the SLR.

Here, we examined the SLR on an upper limb muscle while healthy human subjects either reached toward (pro-) or away from (anti-) a peripheral visual stimulus (**Figure 2.1a**). Our results show that the SLR encodes visual stimulus location even on anti-reach trials, and hence is dissociable from the eventual

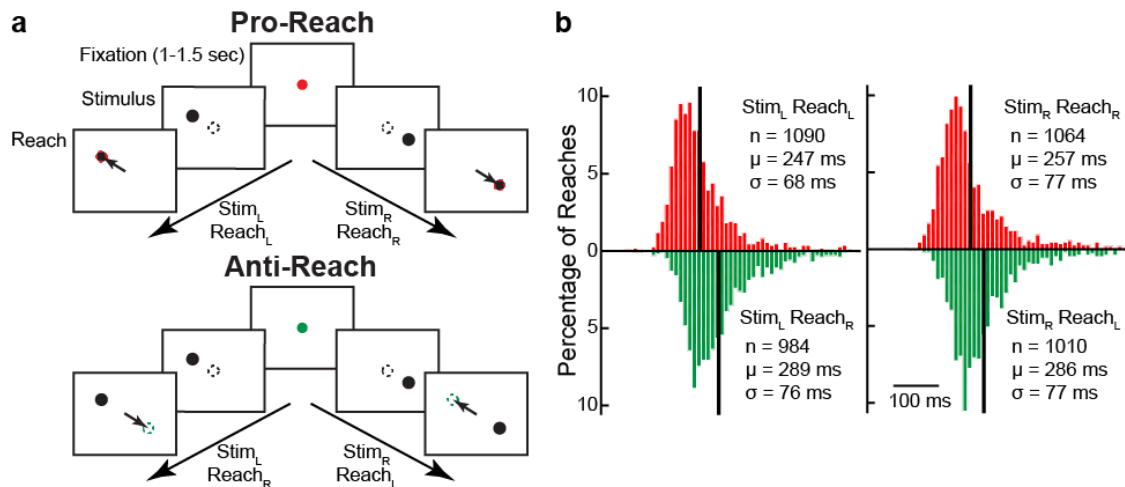


Figure 2.1: Pro-/anti-reach task and behavioural results

(a) Timeline of the 4 different pro-/anti-reach trial conditions. The colour of the central fixation circle indicated either a pro- (red, in this case) or anti-reach (green) trial. (b) Pooled distribution of all 10 subjects' reach RT for all correct trials, sorted by trial condition. Thick black line indicates the mean RT for the given RT distribution.

movement goal. Despite being locked to the sensory input, cognitive control attenuated the magnitude of the SLR on individual correct, but not incorrect, anti-reach trials, with greater attenuation of the SLR preceding short-latency anti-reaches. Such trial-by-trial results link directly with electrophysiological results obtained in non-human primates correlating the magnitude of visual responses in the oculomotor system with ensuing pro- and anti-saccadic reaction times (Everling et al. 1999; Everling and Munoz, 2000), and shows that the SLR in humans can be used to reveal trial-by-trial fluctuations in how visual information is integrated with on-going task demands.

2.3 Materials and Methods

A total of ten healthy participants (nine males and one female, age 22-43, all self-declared right-handed except for one self-declared left-handed male) took part in the experiment. Subjects provided written consent, were paid for their participation, and were free to withdraw from the experiment at any time. All procedures were approved by the University Research Board for Health Science Research at the University of Western Ontario. All subjects reported no history of visual, neurological, and/or musculoskeletal disorders.

2.3.1 Apparatus

Parts of the apparatus, electromyography (EMG) recording setup, and data analyses have been previously described (Wood et al., 2015). Briefly, subjects performed reach movements in the horizontal plane with their right arm while grasping the handle of a robotic manipulandum (InMotion Technologies, Watertown, MA, USA). A six-axis force transducer (ATI Industrial Automation, Apex, NC, USA; resolution of 0.05 N) in the handle measured manual hand forces. Subjects sat at a desk and interacted with the robotic arm on a horizontal plane in line with the subject's elbow height. The x- and y-position of the manipulandum was sampled at 600 Hz. A constant load force of 5.3 N (5 N to the right and 1.75 N toward the subject) was applied to increase the baseline activity of the limb muscle of interest. All stimuli were presented on a horizontal mirror, placed just below chin level, which reflected the display of a downward-facing LCD monitor with a refresh rate of 75 Hz. The precise timing of visual events on the LCD screen was determined by a photodiode. The subject's arm was occluded by the mirror, with real-time feedback of hand position provided by a small red cursor.

2.3.2 Pro-/Anti-Reach Task

To initiate the task, subjects moved the cursor into a grey start circle. Once the cursor entered the circle, the was then changed to either red or green (**Figure 2.1a**). For five of our subjects, a red circle indicated pro-reaches and a green circle indicated anti-reaches; this was reversed for the other 5 subjects. After a variable

delay of 1 to 1.5 seconds, a black peripheral circle appeared 10 cm from the start circle at a counter-clockwise rotation angle (from straight right) of either 160° (a leftward stimulus) or 340° (a rightward stimulus). These two locations have been previously reported to generate the SLR on the limb muscle of interest (Wood et al., 2015). The start circle was extinguished simultaneously with the presentation of the peripheral stimulus. Subjects then had to move the cursor as quickly as possible either toward (pro-) or 180° away from (anti-) the peripheral stimulus. The next trial started after a short randomized delay (0.5 – 1 sec). 9 of our 10 subjects performed at 4 sessions, while one subject performed 3 sessions of interleaved pro- and anti-reach trials with each session consisting of 30 trials at each location and trial type.

2.3.3 Muscle Recordings

Intramuscular EMG activity were recorded using fine-wire electrodes (A-M Systems, Sequim, WA, USA) inserted into the clavicular head of the right pectoralis major (PEC) muscle (see Wood et al., 2015 for insertion procedure). Briefly, for each recording we inserted two monopolar electrodes, enabling recording of multiple motor units. Insertions were aimed ~1 cm inferior to the inflection point of the clavicle. All intramuscular EMG data were recorded with a Myopac Junior system (Run Technologies, Mission Viejo, CA, USA; low-pass filter modified to 2 kHz). Surface EMG was also recorded using silver-chloride electrodes and P15 amplifier (Grass Instruments, Warwick, RI, USA); the electrodes were placed just

lateral to the intramuscular electrodes, on the same muscle fiber belly. Both the surface and intramuscular EMG signals were digitized at 4 kHz.

2.3.4 Data Analysis

In order to achieve sample-to-sample locking between kinematic and EMG data, kinematic data were up-sampled from 600 Hz to 1000 Hz with a lowpass interpolation algorithm, and then lowpass-filtered with a second-order Butterworth filter with a cutoff at 150 Hz. Both the intramuscular and surface recordings were rectified off-line and bin-integrated down to match the 1 kHz sample rate. Reach reaction time (RT) was calculated as the time from the appearance of the visual stimulus (measured by a photodiode) to the initiation of the reach. Reach initiation was identified by first finding the peak tangential hand velocity, and then moving backwards to the closest previous point at which the velocity profile reached 8% of the peak. Trials with RTs less than 170 ms (< 2%) were excluded to prevent contamination of the SLR window by voluntary recruitment associated with very short-latency responses (Wood et al., 2015). Identification of erroneous reach trials were done on a single-trial basis, using kinematic criteria where the initial movement went > 5% (5 mm) towards the incorrect direction.

2.3.5 Receiver-operating characteristic (ROC) analysis

Based on previous works identifying the SLR (Corneil et al., 2004; Pruszynski et al., 2010), we also used a receiver-operating characteristic (ROC) analysis to quantitatively detect the presence of a SLR. We first separated the EMG activity for all correct reaches based on visual stimulus location, and performed separate ROC analyses for pro- and anti-reach trials. For every time-sample (1 ms bin) between 100 ms before to 300 ms after visual stimulus onset, we calculated the area under the ROC curve. This metric indicates the probability that an ideal observer could discriminate the side of the stimulus location based solely on EMG activity. A value of 0.5 indicates chance discrimination, whereas a value of 1 or 0 indicates perfectly correct or incorrect discrimination, respectively. We set the thresholds for discrimination at 0.6 and 0.4; these criteria exceed the 95% confidence intervals of data randomly shuffled with a bootstrap procedure. The time of earliest discrimination was defined as the time after stimulus onset at which the ROC was above 0.6, and remained above that threshold for at least 8 out of the next 10 samples. Based on the ROC analysis, we defined the SLR epoch as an interval spanning 80-120 ms after visual onset.

2.4 Results

Across all of our subjects performing the pro-/anti-reach task, we found the expected increase in reach RT for anti- vs. pro-reach trials (repeated measures 2-

way ANOVA, $F_{(1,9)} = 55.29$, $P < 10^{-4}$, **Figure 2.1b**), but no main effect of stimulus location ($F_{(1,9)} = 2.76$, $P = 0.13$) or an interaction between stimulus location and trial type ($F_{(1,36)} = 4.26$, $P = 0.07$). A SLR was detectable in seven of our ten subjects during pro-reach trials (SLR+) using intramuscular PEC EMG recordings (see below). In five of our seven subjects, we had two separate intramuscular recordings, and in all five cases we were able to detect a SLR on both recordings. An exemplar example of the SLR is shown in **Figure 2.2a,c**, illustrating an increase or a decrease in PEC EMG activity 80-120 ms (crosses and shaded box) after the presentation of leftward (Stim_L, solid) or rightward (Stim_R, open) visual stimuli, respectively. The prevalence of the SLR across our sample (70%) and the recruitment profiles were similar to that reported previously, and as before, the prevalence of the SLR did not relate simply to idiosyncratic RTs (Wood et al., 2015). Six of the ten subjects also participated in our previous study (Wood et al., 2015). We saw consistent intra-subject reliability: three subjects were SLR+ in both studies, whereas three other subjects were SLR- in both studies. These three SLR- subjects also did not exhibit a SLR on anti-trials. Thus, all subsequent EMG analyses were performed only on those seven subjects exhibiting the SLR on pro-reach trials.

2.4.1 The SLR encodes visual stimulus rather than goal location, but is attenuated before correct anti-reaches

Figure 2.2b also shows intramuscular PEC EMG activity from our exemplar subject during individual correctly performed anti-reach trials. Note how the visual stimulus on anti-reach trials continued to evoke a SLR (lower panel of in **Figure 2.2c**, shaded box). Importantly, as on pro-reach trials leftward visual stimuli (solid) evoked an increase, while rightward visual stimuli (open) evoked a decrease in EMG activity. The SLR recruitment profiles were the same regardless of whether the subject reached toward or away from the stimulus, and thus reflected stimulus rather than goal location (**Figure 2.2d**). This interpretation is also clearly supported by the time-series receiver-operating characteristic (ROC) analyses, where we separated EMG activity based on stimulus location (**Figure 2.2e**). For both pro- and anti-reach trials, note how the time-series ROC curves deflected sharply upward above 0.6 yielding discrimination times (i.e. the first time point when there was reliable separation of EMG activity following presentation of leftward or rightward stimuli) of ~90 ms after stimulus onset. After ~120 ms after stimulus onset, EMG activity evolved to drive the voluntary motor command, with the time-series ROC curves for both trial types returning towards chance levels (ROC = 0.5) before diverging to 1 or 0 for pro- or anti-reach trials, respectively. This time-series ROC analysis confirms that the earliest wave of EMG activity reflected the stimulus location and not the eventual reach goal direction.

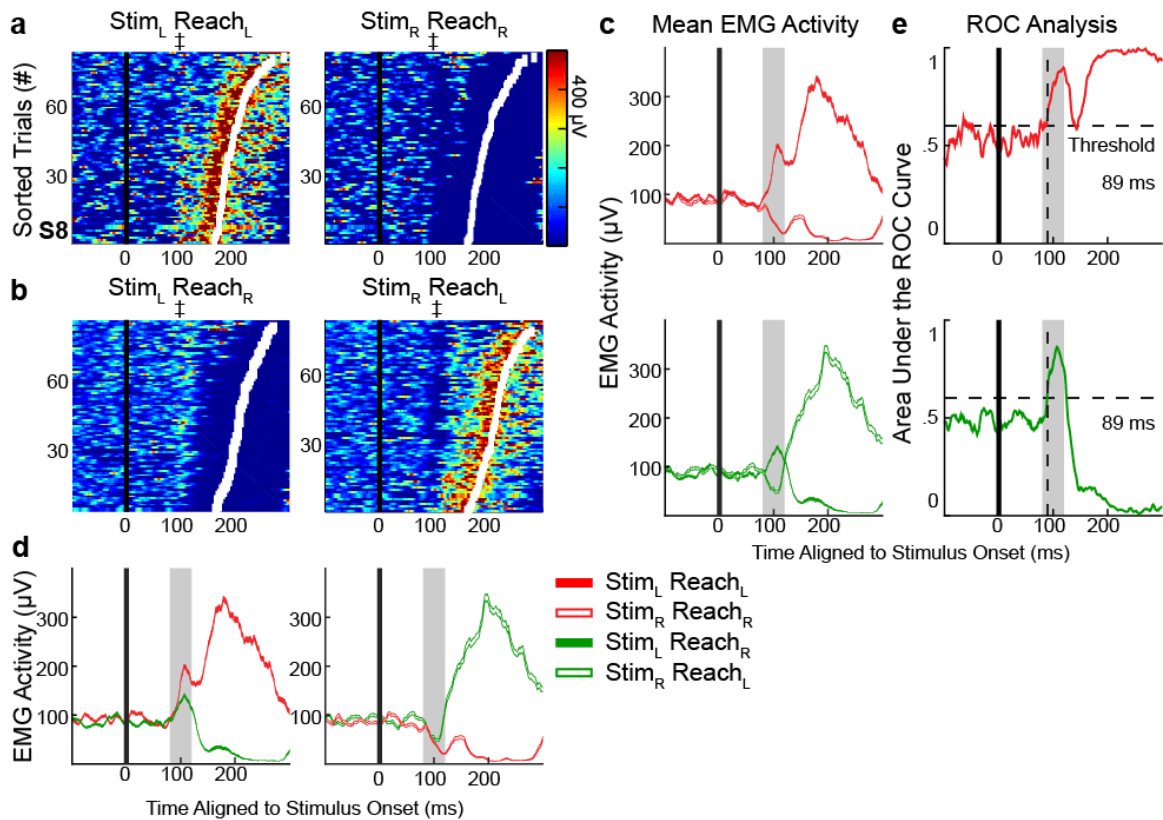


Figure 2.2: Intramuscular EMG results from an exemplar subject

(a) EMG activity for correct pro-reach trials, separated based on stimulus location. Each row represents activity within a single trial, with all trials aligned to stimulus onset (black line) and sorted based on reach RT (white squares). Crosses (\pm) indicate the SLR epoch. (b) EMG activity for correct anti-reach trials. Same layout as (a). (c) Average EMG activity (mean \pm SEM) for leftward (Stim_L, solid) and rightward (Stim_R, open) stimulus locations sorted by pro- or anti-reach type. (d) Same layout as C, except for pro- and anti-reach trials sorted by stimulus location. The SLR epoch (shaded box, 80-120 ms after stimulus onset) was significantly attenuated for anti- vs. pro-reach trials. (e) Time-series receiver-operating characteristic (ROC) analyses. For each time-sample (1 ms bin) the ROC value quantifies the discrimination between EMG activity for leftward and rightward stimulus locations. The discrimination time (dashed vertical line) is the first time-sample where there is a reliable separation between the EMG activities for leftward and rightward stimulus locations (see **Materials and Methods**).

All seven of our SLR+ subjects exhibited discrimination times within 100 ms after stimulus onset for pro-reach trials (range: 84 to 93 ms, **Figure 2.3d**). Four of these subjects also had similar discrimination times for anti-reaches (anti-SLR+, range: 85 to 99 ms top four subjects in **Figure 2.3**). The ROC time-series for the remaining three subjects failed to exceed threshold on anti-reaches, although there were hints of the SLR before anti-reach trials for subjects S7 and S10 (anti-SLR-, bottom three subjects in **Figure 2.3**). Further, for all seven subjects, we observed that the time-series ROC analyses for both pro- and anti-reach trials were in phase 80-120 ms after stimulus onset, initially increasing toward threshold and then briefly decreasing below 0.5. As described previously (Wood et al. 2015), in subjects with longer reach RTs we also observed a 12-15 Hz oscillation of EMG activity following the SLR. This can be clearly observed in S2, S3, and S5; note the reversal of mean EMG activity prior to the movement related activity (**Figure 2.3c**) and how the time-series ROC analyses dip down after initially exceeding threshold (**Figure 2.3d**).

Even though the SLR reflected visual stimulus location and occurred before the larger and later profile of PEC recruitment related to the goal location (**Figure 2.3**, RTs denoted by white squares), it was reliably attenuated for anti-reaches compared to pro-reaches (compare shaded boxes of **Figure 2.3c**). As a group for the seven subjects with a SLR, we observed an interaction between visual stimulus location and trial type during the SLR epoch, (repeated measures 2-way ANOVA, interaction effect, $F_{(1,6)} = 13.88$, $P = 0.01$). The overall difference between

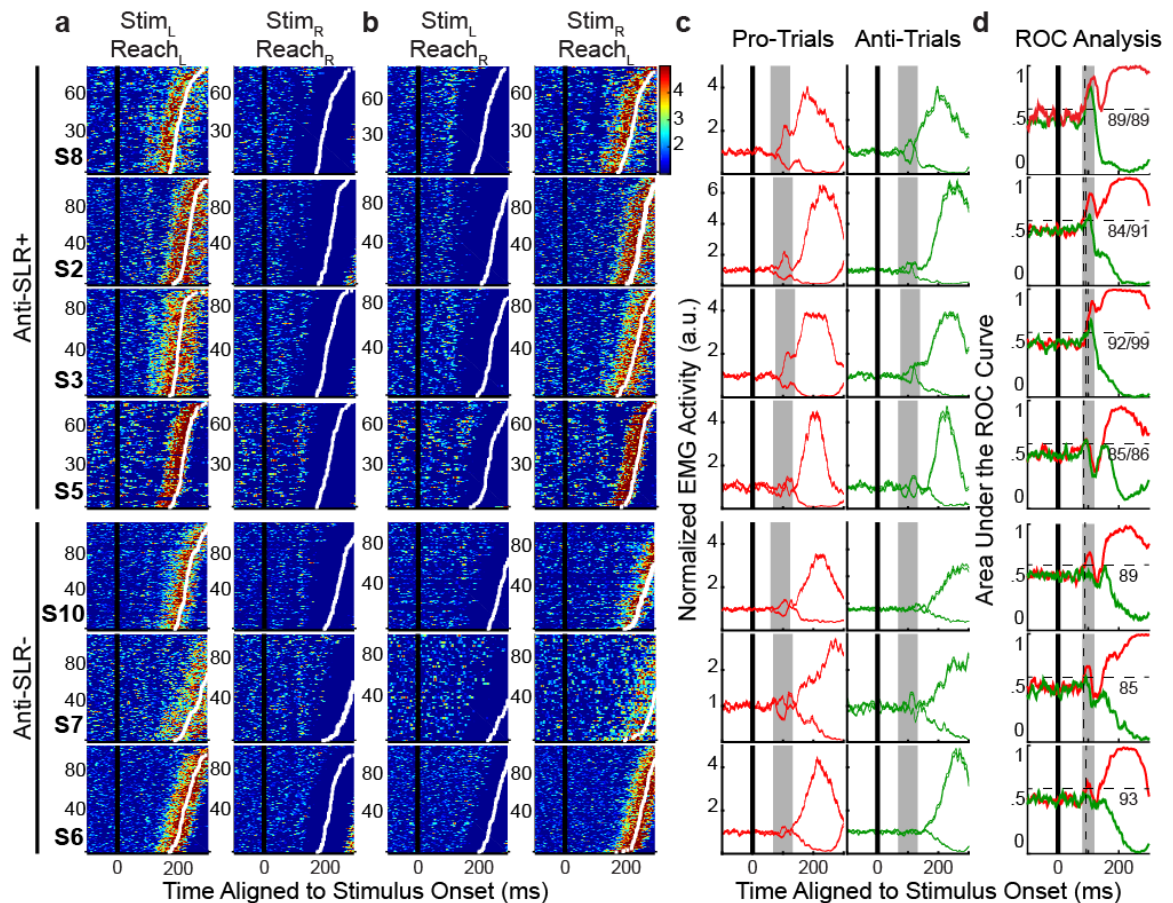


Figure 2.3: EMG activity from seven subjects with a detectable SLR

(a-d) Same format as Figure 2.2, except that all EMG activity were normalized to each subject's individual baseline activity (mean EMG activity in the 100 ms preceding stimulus onset). The top subject is the exemplar subject from **Figure 2.2**. Top four subjects had a detectable SLR for anti-reach trials (anti-SLR+); bottom three subjects did not (anti-SLR-).

leftward and rightward SLR magnitude for pro-reaches was reliably greater than anti-reaches (pair t -test, $t_{(6)} = 3.83$, $P < 0.001$). When we examined the SLR response within each subject, all seven subjects exhibited significantly greater EMG activity for pro- vs. correct anti-reach trials (independent t -test, all $P < 0.025$, Bonferroni corrected) following leftward visual stimulus, and six of seven subjects exhibited significantly weaker EMG activity (independent t -test, $P < 0.025$, Bonferroni corrected) following rightward visual stimulus. Importantly, such differences in SLR magnitude were not simply related to differences in preparatory EMG activity for pro- vs. anti-reach trial types, as there were no difference in a baseline interval in the 40 ms preceding stimulus onset (repeated measures 2-way ANOVA, $F_{(1,6)} = 0.37$, $P = 0.57$, paired t -test, $t_{(6)} = 0.61$, $P = 0.57$).

2.4.2 The SLR generates a transient force towards the visual stimulus for both pro- and anti-reaches

Previous studies of fast visuomotor responses generated during online corrective movements have quantified force profiles (Saijo et al., 2005; Franklin and Wolpert, 2008; Gallivan et al., 2016). To better compare our SLR results with these previous studies, we also examined whether the SLR on the PEC muscle was associated with a transient force toward the visual stimulus on both pro- and anti-reach trials. To analyze this, we separated our 10 subjects into those exhibiting the SLR on pro-reaches (SLR+; seven subjects) or not (SLR-; three subjects), and determined the mean force profile for each subject individually across the four different

conditions, segregated by task (pro- vs. anti-) and stimulus direction. We found that only SLR+ subjects exhibited a profile wherein forces diverged 110-150 ms after stimulus onset for leftward versus rightward stimuli (**Figure 2.4a**). The timing of this divergence is consistent with the SLR epoch, if we accounted for a 30 ms electromechanical delay (Norman and Komi, 1979). Further, in line with EMG activity during the SLR epoch, there was a reliable interaction between stimulus direction and trial type for the mean force 110-150 ms after stimulus onset (repeated measures 2-way ANOVA, interaction effect, $F_{(1,6)} = 13.88$, $P = 0.01$), with pro-reaches exhibiting a greater force difference for leftward vs. rightward stimuli compared to anti-reaches (paired t -test, $t_{(6)} = 3.73$, $P = 0.01$). In contrast, the force

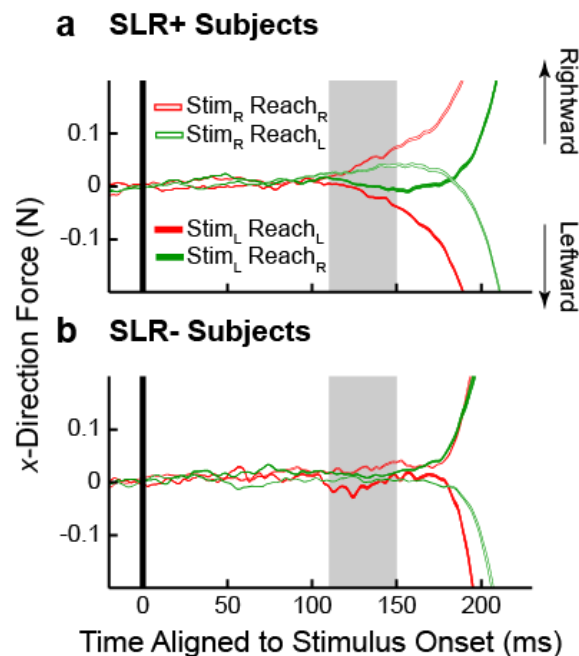


Figure 2.4: Kinetic force profiles offer a crude proxy for EMG activity

(a) Mean \pm SEM x -direction force profiles across the 4 different trial conditions for the seven subjects with a SLR on pro-trials. An interaction was observed between the stimulus direction and trial type at 110-150 ms interval after stimulus onset (shaded box, shifted 30 ms after the SLR epoch). (b) Same format as (a) but for the three subjects without a SLR on pro-trials.

profiles of SLR– subjects did not diverge in the 110-150 ms interval in either the pro- or anti-reach trials (**Figure 2.4b**, repeated measures 2-way ANOVA, $F_{(1,2)} = 5.33$, $P = 0.15$, paired t -test, $t_{(2)} = 2.31$, $P = 0.14$). Thus, the force profiles can be used as a crude proxy for the SLR at a group level basis.

2.4.3 Trials with a larger SLR were associated with shorter-RT pro-reaches, but longer-RT anti-reaches

Next, we determined whether the magnitude of the SLR related in some way to the ensuing reach behaviour. We first investigated the correlation between the magnitude of the SLR and the ensuing RT on a single-trial basis, doing so separately for pro- and anti-reach trials. **Figure 2.5a,b** shows data from the subject in **Figure 2.2**, plotting reach RT against the mean EMG activity during the SLR epoch. As reported previously (Pruszynski et al., 2010) for what were by our definition pro-reaches, i.e. visually-guided reaches, we observed a negative ($r = -0.31$, $P < 0.05$) or positive ($r = 0.30$, $P < 0.01$) correlation for leftward or rightward stimuli, respectively (**Figure 2.5a**; recall that EMG activity during the SLR epoch decreased following rightward stimulus, hence the positive correlation). In other words, larger magnitude SLRs preceded shorter RTs for pro-reaches. Remarkably, such relationships reversed on correct anti-reach trials, with a positive ($r = 0.23$, $P < 0.05$) or negative ($r = -0.31$, $P < 0.01$) correlations emerging for leftward or rightward stimuli, respectively (**Figure 2.5b**). Thus, larger magnitude SLRs preceded longer RTs for correct anti-reach trials. The reversed correlations

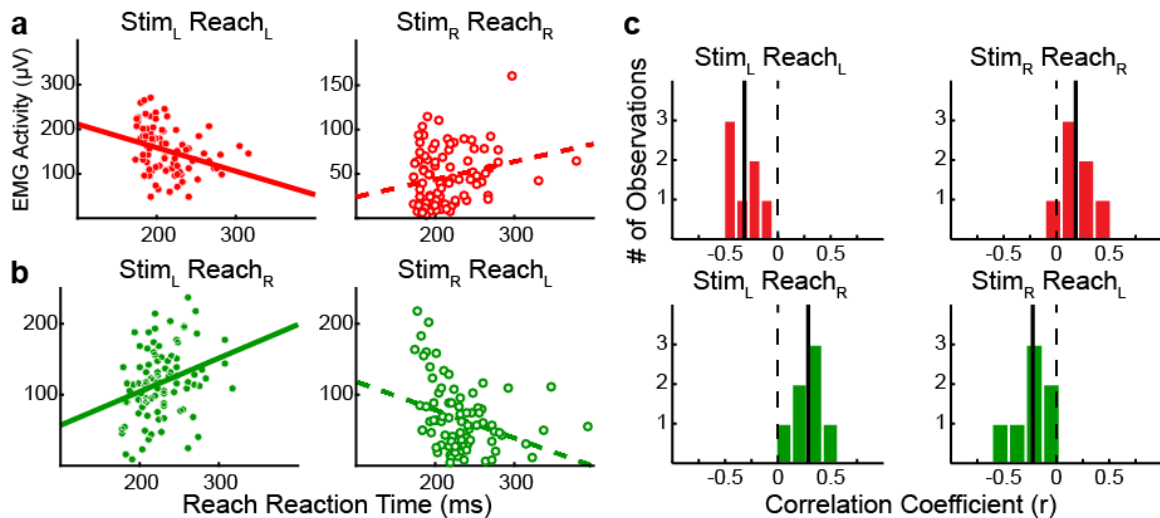


Figure 2.5: Reversed correlations between SLR and ensuing RT for pro- and anti-reach trials
 Single subject scatter plots of correlation between SLR magnitude and RT for pro- (a) and anti-reach trials (b), using data from the exemplar subject in **Figure 2.2**. (c) Group correlation coefficients for all seven subjects with a SLR on pro-trials, even if an SLR was not detected on anti-trials. The black lines indicate the mean correlation coefficient for the 4 different conditions, and the dash lines indicate 0.

between SLR magnitude and RT can also be appreciated in the individual EMG traces in **Figure 2.2a,b**: note how EMG recruitment in the SLR epoch becomes more pronounced going from the longest (top) to shortest (bottom) RTs for leftward pro-reaches, but diminished when going from the longest to shortest RTs for rightward anti-reaches (when the subject moved away from the leftward stimulus).

We observed such correlation reversals in SLR magnitude and RTs for pro- vs. anti-reaches across our seven SLR+ subjects (**Figure 2.5c**). We performed non-parametric bootstrapping analyses to determine the reliability and the reversal of these values. If there was no underlying structure to the correlation coefficients across the 4 different trial types, we would expect our observed mean correlation coefficients to fall within the distribution constructed by randomly assigned trial

types (10,000 times). Instead, we found that all four observed means were reliably different than the bootstrapped distribution (all $P < 0.05$). In addition, the observed differences in correlation coefficients between leftward and rightward stimuli for both pro- and anti-reach trials were also reliably greater than the differences obtained from the bootstrapped distributions ($P = 0.0005$ and $P = 0.0011$ for pro- and anti-reach trials, respectively). This relationship between SLR and ensuing RT was once again not simply a consequence of baseline EMG activity before stimulus onset, as we did not find any reliable correlation between mean EMG activity 40 ms preceding stimulus onset with ensuing reach RT for any of the four conditions (all $P > 0.09$, comparing observed correlations to a bootstrapped distribution) or any reliable difference in correlation coefficient between leftward and rightward stimuli ($P = 0.15$ and $P = 0.20$, for pro- and anti- trials, respectively). These results suggest that the influence of cognitive control on the SLR is such that it reflects stimulus priority, with larger SLRs being beneficial for pro-reaches, but detrimental for anti-reaches; this pattern is similar to what has been observed in the oculomotor system (Kristjánsson et al., 2001).

2.4.4 Similar SLR magnitudes accompanied erroneous anti-reach trials and correct pro-reach trials

Up to now, we have only considered the SLRs for correctly performed anti-reach trials. If the SLR is truly an indicator of cognitive control, we should expect that the SLR is also informative when subjects erroneously reach toward, rather than away

from the visual stimulus on anti-reach trials. Two of the seven SLR+ subjects generated a sufficient number of erroneous anti-reach trials to permit the following analyses (~20% error rate for both subjects, producing > 20 erroneous trials per direction). For these two subjects, we compared SLR magnitudes across three different trial types: correct pro-, correct anti-, and erroneous anti-reach trials (**Fig. 2.6**). For both subjects found reliable difference between the 3 conditions for both leftward and rightward stimuli (1-way ANOVA, both $P < 10^{-7}$). For leftward visual stimulus, the SLR magnitude was significantly greater on erroneous (black) than correct (green) anti-reach trials (independent t -test, $P < 10^{-7}$ and $P < 10^{-5}$, Bonferroni corrected, for S3 and S8 respectively), but not significantly different between the SLRs on erroneous anti-reach and correct pro-reach (red) trials (independent t -test, $P = 0.09$ and $P = 0.88$, respectively). Similarly, for rightward visual stimulus, significantly stronger SLRs were observed for erroneous vs. correct anti-reach trials (independent t -test, $P < 0.01$ and $P < 0.01$, respectively; recall the SLR is a decrease in EMG in this direction, hence stronger SLRs produce greater decreases in EMG activity), but similar magnitude SLRs were observed on correct pro-reaches and erroneous anti-reaches (independent t -test, $P = 0.30$ and $P = 0.11$, respectively). Thus, as observed for visual responses in previous neurophysiological studies during the pro-/anti-saccade task (Everling et al., 1998; Everling and Munoz, 2000), the SLR on erroneous anti-reach resembled that prior to correct pro-reaches. These results further support the idea that the SLR can be used as an indicator of cognitive control on a trial-by-trial basis.

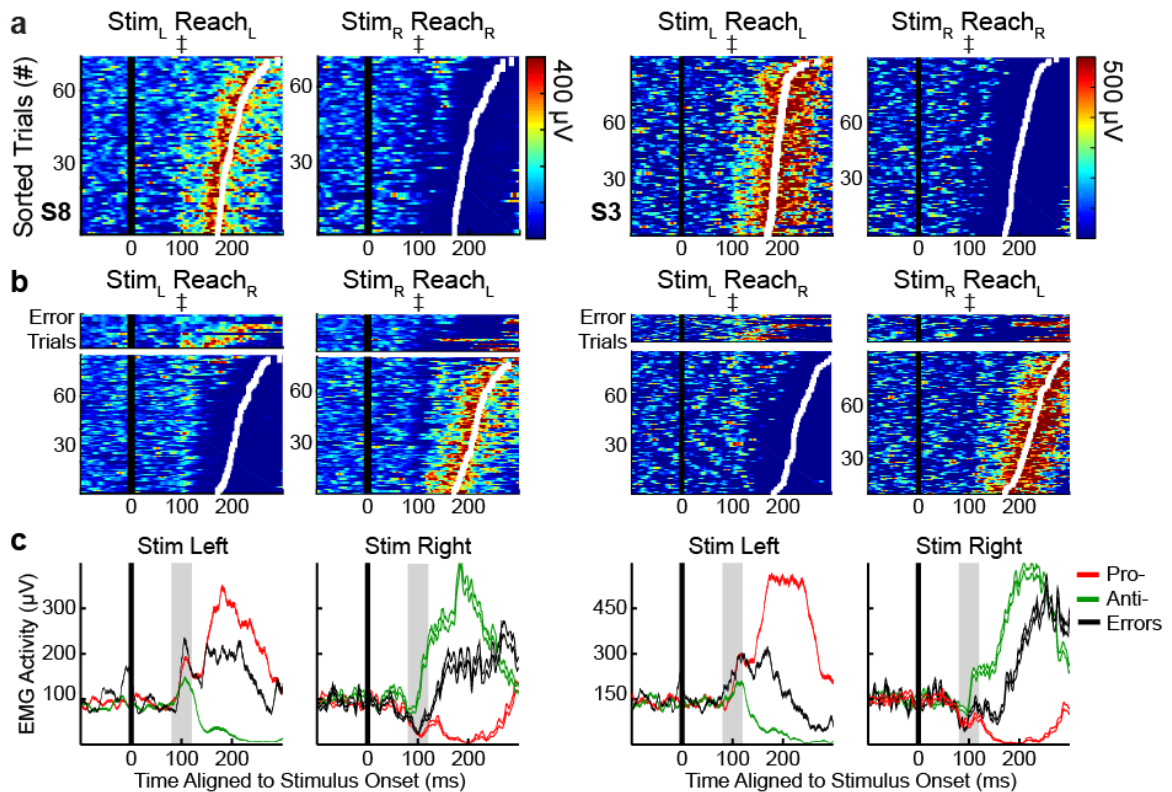


Figure 2.6: SLR magnitudes were similar on pro-reach and erroneous anti-reach trials

(a-c) Data from the two subjects, S3 and S8, with enough erroneous anti-reach trials. Same format as **Figure 2.2**, except erroneous anti-reach trials are displayed on top of correct anti-reach trials or shown in black. See **Materials and Methods** for how erroneous trials were detected.

2.4.5 Surface EMG recordings can also detect the SLR

To date, almost all the previous studies on the SLR in humans or non-human primates have relied on intramuscular EMG recordings (Corneil et al., 2004; Chapman and Corneil, 2011; Goonetilleke et al., 2015; Wood et al., 2015). Reliance on intramuscular recordings may hinder widespread examination of the SLR in variety of paradigms in both healthy and patient populations. One study that detected SLRs with intramuscular recordings (Pruszynski et al., 2010) reported that surface EMG recordings were ‘almost universally unsuccessful’, with

only four detectable SLR out of 108 recordings. They suggested that intramuscular electrodes may be recording from slower (but first-recruited) motor units located deeper in the muscle. In sharp contrast, we were able to detect the SLR (using the same criteria as described in the **Materials and Methods**) with surface EMG recordings in six out of the seven SLR+ subjects. **Figure 2.7** shows surface recordings from our exemplar subject and hence is directly comparable with the intramuscular recordings shown in **Figure 2.2**. While surface recordings were noisier, such recordings still exhibited all the same characteristics as observed with intramuscular recordings. Across all six of these subjects, their SLRs were significantly attenuated before correct anti-reaches compared to pro-reaches (paired t -test, $t_{(5)} = 3.11$, $P < 0.05$), the correlation between SLR magnitude and ensuing RT were reversed for pro-reaches vs. anti-reaches for both leftward and rightward stimuli ($P = 0.037$ and $P = 0.0142$, respectively), and for the two subjects with sufficient erroneous anti-reach trials, the SLRs preceding anti-reach errors resembled that of pro-reach trials (independent t -test, all $P > 0.1$) but were significantly stronger than those preceding correct anti-reach trials (independent t -test, all $P < 0.05$). Our successful detection of the SLR may be related to a combination of the posture adopted by the subject, the robotic manipulandum used, and the application of a constant load to increase background EMG activity on the muscle of interest. Regardless, demonstrating the efficacy of surface recordings will help broaden the study of the SLR, particularly in clinical populations.

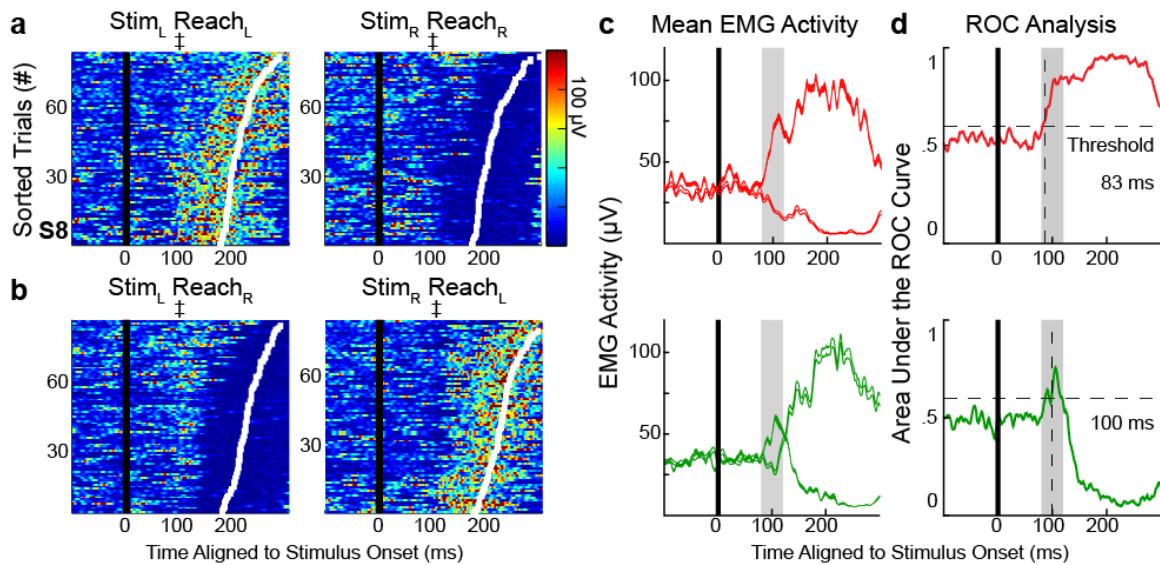


Figure 2.7: SLRs can be detected with surface EMG recordings

(a-d) Surface EMG recordings from the exemplar subject, using the same format as **Figure 2.2**.

2.5 Discussion

2.5.1 Summary of results

Our results demonstrate that a fast visuomotor response, the SLR, can provide a window into the integration of visual input with cognitive control in humans. Here, by having subjects reach either toward (pro-) or away (anti-reach) from a peripheral visual stimulus, we showed that the initial recruitment of an upper limb muscle encodes the location of the visual stimulus, with subsequent muscle recruitment evolving to drive the task-appropriate command. SLR magnitude attenuated when subjects correctly reached away from the stimulus. Furthermore, SLR magnitude correlated with ensuing reach RT, but such correlations were reversed when subjects moved either toward or away from the visual stimulus. Overall, our results bear remarkable resemblance to neurophysiological recordings of visual

responses from the frontal eye fields (FEF) and the intermediate layers of the superior colliculus (SC) in non-human primates performing pro-/anti-saccades (Everling et al., 1999; Everling and Munoz, 2000). Accordingly, the SLR may provide a new way of assessing how sensory input is integrated with cognitive control on a trial-by-trial basis in humans.

2.5.2 Influence of task instruction on visual processing

Previous work has shown that visual representations can be modulated by task instruction as early as the lateral geniculate nucleus (McAlonan et al., 2008), with such modulation being ubiquitous throughout visual and oculomotor areas in striate, extra-striate, parietal, frontal cortices, and the SC (Wurtz and Goldberg, 1972; Goldberg and Bushnell, 1981; Moran and Desimone, 1985; Colby et al., 1996). Our results show that the human SLR is also modulated by task instruction, with trial-by-trial fluctuation in SLR magnitude correlating with aspects of the ensuing behavioural response. Many neurophysiological results have reported similar trial-by-trial correlation between the magnitude of the visual response with ensuing RT (Lee et al., 2010; Marino et al., 2012; Galashan et al., 2013; Sharma et al., 2015). Furthermore, the strength of single trial correlations between SLR magnitude and ensuing RT are comparable to that observed previously for correlations between activity of neurons in the SC and FEF with saccadic RT (Dorris et al., 1997; Everling and Munoz, 2000). Indeed, the relationship between the SLR and ensuing RT is particularly noteworthy, as it marks the first time to our

knowledge that a direct, within trial measurement of visual encoding has been reported in healthy humans using non-invasive measurements.

As mentioned above, the SLR recorded from the human limb exhibits many of the same characteristics as seen for visual responses in the oculomotor system during interleaved pro- and anti-saccade trials. While there have been neurophysiological investigations of pro- and anti-reaches, such studies were not designed to assess the effects of task instruction on processing of the initial visual stimulus. Some studies have used a variation of a stimulus-response compatibility task, where a different peripheral visual stimulus instructed the subjects to make pro- vs. anti-reaches (Georgopoulos et al., 1989; Crammond and Kalaska, 1994; Zhang et al., 1997). Other studies have provided the task instruction and stimulus simultaneously, but required subjects withhold movement onset for a proscribed delay period (Gail and Andersen, 2006; Gail et al., 2009; Klaes et al., 2011). Our results strongly imply that many of the lessons learned from the oculomotor system about contextual processing of visual information extends to the reaching system, providing one uses a similar task structure.

2.5.3 A visual, not goal-directed, nature to the SLR

The SLR encoding the visual stimulus and not the motor goal is inconsistent with the involvement of the corticospinal system for the SLR. First, although transient visual responses have been reported in reach-related areas such as primary motor (Kwan et al., 1981), premotor (Weinrich and Wise, 1982), and parietal cortices

(Snyder et al., 1998; Cui and Andersen, 2011), the latencies of such responses in non-human primates exceed 100 ms and consequently, are too late to be driving the SLR in humans. Furthermore, the central observation that the SLR encodes the location of the visual stimulus is inconsistent with involvement of the motor cortices: although preparatory- or delay-period activity in primary, premotor, and parietal cortices can encode multiple potential reaching targets (Cisek and Kalaska, 2005; Cui and Andersen, 2011), even in the context of an anti-reaching task (Klaes et al., 2011), such activity remains divorced from muscle recruitment in the periphery up until the subject makes a commitment to move (Tanji and Evarts, 1976; Kaufman et al., 2014). Based on these considerations, it seems unlikely that the SLR arises from signals relayed along a direct corticospinal pathway.

2.5.4 SLR potentially mediated through a reticulospinal pathway

An alternative descending motor pathway for the SLR is the reticulospinal pathway (Lemon, 2008), which is very important for postural control and orienting of the trunk (Lawrence and Kuypers, 1968). The reticulospinal pathway is thought to have a comparatively weaker effect on motoneurons than the corticospinal pathway (Riddle et al., 2009), which is consistent with the relatively small magnitude of the SLR. The reticulospinal pathway has also been implicated in on-line corrective reach movements, which can be initiated within 150 ms after stimulus displacement (Carlton, 1981; Saunders and Knill, 2004; Saijo et al., 2005; Franklin and Wolpert, 2008), can occur without perception of stimulus displacement

(Goodale et al., 1986), and persist even in a subject with a complete agenesis of their corpus callosum (Day and Brown, 2001). Our results resemble those reported by Day and Lyon (2000) who studied on-line corrective movements in healthy subjects who had to point either toward (pro-trials) or away from (anti-trials) a displaced stimulus. They reported two distinct phases in subjects' hand trajectory: an early (<160 ms) small component that invariably moved toward the displaced visual stimulus on both pro- and anti-trials which they attributed to the reticulospinal pathway, and a later (>160 ms) component that corresponded to the task goal. When considered alongside these findings, our results strongly imply that the SLR is relayed to the motor periphery via the reticulospinal system.

2.5.5 Potential sources for task dependent modulation of the SLR

Assuming that the SLR is relayed through a reticulospinal pathway, and given that its short latency precludes processing in motor cortices, presumably some node between the retina and reticular formation must be modulated by task-related signals prior to the arrival of visual information. Within the brainstem, the SC is an obvious candidate, and we have emphasized the similarity between our results and SC activity on anti-saccade trials (Everling et al., 1998; 1999). The SC receives extensive projections from frontal and parietal cortices that convey task-related signals, and the SC is itself strongly interconnected with premotor centres for orienting eye, head, and limb and torso movements (see Corneil and Munoz, 2014 for review). Visual neurons in the SC respond within 50 ms of stimulus onset

(Wurtz and Goldberg, 1972), and a subset of these neurons are active only prior to reaches, but not saccades (Song and McPeck, 2015). The SC is also thought to mediate SLRs on neck muscles in primates (Rezvani and Corneil, 2008; Chapman and Corneil, 2011), which bears many similarities to the limb SLR shown here. In addition, neurons in intermediate and deep SC are active prior to reaching movements (Werner, 1993), with activity of such neurons correlating well with EMG activity on upper limb muscles (Werner et al., 1997; Stuphorn et al., 1999). Electrical stimulation within the SC can also evoke limb movements in both cats and primates (Cowie et al., 1994; Courjon et al., 2004; Philipp and Hoffmann, 2014). Finally, human fMRI experiments have reported reach-related BOLD activity in the deep layers of SC which is distinct from saccade-related activity (Linzenbold and Himmelbach, 2012; Himmelbach et al., 2013). Taken together, the SC appears to be a logical node for where cognitive control could influence the vigor of short-latency visual signals that are destined for the reticular formation.

2.5.6 SLR as an alternative biomarker for the fast visuomotor response

While neurophysiological studies are required to prove that the tectoreticulospinal system provides the substrate for the SLR, and perhaps on-line corrections more generally, there are a number of important implications for our findings. First, the SLR can be detected even though the subject started from a static posture, and evolves well in advance of voluntary movement (**Figure 2.3**). Attributing different components of muscle recruitment to different descending pathways during on-

line corrective movements is far more complicated, both because of the ongoing muscle recruitment accompanying the initial movement, and because the voluntary component of the corrective movement is itself expedited due to an already-made commitment to move (Cluff and Scott, 2015). Studying the SLR from a static posture may, somewhat paradoxically, simplify the study of the fast visuomotor response. Perhaps more fundamentally, it is clear that SLR magnitude is modulated by top-down control, with such modulation being quantifiable at a trial-by-trial resolution that is unprecedented for human studies. In this regard, our ability to detect the SLR with surface recordings is particularly encouraging, as the SLR may provide a novel and accessible biomarker to better understand how visual input integrates with cognitive control in both clinical (Chan et al., 2005; Antoniadou et al., 2013) and developmental (Luna et al., 2015) studies in humans.

2.6 References

- Antoniades C, Ettinger U, Gaymard B, Gilchrist I, Kristjánsson A, Kennard C, John Leigh R, Noorani I, Pouget P, Smyrnis N, Tarnowski A, Zee DS, Carpenter RHS (2013) An internationally standardised antisaccade protocol. *Vision Research* 84:1–5.
- Carlton LG (1981) Processing visual feedback information for movement control. *J Exp Psychol Hum Percept Perform* 7:1019–1030.
- Carpenter RH, Williams ML (1995) Neural computation of log likelihood in control of saccadic eye movements. *Nature* 377:59–62.

- Chan F, Armstrong IT, Pari G, Riopelle RJ, Munoz DP (2005) Deficits in saccadic eye-movement control in Parkinson's disease. *Neuropsychologia* 43:784–796.
- Chapman BB, Corneil BD (2011) Neuromuscular recruitment related to stimulus presentation and task instruction during the anti-saccade task. *Eur J Neurosci* 33:349–360.
- Churchland MM et al. (2010) Stimulus onset quenches neural variability: a widespread cortical phenomenon. *Nature Neurosci* 13:369–378.
- Cisek P, Kalaska JF (2005) Neural Correlates of Reaching Decisions in Dorsal Premotor Cortex: Specification of Multiple Direction Choices and Final Selection of Action. *Neuron* 45:801–814.
- Cluff T, Scott SH (2015) Online Corrections are Faster Because Movement Initiation Must Disengage Postural Control. *Motor Control*.
- Colby CL, Duhamel JR, Goldberg ME (1996) Visual, presaccadic, and cognitive activation of single neurons in monkey lateral intraparietal area. *J Neurophysiol* 76:2841–2852.
- Corneil BD, Munoz DP (2014) Overt Responses during Covert Orienting. *Neuron* 82:1230–1243.
- Corneil BD, Olivier E, Munoz DP (2004) Visual responses on neck muscles reveal selective gating that prevents express saccades. *Neuron* 42:831–841.
- Courjon JH, Olivier E, Pelisson D (2004) Direct evidence for the contribution of the superior colliculus in the control of visually guided reaching movements in the cat. *J Physiol* 556:675–681.
- Cowie RJ, Smith MK, Robinson DL (1994) Subcortical contributions to head movements in macaques. II. Connections of a medial pontomedullary head-movement region. *J Neurophysiol* 72:2665–2682.
- Crammond DJ, Kalaska JF (1994) Modulation of preparatory neuronal activity in dorsal premotor cortex due to stimulus-response compatibility. *J Neurophysiol* 71:1281–1284.

- Cui H, Andersen RA (2011) Different representations of potential and selected motor plans by distinct parietal areas. *J Neurosci* 31:18130–18136.
- Day BL, Brown P (2001) Evidence for subcortical involvement in the visual control of human reaching. *Brain* 124:1832–1840.
- Day BL, Lyon IN (2000) Voluntary modification of automatic arm movements evoked by motion of a visual target. *Exp Brain Res* 130:159–168.
- Dorris MC, Paré M, Munoz DP (1997) Neuronal activity in monkey superior colliculus related to the initiation of saccadic eye movements. *J Neurosci* 17:8566–8579.
- Everling S, Dorris MC, Klein RM, Munoz DP (1999) Role of primate superior colliculus in preparation and execution of anti-saccades and pro-saccades. *J Neurosci* 19:2740–2754.
- Everling S, Dorris MC, Munoz DP (1998) Reflex suppression in the anti-saccade task is dependent on prestimulus neural processes. *J Neurophysiol* 80:1584–1589.
- Everling S, Munoz DP (2000) Neuronal correlates for preparatory set associated with pro-saccades and anti-saccades in the primate frontal eye field. *J Neurosci* 20:387–400.
- Franklin DW, Wolpert DM (2008) Specificity of reflex adaptation for task-relevant variability. *J Neurosci* 28:14165–14175.
- Gail A, Andersen RA (2006) Neural dynamics in monkey parietal reach region reflect context-specific sensorimotor transformations. *J Neurosci* 26:9376–9384.
- Gail A, Klaes C, Westendorff S (2009) Implementation of spatial transformation rules for goal-directed reaching via gain modulation in monkey parietal and premotor cortex. *J Neurosci* 29:9490–9499.
- Galashan FO, Saßen HC, Kreiter AK, Wegener D (2013) Monkey area MT latencies to speed changes depend on attention and correlate with behavioral reaction times. *Neuron* 78:740–750.

- Gallivan JP, Logan L, Wolpert DM, Flanagan JR (2016) Parallel specification of competing sensorimotor control policies for alternative action options. *Nature Neurosci* 19:320–326.
- Georgopoulos AP, Lurito JT, Petrides M, Schwartz AB, Massey JT (1989) Mental rotation of the neuronal population vector. *Science* 243:234–236.
- Goldberg ME, Bushnell MC (1981) Behavioral enhancement of visual responses in monkey cerebral cortex. II. Modulation in frontal eye fields specifically related to saccades. *J Neurophysiol* 46:773–787.
- Goodale MA, Pelisson D, Prablanc C (1986) Large adjustments in visually guided reaching do not depend on vision of the hand or perception of target displacement. *Nature* 320:748–750.
- Goonetilleke SC, Katz L, Wood DK, Gu C, Huk AC, Corneil BD (2015) Cross-species comparison of anticipatory and stimulus-driven neck muscle activity well before saccadic gaze shifts in humans and non-human primates. *J Neurophysiol* 114:902–913.
- Gottlieb J, Goldberg ME (1999) Activity of neurons in the lateral intraparietal area of the monkey during an antisaccade task. *Nature Neurosci* 2:906–912.
- Hallett PE (1978) Primary and secondary saccades to goals defined by instructions. *Vision Research* 18:1279–1296.
- Himmelbach M, Linzenbold W, Ilg UJ (2013) Dissociation of reach-related and visual signals in the human superior colliculus. *NeuroImage* 82:61–67.
- Kaufman MT, Churchland MM, Ryu SI, Shenoy KV (2014) Cortical activity in the null space: permitting preparation without movement. *Nature Neurosci* 17:440–448.
- Klaes C, Westendorff S, Chakrabarti S, Gail A (2011) Choosing Goals, Not Rules: Deciding among Rule-Based Action Plans. *Neuron* 70:536–548.
- Kristjánsson A, Chen Y, Nakayama K (2001) Less attention is more in the preparation of antisaccades, but not prosaccades. *Nature Neurosci* 4:1037–1042.

- Kwan HC, MacKay WA, Murphy JT, Wong YC (1981) Distribution of responses to visual cues for movement in precentral cortex of awake primates. *Neuroscience Lett* 24:123–128.
- Lawrence DG, Kuypers HG (1968) The functional organization of the motor system in the monkey. II. The effects of lesions of the descending brain-stem pathways. *Brain* 91:15–36.
- Lee J, Kim HR, Lee C (2010) Trial-to-trial variability of spike response of V1 and saccadic response time. *J Neurophysiol* 104:2556–2572.
- Lemon RN (2008) Descending pathways in motor control. *Annu Rev Neurosci* 31:195–218.
- Linzenbold W, Himmelbach M (2012) Signals from the deep: reach-related activity in the human superior colliculus. *J Neurosci* 32:13881–13888.
- Luce RD (1986) *Response Times: Their Role in Inferring Elementary Mental Organization*. New York: Oxford University Press.
- Luna B, Marek S, Larsen B, Tervo-Clemmens B, Chahal R (2015) An integrative model of the maturation of cognitive control. *Annu Rev Neurosci* 38:151–170.
- Marino RA, Levy R, Boehnke SE, White BJ, Itti L, Munoz DP (2012) Linking visual response properties in the superior colliculus to saccade behavior. *Eur J Neurosci* 35:1738–1752.
- McAlonan K, Cavanaugh J, Wurtz RH (2008) Guarding the gateway to cortex with attention in visual thalamus. *Nature* 456:391–394.
- Moran J, Desimone R (1985) Selective attention gates visual processing in the extrastriate cortex. *Science* 229:782–784.
- Munoz DP, Everling S (2004) Look away: the anti-saccade task and the voluntary control of eye movement. *Nat Rev Neurosci* 5:218–228.
- Norman RW, Komi PV (1979) Electromechanical delay in skeletal muscle under normal movement conditions. *Acta Physiol Scand* 106:241–248.

- Philipp R, Hoffmann KP (2014) Arm movements induced by electrical microstimulation in the superior colliculus of the macaque monkey. *J Neurosci* 34:3350–3363.
- Posner MI (1986) *Chronometric Explorations of Mind*. New York: Oxford University Press.
- Pruszynski JA, King GL, Boisse L, Scott SH, Flanagan JR, Munoz DP (2010) Stimulus-locked responses on human arm muscles reveal a rapid neural pathway linking visual input to arm motor output. *Eur J Neurosci* 32:1049–1057.
- Rezvani S, Corneil BD (2008) Recruitment of a head-turning synergy by low-frequency activity in the primate superior colliculus. *J Neurophysiol* 100:397–411.
- Riddle CN, Edgley SA, Baker SN (2009) Direct and indirect connections with upper limb motoneurons from the primate reticulospinal tract. *J Neurosci* 29:4993–4999.
- Saijo N, Murakami I, Nishida S, Gomi H (2005) Large-field visual motion directly induces an involuntary rapid manual following response. *J Neurosci* 25:4941–4951.
- Saunders JA, Knill DC (2004) Visual feedback control of hand movements. *J Neurosci* 24:3223–3234.
- Schall JD (2003) Neural correlates of decision processes: neural and mental chronometry. *Curr Opin Neurobiol* 13:182–186.
- Schmolesky MT, Wang Y, Hanes DP, Thompson KG, Leutgeb S, Schall JD, Leventhal AG (1998) Signal timing across the macaque visual system. *J Neurophysiol* 79:3272–3278.
- Sharma J, Sugihara H, Katz Y, Schummers J, Tenenbaum J, Sur M (2015) Spatial Attention and Temporal Expectation Under Timed Uncertainty Predictably Modulate Neuronal Responses in Monkey V1. *Cereb Cortex* 25:2894–2906.

- Snyder LH, Batista AP, Andersen RA (1998) Change in motor plan, without a change in the spatial locus of attention, modulates activity in posterior parietal cortex. *J Neurophysiol* 79:2814–2819.
- Song J-HH, McPeck RM (2015) Neural correlates of target selection for reaching movements in superior colliculus. *J Neurophysiol* 113:1414–1422.
- Stuphorn V, Hoffmann KP, Miller LE (1999) Correlation of primate superior colliculus and reticular formation discharge with proximal limb muscle activity. *J Neurophysiol* 81:1978–1982.
- Tanji J, Evarts EV (1976) Anticipatory activity of motor cortex neurons in relation to direction of an intended movement. *J Neurophysiol* 39:1062–1068.
- Weinrich M, Wise SP (1982) The premotor cortex of the monkey. *J Neurosci* 2:1329–1345.
- Werner W (1993) Neurons in the primate superior colliculus are active before and during arm movements to visual targets. *Eur J Neurosci* 5:335–340.
- Werner W, Dannenberg S, Hoffmann KP (1997) Arm-movement-related neurons in the primate superior colliculus and underlying reticular formation: comparison of neuronal activity with EMGs of muscles of the shoulder, arm and trunk during reaching. *Exp Brain Res* 115:191–205.
- Wood DK, Gu C, Corneil BD, Gribble PL, Goodale MA (2015) Transient visual responses reset the phase of low-frequency oscillations in the skeletomotor periphery. *Eur J Neurosci* 42:1919–1932.
- Wurtz RH, Goldberg ME (1972) Activity of superior colliculus in behaving monkey. 3. Cells discharging before eye movements. *J Neurophysiol* 35:575–586.
- Zhang J, Riehle A, Requin J, Kornblum S (1997) Dynamics of single neuron activity in monkey primary motor cortex related to sensorimotor transformation. *J Neurosci* 17:2227–2246.

Chapter 3 – Done in 100 ms: Path-Dependent Visuomotor Transformation in the Human Upper Limb

Chao Gu (顾超)^{1,3}, J. Andrew Pruszynski¹⁻⁴, Paul L. Gribble¹⁻³, and Brian D. Corneil¹⁻⁴

Department of ¹Psychology and ²Physiology & Pharmacology, University of Western Ontario, London, Ontario, Canada N6A 5B7

³Brain and Mind Institute and ⁴Robarts Research Institute, University of Western Ontario, London, Ontario, Canada N6A 5B7

Keywords: Hand-eye coordination, human reaching movements, movement planning, trajectory, visual response

Gu C, Pruszynski JA, Gribble PL, Corneil BD (2018) Done in 100ms: path-dependent visuomotor transformation in the human upper limb. *J Neurophysiol* 119:1319-1328.

3.1 Abstract

A core assumption underlying mental chronometry is that more complex tasks increase cortical processing, prolonging reaction times. In this study, we show that increases in task complexity alter the magnitude, rather than the latency, of the output for a circuitry that rapidly transforms visual information into motor actions. We quantified visual stimulus-locked responses (SLRs), which are changes in upper limb muscle recruitment that evolve at fixed latency ~ 100 ms after novel stimulus onset. First, we studied the underlying reference frame of the SLR by dissociating the initial eye and hand positions. Despite its quick latency, we found that the SLR was expressed in a hand-centric reference frame, suggesting that the circuit mediating the SLR integrated retinotopic visual information with body configuration. Next, we studied the influence of planned movement trajectory, requiring participants to prepare and generate either curved or straight reaches in the presence of obstacles to attain the same visual stimulus location. We found that SLR magnitude was influenced by the planned movement trajectory to the same visual stimulus. On the basis of these results, we suggest that the circuit mediating the SLR lies in parallel to other well-studied corticospinal pathways. Although the fixed latency of the SLR precludes extensive cortical processing, inputs conveying information relating to task complexity, such as body configuration and planned movement trajectory, can pre-set nodes within the circuit underlying the SLR to modulate its magnitude.

3.2 Introduction

The reaction time (RT) needed to initiate a visually-guided action is a core measure in behavioural neuroscience (Luce 1986). In humans, visually-guided reaches from a static posture typically start within ~200-300 ms of stimulus presentation (Welford 1980), with RTs increasing for more complex tasks that require additional cortical processing (Donders 1969). A more precise measurement of RT can be obtained via electromyographic (EMG) recordings of limb muscle activity, which circumvent the electromechanical delays that arise between the neural command to initiate a movement and movement itself (e.g. due to the arm's inertia, Norman & Komi, 1979). In addition to the large and well-studied volley of neuromuscular activity that initiates the movement, a brief and small burst of activity occurs time-locked ~100 ms after novel visual stimulus presentation, regardless of the ensuing movement RT (Pruszynski et al. 2010). These visual stimulus-locked responses (SLRs) are directionally tuned, with EMG activity increasing or decreasing for stimulus locations to which the muscle would serve as an agonist or antagonist, respectively. Furthermore, the SLR persists toward the stimulus location even when movement is temporarily withheld (Wood et al. 2015) or proceeds in the opposite direction (Gu et al. 2016).

The SLR evolves during the earliest interval in which visual information can influence limb muscle recruitment, and its short latency limits the opportunity for extensive cortical processing. To better understand the properties of the circuit underlying this rapid sensorimotor transformation, we characterized the SLR

across three different visually guided reach experiments by altering task complexity. We studied whether the SLR was expressed in an eye- or hand-centred reference frame by dissociating initial eye and hand position (Experiment 1), and the influence of different pre-planned straight or curved movement trajectories on the SLR (Experiments 2 & 3). We found that while the SLR latencies remained constant in all three experiments, changes in SLR magnitude showed that the underlying circuit rapidly transforms retinotopic visual information into a hand-centred reference frame in a manner that is influenced by the planned movement trajectory.

3.3 Materials and Methods

In total, we had 30 participants (19 males, 11 females; mean age: 26 ± 5 years SD) performed at least one of the three experiments. All were self-declared right-handed except for two left-handed males and two left-handed females. All participants had normal or corrected-to-normal vision and reported no current visual, neurological, and/or musculoskeletal disorders. Participants provided written consent, were paid for their participation, and were free to withdraw from any of the experiments at any time. All procedures were approved by the Health Science Research Ethics Board at the University of Western Ontario. Parts of the apparatus, electromyography (EMG) recording setup, and data analyses have been previously described (Gu et al., 2016; Wood et al., 2015).

3.3.1 Apparatus and Kinematic Acquisition

Briefly, in all three experiments, participants performed reach movement in the horizontal plane with their right arm while grasping the handle of a robotic manipulandum (InMotion2, InMotion Technologies, Watertown, MA, USA). Participants sat at a desk and interacted with the robotic manipulandum with their elbow supported by a custom-built air-sled (see **Fig. 1a** of Wood et al. 2015). A constant load force of 5 N to the right was applied to increase the baseline activity for the limb muscle of interest for all three experiments. The x - and y - positions of the manipulandum were sampled at 600 Hz. All visual stimuli were presented onto a horizontal mirror, located just below the participant's chin level, which reflected the display of a downward-facing LCD monitor with a refresh rate of 75 Hz. The precise timing of visual stimulus onsets on the LCD screen were determined by a photodiode. The mirror occluded the participant's arm and visual feedback of the hand was given as a small red cursor.

3.3.2 EMG and EOG Acquisition

EMG activities from the clavicular head of the right pectoralis major (PEC) muscle were recorded using either intramuscular (Experiment 1) and/or surface recordings (all Experiments). Intramuscular EMG activity was recorded using fine-wire (A-M Systems, Sequim, WA, USA) electrodes inserted into the PEC muscle (see Wood et al., 2015 for insertion procedure). Briefly, for each recording we inserted two monopolar electrodes ~2.5 cm into the muscle belly of the PEC muscle, enabling

recording of multiple motor units. Insertions were aimed ~1 cm inferior to the inflection point of the participant's clavicle, and staggered by 1 cm along the muscle's fiber direction. All intramuscular EMG data were recording with a Myopac Junior System (Run Technologies, Mission Viejo, CA, USA). Surface EMG was recorded with doubled-differential electrodes (Delsys Inc., Natick, MA, USA), placed either near or at the same location as the intramuscular recordings. In Experiment 1, horizontal eye position was measured using bitemporal direct current electrooculography (EOG, Grass Instruments, Astro-Med Inc.). EMG and EOG data were digitized and sampled at 4 kHz.

3.3.3 Data Analyses

To achieve sample-to-sample matching between kinematic and EMG data, kinematic data were up-sampled from 600 Hz to 1000 Hz with a lowpass interpolation algorithm, and then lowpass-filtered with a second-order Butterworth filter with a cutoff at 150 Hz. Off-line, EMG data were rectified, and either bin-integrated into 1 ms bins (intramuscular) or down-sampled (surface) to match the 1000 Hz sample rate. Reach reaction times (RTs) were calculated as the time from the onset of the visual stimulus (measured by a photodiode) to the initiation of the reach movement. Reach initiation was identified by first finding the peak tangential movement velocity, and then moving backwards to the closest time-point at which the velocity profile reached 8% of the peak velocity. We defined the SLR epoch as 85 ms to 125 ms after stimulus onset. Trials with RTs less than 185 ms were

excluded to prevent contamination of the SLR epoch by recruitment associated with very short-latency responses (Wood et al. 2015; Gu et al. 2016). We also defined the voluntary movement (MOV) epoch as -20 to 20 ms around the reach RT.

To determine the normalized movement trajectory for Experiments 2 and 3, we first defined the movement duration for each trial individually. The movement duration was defined as 50 ms prior to when the hand position surpassed 2 cm from the centre of the start position to 50 ms after the time when the hand position surpassed 20 cm (14 cm for the Catch Trials in Experiment 3) from the centre of the start position. We then interpolated the movement duration into 101 equal time samples. Then for each normalized time sample we calculated the x - and y -positions to get the normalized movement trajectory for each trial.

3.3.4 SLR Detection and Latency Analysis

Based on previous works identifying the SLR (Corneil et al. 2004; Pruszynski et al. 2010), we used a receiver-operating characteristic (ROC) analysis to quantitatively detect the presence of a SLR. In all Experiments, we first separated the EMG activity for all correct control reaches based on visual stimulus location, and performed the following ROC analysis. For every time-sample (1 ms bin) between 100 ms before to 300 ms after visual stimulus onset, we calculated the area under the ROC curve. This metric indicates the probability that an ideal observer could discriminate the side of the stimulus location based solely on EMG activity. A value

of 0.5 indicates chance discrimination, whereas a value of 1 or 0 indicates perfectly correct or incorrect discrimination, respectively. We set the thresholds for discrimination at 0.6; these criteria exceed the 95% confidence intervals of data randomly shuffled with a bootstrap procedure (Chapman and Corneil 2011). The earliest discrimination time was defined as the time after stimulus onset at which the ROC was above 0.6 and remained above that threshold for at least 5 out of the next 10 samples. Based on the ROC analyses we defined the SLR epoch as from 85 to 125 ms after visual stimulus onset and categorized any participant with a discrimination time <125 ms as having a SLR (SLR+ participant). Across the 5 experiments we could reliably detect a SLR in 24 out of 30 participants (~80% detection rates). This rate is comparable to previous reports of the SLR detection on the limb with either intramuscular and surface recordings in this setup (Wood et al. 2015; Gu et al. 2016). To determine the onset latency of the SLR on the upper limb, we used the same procedure as previously described for SLR on neck muscle activity (Goonetilleke et al. 2015). Briefly, we used the same time-series ROC mentioned above and fit a two-piece piecewise linear regression (Cashaback et al. 2013). The first linear regression is based on baseline activity preceding any SLR (from 0 to 80 ms after stimulus onset) and the second linear regression is based on activity for candidate inflection point to the peak of the SLR (max ROC value in an interval from 80 to 140 ms). The inflection point was determined as the latency that minimized the sum of the squared error between the observed ROC curve and the two linear regressions. Relative to the ROC value at the inflection

point, the onset latency was the time where the ROC increased by 0.05 for the next 5 out of 10 samples.

3.3.5 Experiment 1: Reference Frame Task

To initiate each trial, participants ($N = 7/8$; 7 SLR+ participants) brought the cursor into a starting hand position (**Figure 3.1a**, green circle). After a randomized (0.5 - 1 sec) delay, participants had to look towards the starting eye position (red circle). three different initial positions were possible: either the hand and the eye were in line with the participant's midline (Position 1), or the hand was 10 cm to the right and the eye was 10 cm to left of midline (Position 2), or vice versa where the hand was 10 cm to the left and the eye was 10 cm to the right of midline (Position 3). After another randomized (1 - 1.5 sec) delay, a black visual stimulus appeared concurrently with the offset of both the starting hand and eye position stimuli. This served as the go cue to make a coordinated hand-eye movement towards the black visual stimulus. The black stimulus could be in one of three possible locations: either at the midline (Stim_C) or 20 cm to the left (Stim_L) or right of midline (Stim_R). Participants had to attain the stimulus location to start the next trial. In the case of Position 1 and Stim_C the participant did not have to move, hence the next trial started 1 sec after stimulus onset. If the participant moved their hand outside of the starting hand position at any point prior to the onset of the black stimulus, the trial was aborted and reset. Each participant performed 8 blocks, with each block consisted of 72 trials, in which the 9 different trial types (3 Start Positions x 3

Stimulus Locations) were tested pseudo-randomly 8 different times per block. For Stim_C in Position 1 participants were not required to move. To analyze the data during the presumed MOV epoch on these trials, we assumed that the RT for these trials would be from a similar distribution of RT as Stim_L and Stim_R reach movements. Thus, we randomly assigned a reach RT for each Stim_C trial from the pooled RT of Stim_L and Stim_R in Position 1.

3.3.6 Experiment 2: Obstacle Task

Each trial began with the appearance of a start position stimulus; on 2/3rd of all trials the gray visual obstacle was presented concurrently. No obstacle was presented on the other 1/3rd of trials, which served as a control condition. Two different sets of obstacles could appear, either a horizontal bar or two upside-down L-shape obstacles (**Figure 3.2**). To initiate the trial participants ($N = 15/20$ SLR+) moved the cursor into the start position. After a variable delay (1 - 1.25 sec) a black peripheral stimulus appeared 20 cm from the position, at either a left-outward (135° CCW from straight right) or right-outward (45° CCW) location away from the participant. The start position was extinguished simultaneously with the presentation of the peripheral stimulus. Participants then had to move the cursor as quickly as possible to the peripheral stimulus. Each participant performed four blocks; in two blocks participants were instructed to avoid the gray obstacles while in the other two blocks they were instructed to reach through the obstacles when reaching for the peripheral stimulus. The order of instruction was counterbalanced

across our participants. Each block consisted of 150 trials in total, with 25 trials for each of the 6 different conditions.

3.3.7 Experiment 3: Choice Task

Each trial began with the appearance of a start position stimulus and a gray obstacle (**Figure 3.3a**). To initiate the trial participants ($N = 14/15$ SLR+) moved the cursor into the start position. After a variable delay (1 - 1.25 sec) the start position was extinguished simultaneously with the presentation of the peripheral black visual stimulus. On Test Trials ($2/3^{\text{rd}}$ of all trials) the peripheral stimulus was presented 20 cm left-outward from the start position (135° CCW), while in Catch Trials ($1/3^{\text{rd}}$ of all trials) the peripheral stimulus was presented 14 cm from the start position directly outward (90° CCW) or leftward (180° CCW) with equal likelihood. Participants were instructed to move the cursor as quickly as possible to the peripheral stimulus, while avoiding the gray obstacle by choosing the shortest movement trajectory. The shape of the gray obstacle varied on a trial-by-trial basis but the overall area remained constant. The obstacle shape displayed was based on an adaptive estimation of the psychometric function for each participant. We assumed that the psychometric function of the choice of the movement trajectory around the obstacle took the form of a logistic function (**Equation 3-1**).

$$p(x) = \frac{1}{1 + e^{\beta(x-\alpha)}} \quad \text{(Equation 3-1)}$$

in which x was the shape of the obstacle (ranging from a purely horizontal bar, $x = -68$, through L-shaped obstacles, through to a vertical bar, $x = 68$; for shapes see x -axis of **Figure 3.3b**); $p(x)$ indicated the probability of leftward curved reach around the obstacle for the given midpoint of the obstacle; and α and β were the threshold and the slope of the logistic function. To estimate this function, we used a modified updated maximum likelihood procedure (Shen and Richards, 2012), with the parameter space consisting of a grid of α and β values. The α parameter spanned 69 values ranging from -68 to 68 in 2 unit increments. The β parameter spanned value ranging from 0 to 0.5 in 0.05 increments. A uniform prior ($\alpha, \beta = 0$) was used for the 1st block, while subsequent blocks used the estimated parameters from the last trial of the previous block. To initialize each block, the first 5 trials had obstacles that were at the: 0th, 100th, 50th, 25th, and 75th percentiles ($x = -68, 68, 0, -34, 34$ unit, respectively). Afterwards, the obstacle shape was set either at the estimated threshold, $p(x) = 0.5$, or at either the lower, $p(x) = 0.25$, or upper deflections, $p(x) = 0.75$, in a pseudorandom order at a 2:1:1 ratio. Test, Catch leftward, and Catch rightward Trials were also presented in a pseudorandom order at a 4:1:1 ratio, respectively. Each participant performed 6 blocks, except for 1 who performed 5 blocks, with each block consisting of 197 trials: 5 initial trials, 128 Test, 32 Catch leftward and outward Trials. All participants had at least 100 correct Test Trials for the threshold visual obstacle, at which $p_{(leftward)}$ was closest to 0.5.

3.3.8 Experimental Design and Statistical Analysis

All statistical analyses were performed with custom-written script in Matlab (version R2014b, Mathworks Inc, Natick, MA, USA). In Experiment 1, the within subject analysis was a 2-way ANOVA, with the mean factors of start position and stimulus location, while the between subject analysis was a 1-way ANOVA for the mean adjusted normalized EMG activity of each start position. In Experiment 2, the within subject analysis was a 2-way ANOVA, with the mean factors of stimulus location and movement trajectory, while the between subject analysis was a 1-way ANOVA of the normalized EMG activity for movement trajectory. Finally, in Experiment 3, for both within and between subject analyses, we performed a 2-way ANOVA, with the mean factors of initial reach direction (i.e. leftward or outward) and movement trajectory (i.e. straight or curved). The level of significance was set to $P < 0.05$ at the group level, and $P < 0.05$ post-hoc Tukey's HSD corrected.

3.4 Results

In total 30 participants took part in at least one of the three experiments (42 separate sessions in total). Across, our three experiments, a reliable SLR was detected in 24 out of 30 participants (SLR+, 80%) participants (see **Materials and Methods** for detection criteria). This SLR detection rate was similar to our previous studies (Wood et al. 2015; Gu et al. 2016). Data from participants that did not exhibit a SLR were excluded from all subsequent analyses.

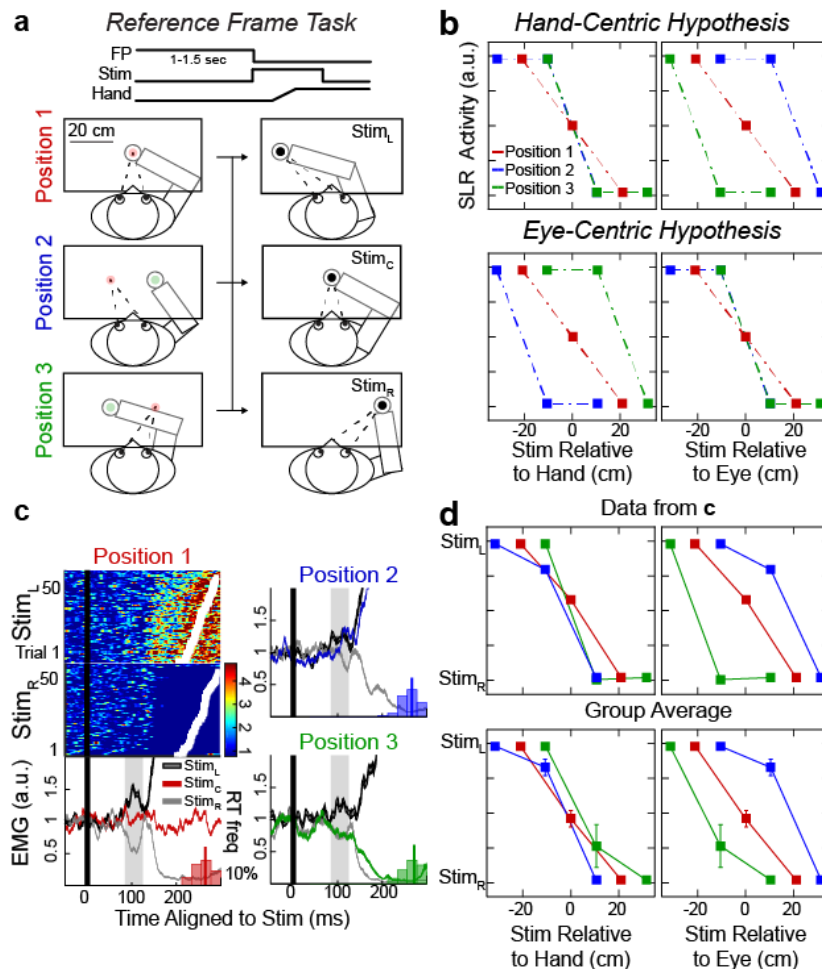


Figure 3.1: The SLR generates a motor command toward the visual stimulus in a hand-centric reference frame

(a) Experimental paradigm. Participants started in 1 of 3 different initial positions, and moved both their eyes and right hand to a black visual stimulus. (b) These various initial positions and stimulus locations allowed us to predict SLR magnitude as either a function of stimulus location relative to either the hand (hand-centric, top) or the eye (eye-centric reference frame, bottom panels). (c) Individual and mean EMG activity from a participant. The colour subpanels are individual Stim_L and Stim_R trials from Position 1. Each row represents EMG activity from a single trial, with all trials aligned to stimulus onset (black line) and sorted based on reach RT (white squares). All other subpanels represent mean EMG activities for correct trials, segregated by initial position and stimulus location. Overlaid on top of each mean EMG plot are the RT distribution (bar) and median RT (vertical line) for each position. Shaded boxes indicate the SLR epoch. (d) The participant for c. (top) and the group ($n = 7$, bottom panels) mean adjusted normalized SLR magnitudes conform to the prediction of a hand-centric reference frame.

3.4.1 The SLR encodes stimulus location relative to hand, not eye, position

Although previous studies have reported that SLRs are tuned to the position of the visual stimulus (Pruszynski et al. 2010; Wood et al. 2015; Gu et al. 2016), these studies did not manipulate the initial position of the eyes and hand and thus could not differentiate whether the SLR encoded stimulus position relative to the eye or hand. The underlying reference frame of the SLR may start to reveal the underlying neural circuitry since many fMRI and neurophysiological studies have shown that visual stimuli can be encoded in different reference frames throughout the parietal and motor cortices (Batista et al. 1999; Buneo et al. 2002; Medendorp et al. 2003; Crawford et al. 2004; Pesaran et al. 2006).

In Experiment 1, we assessed if the SLR encoded stimulus location relative to the eye (an *eye-centric*) or the hand position (a *hand-centric* reference frame). Participants ($N = 7/8$, 7 SLR+ participants) began each trial in 1 of 3 initial positions (**Figure 3.1a**), with either the hand and eye in line with the participant's midline (Position 1, red), with either the hand 10 cm right and the eye 10 cm left of midline (Position 2, blue), or with the hand 10 cm left and the eye 10 cm right of midline (Position 3, green). Participants then made a coordinated hand-eye movement towards a black visual stimulus that appeared either 20 cm left (Stim_L), 20 cm right (Stim_R), or at the midline (Stim_C). These various initial positions and stimulus locations allowed us to predict SLR magnitude as a function of stimulus location

relative to either the hand or eye position (**Figure 3.1b**). Note that if the SLR magnitude is plotted as a function of stimulus eccentricity in the correct reference frame, then such functions should overlap for the three different starting positions. In contrast, such functions should be staggered if plotted in the incorrect reference frame (**Figure 3.1b**).

Figure 3.1c shows a participant's EMG activity aligned to visual stimulus onset (black line) from all 3 initial positions. Trials were segregated based on initial position and visual stimulus location. EMG activity was normalized to baseline activity (mean EMG activity 41 ms prior to stimulus onset) for each position separately. In Position 1, similar to previous reports, we observed a reliable difference in SLR magnitude (shaded box spanning 85-125 ms after stimulus onset, left bottom panel) between Stim_L and Stim_R trials (2-way ANOVA – start position and stimulus location, interaction effect, $F_{(4,553)} = 4.88$, $P = 0.0007$, post-hoc Tukey's HSD, $P < 10^{-7}$). This increase and decrease in EMG activity could also be seen on individual EMG traces from the Stim_L and Stim_R trials, respectively (top-left and middle-left panels). The SLR was relatively brief and evolved before the much larger change in EMG activity associated with either the leftward or rightward reach movement (RTs denoted by white squares). The SLR persisted in the other 2 initial Positions, with SLR magnitude being reliably greater for Stim_L compared to Stim_R trials (**Figure 3.1c**, $P = 0.0002$ and $P < 10^{-6}$, for Positions 2 and 3, respectively). Across our participants, we found no difference in the onset latency of the SLR for Stim_L and Stim_R trials between when the hand and eye started in

the same (Position 1, mean \pm SEM latency = 87.4 ± 1.2 ms) versus different locations (Positions 2 and 3, 86.7 ± 2.2 ms; paired t -test, $t_{(6)} = 0.28$, $P = 0.79$), even though the median RTs were slightly shorter when the eye and hand started at the same (272.4 ± 9.4 ms) versus different positions (286.0 ± 11.2 ms; paired t -test, $t_{(6)} = -3.1$, $P = 0.02$).

In Positions 2 and 3, the Stim_C trials (colour trials) can be used to differentiate between hand-centric and eye-centric reference frames, since the stimulus falls between the initial positions of the hand and eye. In Position 2, SLR magnitude increased relative to the baseline activity by an equal amount for both Stim_C and Stim_L trials ($P = 0.89$), when the stimulus fell to the left of the hand. In Position 3, SLR magnitude decreased by an equal amount for both the Stim_C and Stim_R trials ($P = 0.99$), when the stimulus fell to the right of the hand. Thus, for this participant, the pattern of SLR magnitudes was consistent with a hand-centric reference frame. To account for the differences in SLR magnitude for each Position and across our participants, we scaled the SLR magnitude for Stim_C trials based on the SLR magnitudes observed for Stim_L and Stim_R trials (+1, -1 a.u., respectively). This allowed us to test our data against the 2 initial predictions, expressing the adjusted normalized SLR magnitudes aligned to stimulus location relative to either the hand or eye position for this participant (top row, **Figure 3.1d**) and across the group (bottom row). Our results clearly indicate that the SLR is encoded in a hand-centric reference frame (compare to the *hand-centric hypothesis* in **Figure 3.1b**). Across the group, we found reliably greater SLR

magnitudes for Stim_C trials in Position 2 compared to Position 3 (repeated measures 1-way ANOVA - start position, $F_{(2,12)} = 10.51$, $P = 0.002$, post-hoc Tukey's HSD, $P = 0.002$). We found a similar response pattern during the MOV epoch, where Position 2 evoked a greater MOV response compared to Position 3 ($F_{(2,12)} = 315.9$, $P < 10^{-10}$, post-hoc Tukey's HSD, $P < 10^{-8}$). This result suggests that, despite its short latency, the circuit mediating the SLR rapidly integrates visual stimulus location and the underlying body position, generating a motor command in a hand-centric reference frame.

3.4.2 Movement trajectory influences SLR magnitude for reaches to the same visual stimulus

Given that the SLR encoded the visual stimulus relative to the current hand position, we next examined if the SLR simply encoded visual stimulus location in space, or if it is influenced by the planned movement trajectory. To start differentiating these two possibilities, in Experiment 2, participants ($N = 15/20$ SLR+) performed either curved or straight reaches to two potential visual stimulus locations. In different blocks, participants were instructed to either avoid or reach through different visual obstacles to attain the left-outward or right-outward visual stimulus. Except for control trials without the obstacle, obstacles were present at trial onset so that participants could plan their trajectory to the two potential stimulus locations. **Figure 3.2** shows the mean normalized movement trajectories

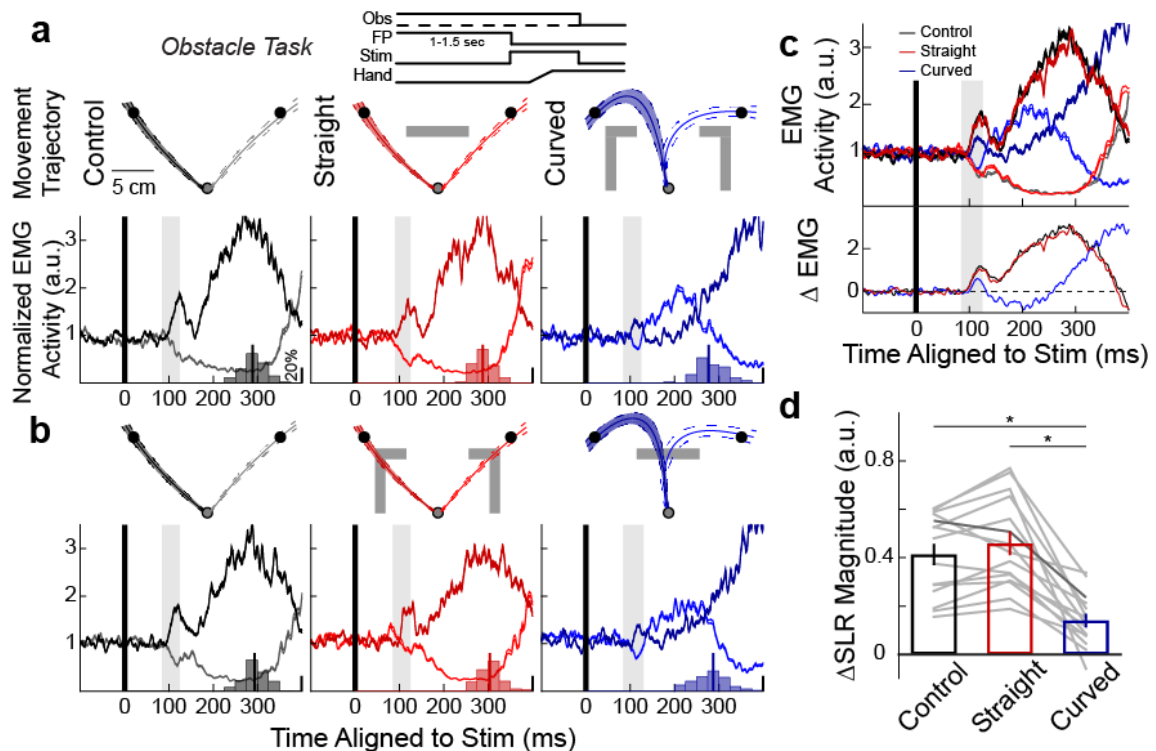


Figure 3.2: Decreased SLR magnitude for curved compared to straight reaches to the same visual stimulus

(a,b) Kinematic and EMG data from a participant during the obstacle task when instructed to avoid or reach through the visual obstacle (gray rectangles). Left-outward (dark) and right-outward (light shaded contours) reach trials were segregated by movement trajectory: reaches with no obstacles (Control – black), straight reaches with obstacles (Straight – red), or curved reaches with obstacles (Curved – blue). All obstacles were shown to the participants for at least 1 sec prior to the onset of the peripheral visual stimulus. Top panels show the mean \pm SD normalized movement trajectories for each condition, while the bottom panels show the corresponding mean \pm SEM EMG activities aligned to stimulus onset, with the SLR epoch highlighted (shaded boxes). Overlaid on top of each mean EMG plot are the RT distribution (bar) and median RT (vertical line) for condition. (c) Top subpanel shows the same EMG data as a and b, but combining EMG data for the three difference movement trajectories regardless of visual obstacle and task instruction. Bottom subpanel shows the difference in mean EMG activity (Δ EMG) between left-outward and right-outward reach trials for the three trajectories. (d) Group mean \pm SEM of the Δ EMG during the SLR epoch (Δ SLR magnitude) for the three different movement trajectories. Each gray line represents an individual participant, with the darker line representing data from the participant in c. * $P < 0.0001$.

and EMG activities when a participant either avoided (**Figure 3.2a**) or reached through (**Figure 3.2b**) the obstacle. Trials were categorized based on movement trajectories: straight with no obstacle (Control - black), straight either avoiding or reaching through an obstacle (Straight - red), or curved either avoiding or reaching through an obstacle (Curved - blue). When categorized this way, we found no reliable difference in mean SLR magnitude across our sample for avoiding compared to reaching through the different visual obstacles (repeated measures 3-way ANOVA – stimulus location, trajectory, and instruction, main effect for instruction $F_{(1,161)} = 0.04$, $P = 0.85$). Thus, all subsequent analyses examined mean SLR magnitudes as a function of stimulus location and movement trajectory.

Figure 3.2c shows the same participant's EMG data, but now with the EMG activity combined between the two different instructions (top panel). To compare the difference in SLR magnitude (Δ SLR magnitude) between curved and straight reach trials, we calculated the mean EMG difference between left-outward and right-outward stimulus locations (bottom panel) during the SLR epoch for the three different movement trajectories. Once again, across our participants we could not find a difference in SLR latency between Straight and Curved trajectories (95.1 ± 1.6 ms and 99.8 ± 2.8 ms, paired t -test, $t_{(14)} = -1.9$, $P = 0.07$). Note the increase in SLR latency compared to Experiment 1 is probably due to the change in stimulus locations, as left- and right-outward are not the PD and non-PD of the SLR (Pruszynski et al. 2010). Instead, we did find a reliable decrease in Δ SLR magnitude for Curved reaches compared to both Control and Straight reaches

(**Figure 3.2d**, repeated measures 1-way ANOVA – movement trajectory, $F_{(2,28)} = 37.13$, $P < 10^{-7}$, post-hoc Tukey's HSD, both $P < 10^{-6}$). The decrease in Δ SLR magnitude between Curved and Straight reaches was likely not due to a potential confound of increased RTs (Pruszynski et al. 2010; Gu et al. 2016), as Curved reaches had shorter median RTs than Straight reaches (268.1 ± 6.6 ms and 277.3 ± 6.4 ms, respectively, paired t -test, $t_{(14)} = 2.76$, $P = 0.015$). Next, we re-examined the EMG activity during the MOV epoch. As expected given the initial outward trajectory for the Curved reaches, which is associated with less PEC muscle recruitment, EMG activity for the MOV response was also attenuated for Curved compared to Control and Straight reaches (repeated measures 1-way ANOVA $F_{(2,28)} = 30.54$, $P < 10^{-7}$, post-hoc Tukey's HSD, both $P < 10^{-5}$). However, it was not the case that EMG activity during the SLR simply correlated with a given initial movement trajectory, as the SLR still differed between left-outward versus right-outward stimulus locations for curved reaches (**Figure 3.2b**). These results suggest that the SLR is not simply encoding either the spatial location of a stimulus or the movement trajectory, but rather that the SLR to a given stimulus location is modulated by the planned movement trajectory.

3.4.3 Initial movement trajectory, not task demands, influences SLR magnitude for curved reaches

A potential confound in Experiment 2 was the overall difference in task demand related to planning a curved versus a straight reach movement. Previous work has

shown that curved reaches were more task demanding than straight point-to-point reaches (Wong et al. 2016), and we previously showed that SLR magnitude decreased with increase task demands, i.e. when participants had to move away rather than towards a visual stimulus (Gu et al. 2016). In Experiment 3, we controlled for task demand by having participants ($N = 14/15$ SLR+) perform two different curved reach trajectories to attain the same visual stimulus (**Figure 3.3a**). At the beginning of each trial a visual obstacle, which participants were instructed to avoid, was shown. In Test Trials, participants made either an initially leftward (dark) or outward (light red) curved movement to a left-outward stimulus. We varied the shape of the obstacle on a trial-by-trial basis (see **METHODS: Experiment 3** for exact detail). **Figure 3.3b** shows the probability of a leftward Curved reach as a function of the possible obstacle shape. The obstacle where $p_{(\text{leftward})} \approx 0.5$ was preferentially sampled and termed the threshold obstacle (filled circle). In addition, we interleaved Catch Trials so that participants made straight leftward (black) and outward (gray) movements that had similar initial trajectories as the curved movements (see insert for movement trajectories in **Figure 3.3c, e**). Once again, we found no difference in the SLR latency for Curved vs Catch trials (95.9 ± 1.3 ms and 101.3 ± 4.1 ms, respectively, paired t -test, $t_{(13)} = 1.33$, $P = 0.21$).

To analyze this dataset, we first pooled all correct trials together regardless of the obstacle's shape for a single participant. On Catch Trials, the SLR magnitude was greater for leftward compared to outward straight reaches (**Figure 3.3c**, 2-way ANOVA – initial direction and trajectory type, interaction effect, $F_{(1,1113)}$

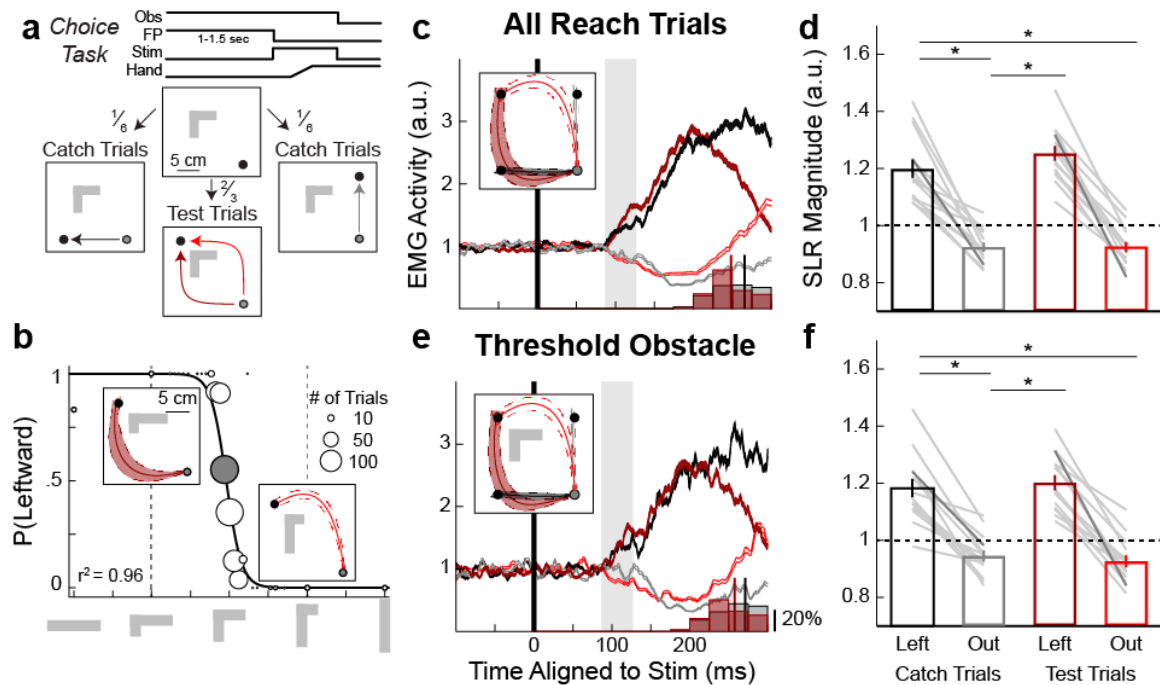


Figure 3.3: SLR magnitude modulated by pre-planned movement trajectory

(a) Experiment paradigm. Participants were instructed to reach to a visual stimulus using the shortest movement trajectory while avoiding an obstacle. The shape of the obstacle varied on a trial-by-trial basis. For Test Trials, participants made either initially curved leftward (dark red) or outward (light red) reaches toward a left-outward visual stimulus. For Catch Trials, participants reached straight leftward (black) or outward (gray). Once again, the obstacle was presented at least 1 sec prior to the onset of peripheral visual stimulus. (b) Behavioural performance for all Test Trials from a participant. The probability of an initial leftward curved reach is plotted as a function of obstacle shape. Insert shows the mean \pm SD normalized movement trajectories for two different obstacle shapes. Black line is the best fit of the participant's behaviour. (c, e) The participant's mean EMG \pm SEM different reach types for all reach trials (c) and for the threshold obstacle (e, shaded circle from b) aligned to stimulus onset. Overlaid on top of each mean EMG plot are the RT distribution (bar) and median RT (vertical line) for curved and straight reaches. Group mean \pm SEM of SLR magnitudes for all reach trials (c) and for the threshold obstacle (f) for the 4 different reach conditions. Each gray line represents an individual participant, with the darker line indicating data from the participant in b. * $P < 10^{-6}$.

= 5.31, $P = 0.02$, post-hoc Tukey's HSD, $P < 10^{-8}$). Similarly, on Test Trials the SLR magnitude was also greater for leftward compared to outward curved reaches ($P < 10^{-8}$). When we compared reaches with the same initial movement trajectory (straight vs curved reaches), we found no reliable difference in SLR magnitudes for both initially leftward and outward reaches ($P = 0.15$ and $P = 0.68$, respectively). To further examine the influence of the planned movement trajectories on the SLR magnitude, we next examined trials at the threshold obstacle, where the exact same visual obstacle was presented and the participant generated leftward or outward curved movement trajectories approximately half the time ($p_{(\text{leftward})} = 0.55$, filled circle in **Figure 3.3b**). As before, the SLR magnitude was greater for leftward versus outward reaches for both Catch and Test Trials, (**Figure 3.3e**, 2-way ANOVA, interaction effect, $F_{(1,279)} = 41.4$, $P < 10^{-9}$, post-hoc Tukey's HSD, $P < 10^{-8}$ and $P = 0.03$, respectively). Furthermore, the SLR magnitudes were not different for straight versus curved reaches with the same initial trajectory ($P = 0.31$ and $P = 0.78$, for initially leftward and outward reaches, respectively).

We observed the same pattern of SLR magnitude modulation based on initial movement trajectory across our participants: SLR magnitude was greater for leftward versus outward reaches when pooled for all obstacles (**Figure 3.3d**) and for the threshold obstacle (**Figure 3.3f**, repeated measures 2-way ANOVA, main effect of direction, $F_{(1,13)} = 129.3$ and 143.7 , respectively, both $P < 10^{-7}$, post-hoc Tukey's HSD, all $P < 10^{-4}$). Again, we found no differences in SLR magnitude for the same initial movement trajectory (all $P > 0.38$). Thus, even when we controlled

for task demand by having participants perform curved reaches with different initial trajectories to the same visual stimulus location, we found that the SLR was still modulated by the initial movement trajectory. Likewise, when we re-examined the data for the MOV response we found increased PEC muscle recruitment for leftward versus outward movement trajectories (repeated measures 2-way ANOVA, main effect of direction, $F_{(1,13)} = 66.61$ and 77.21 , respectively, both $P < 10^{-5}$, post-hoc Tukey's HSD, all $P < 10^{-5}$). Thus, SLR magnitude for the same visual stimulus is modulated by the initial planned movement trajectory.

3.4.4 SLR magnitude during Catch Trials were modulated based on the pre-planned movement

Finally, to further demonstrate that the SLR magnitude was modulated based on the pre-planned movement we further examined the SLR on Catch Trials. Recall that Catch trials were randomly interleaved throughout the experiment, appearing at the Leftward or Outward locations regardless of obstacle shape. Given that the obstacle was present at the start of the trial, Catch trials could be classified as being either congruent (i.e. the pre-planned movement was in the same direction as the Catch Trial) or incongruent (i.e. in the opposite direction; **Figure 3.4a**). For example, obstacles more horizontal than the threshold obstacle (light grey shaded region in **Figure 3.4a**) were congruent for Leftward and incongruent for Outward Catch Trials. In contrast, obstacles more vertical than the threshold obstacle (non-

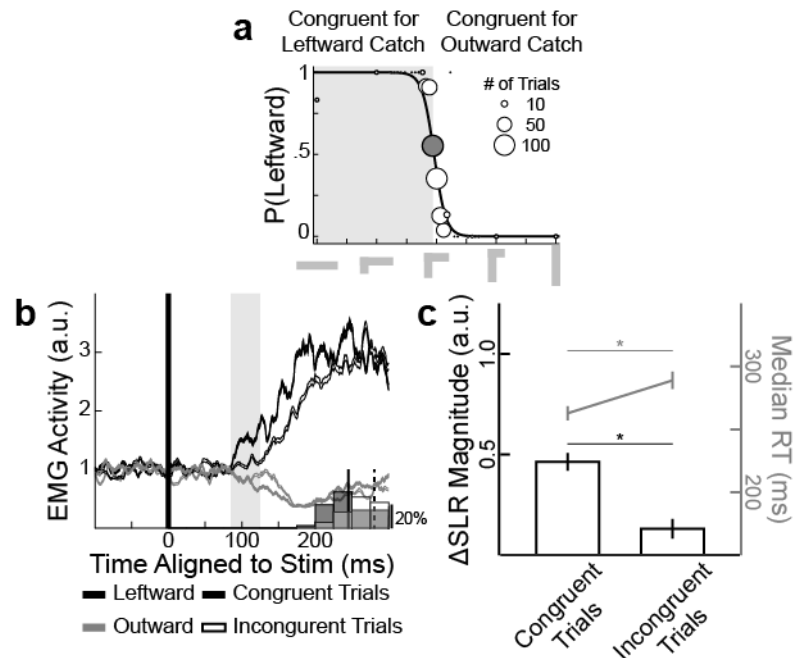


Figure 3.4: SLR magnitude and RT modulation for Catch Trials based on obstacle shape
 (a) Catch Trials were separated into Congruent and Incongruent Catch Trials. For example, leftward Congruent and Incongruent Trials were any trials with an obstacle more horizontal (gray shaded region) and vertical (non-shaded region) than the threshold obstacle (filled circle), respectively. (b) Mean for Congruent (filled) and Incongruent (open) Catch Trials sorted by either Leftward (black) or Outward (gray) stimulus location from the same participant as in **Figure 3.3**. Overlaid on top of each mean EMG plot are the RT distribution (bar) and median RT (vertical line) for curved and straight reaches. (c) The mean \pm SEM Δ SLR magnitude (Leftward – outward, black) and median RT (gray) for both Congruent and Incongruent Trials across our participants. * $P < 10^{-4}$.

shaded region in **Figure 3.4a**) were congruent to Outward and incongruent to Leftward Catch Trials.

Figure 3.4b shows the mean EMG activity for all Catch Trials when we separated for both direction (Leftward – black and Outward – gray) and congruency (Congruent – filled and Incongruent – open). Note that we observed a reliable difference in EMG activity during the SLR epoch for both Congruent and Incongruent Trials, but the magnitude of the SLR was smaller for incongruent trials.

Figure 3.4c shows the mean Δ SLR magnitude (black bars, Leftward – Outward

Catch Trials) and median RT (gray line) across all our participants, for Congruent and Incongruent trials. We found a reliably larger Δ SLR magnitude for Congruent compared to Incongruent Trials (paired t -test, $t_{(13)} = 6.88$, $P < 10^{-4}$), but the Incongruent Δ SLR magnitude was still present (one-sample t -test, $t_{(13)} = 2.71$, $P = 0.018$). Consistent with the changes in Δ SLR magnitude, we also observed difference in the ensuing RT, where participants had substantially shorter RTs for Congruent compared to Incongruent Trials (262.8 ± 5.7 and 288.9 ± 6.9 ms, respectively, paired t -test, $t_{(13)} = -6.55$, $P < 10^{-4}$).

3.5 Discussion

Here, we characterized the visual stimulus-locked response (SLR) on the human pectoralis major muscle during three different visually-guided reach tasks. Previous work has shown that the SLR is the first wave of muscle recruitment that is evoked by the onset of a novel visual stimulus, occurring within 100 ms of stimulus onset and preceding the larger volley of EMG activity associated with movement initiation (Pruszynski et al. 2010; Wood et al. 2015). The design of each task was based on earlier work conducted in either human or non-human primates, allowing for a direct comparison of SLR measurements to neurophysiological and behavioural concepts of sensorimotor control of reaching. The outcomes of these three experiments can be summarized into 3 main points. First, the onset latency of the SLR does not change with increases in task complexity during any of the three experiments. Second, the SLR is directionally tuned to the stimulus location

relative to the hand, not eye, position. Finally, the SLR magnitude is influenced by, but not completely determined by, the pre-planned initial movement trajectory.

There are many similarities between the SLR's visuomotor properties, which is evoked from a static posture, and rapid online corrective reaching movements to displaced visual (Gaveau et al. 2014) or tactile stimuli (Pruszynski et al. 2016). For example, the ~100 ms latency of the SLR is consistent with previous reports of EMG response latencies to a displaced visual stimulus (Soechting and Lacquaniti 1983; Fautrelle et al. 2010), and occurs early enough to change reach kinematics within ~150 ms (Carlton 1981). Like the SLR, the latency of the online corrective movement is not modulated by changes in task demand (Oostwoud Wijdenes et al. 2011; Franklin et al. 2016). In an anti-reach paradigm, both the SLR (Gu et al. 2016) and the initial trajectory of the corrective movements (Day and Lyon 2000) are invariably directed towards the stimulus, even though the participants eventually moved in the opposite direction. Additionally, both the SLR (**Figure 3.1**) and corrective movements (Diedrichsen et al. 2004) are encoded in a hand-centric reference frame, reflecting stimulus location relative to the hand regardless of current eye position. Given the similarities between the SLR and corrective reach movements, we suggest that both are driven by a fast visuomotor system that lies in parallel to the well-studied corticospinal pathways (Alstermark and Isa 2012).

It is tempting to speculate about the pathway that could be underlying the SLR, and by extension, corrective reach movements. Our findings are consistent with previous suggestions that corrective movements are mediated by visual inputs

relayed through the superior colliculus (SC) via the reticulospinal pathway (Day and Brown 2001; Reynolds and Day 2012). For example, many neurons in intermediate and deep layers of the SC discharge a volley of action potentials with 50 ms of visual stimulus onset (Wurtz and Goldberg 1972) that depends on the integrity of the lateral geniculate nucleus and primary visual cortex (Schiller et al. 1979). Moreover, axons of these visually-responsive SC neurons contribute to the descending predorsal bundle that branches into the reticular formation (Rodgers et al. 2006), leading to SLRs on neck muscles that promote orienting head movements (Corneil et al. 2004, 2008; Rezvani and Corneil 2008). In addition to its role in oculomotor control, the SC also plays a more general role in whole-body orienting (Gandhi and Katnani 2011; Corneil and Munoz 2014) and proximal limb control (Lünenburger et al. 2001). Stimulation (Philipp and Hoffmann 2014) and chemical inactivation (Song et al. 2011) of the SC can influence reaching behaviour in non-human primates, in line with human imaging studies of selective SC BOLD-activation during reaching tasks (Linzenbold and Himmelbach 2012; Himmelbach et al. 2013). Reach-related SC neurons can also exhibit similar short-latency visual responses (Song and McPeck 2015), and movement-related activity correlates with recruitment of proximal limb muscle activity (Werner et al. 1997; Stuphorn et al. 1999). Furthermore, like the SLR, a subset of these neurons operate in a hand-centric reference frame (Stuphorn et al. 2000).

Others have proposed that corrective movements are mediated through a cortical pathway, specifically via the posterior parietal cortex (PPC) (Desmurget et

al. 1999; Pisella et al. 2000). The ~100 ms latency of the SLR and its expression in hand-centric reference frame are both inconsistent with the known properties of PPC activity. For example, the SLR latency in the human limb occurs at, or around the same time, as the peak of the visual response of the monkey PPC (Snyder et al. 1998). Most of these visual responses are also not encoded in a hand-centric reference frame that we observed with the SLR (Batista et al. 1999; Buneo et al. 2002). Thus, while the PPC may be involved in the later phases of online corrections (Franklin et al. 2016), it seems unlikely that the PPC is involved in generating the SLR. Additionally, while primary motor cortex and premotor cortex do exhibit rapid visual transient responses (Kwan et al. 1981; Weinrich and Wise 1982), a recent study has suggested that these visual transient responses do not affect the neural output in both primary and premotor cortices (Stavisky et al. 2017).

Finally, the results shown in Experiments 2 and 3 demonstrate that advanced planning of a movement trajectory can influence SLR magnitude. In both experiments, participants viewed an obstacle with which they either had to avoid or intersect for an extended period of time prior to the presentation of the visual stimulus. Moreover, the stimuli could only appear at a limited number of locations (two and three for Experiments 2 and 3, respectively). The influence of such advanced planning on the SLR is particularly apparent in Catch Trials in Experiment 3, where ‘Congruent’ stimulus location in line with the initial phase of the planned curved trajectory evoked a larger SLR than ‘Incongruent’ stimulus location (**Figure 3.4**). Importantly, such advanced planning did not influence

baseline EMG activity just before the SLR epoch. Previous neurophysiological studies have shown anticipatory build-up neural activity well before movement onset to both spatial and non-spatial cues throughout the primary (Tanji and Evarts 1976; Confais et al. 2012) and premotor cortices (Mauritz and Wise 1986; Cisek and Kalaska 2005), as well as within the PPC (MacKay and Crammond 1987; Snyder et al. 2006); however, such anticipatory activity did not lead to EMG recruitment. Further, other studies have also shown that advanced planning of multiple alternatives did not lead to increased EMG activity or behavioural output during the planning phase (Cisek and Kalaska 2005; Klaes et al. 2011; Stewart et al. 2014). Instead, we speculate that anticipatory signals from higher-order skeletomotor regions are relayed to the SC (Fries 1984, 1985; Distler and Hoffmann 2015), providing a means to pre-set SC activity prior to the arrival of visually-related information, so that the resulting SLR reflects both stimulus location relative to the hand and the pre-selected motor plan.

3.6 References

- Alstermark B, Isa T. Circuits for skilled reaching and grasping. *Annu Rev Neurosci* 35: 559–578, 2012.
- Batista AP, Buneo CA, Snyder LH, Andersen RA. Reach plans in eye-centered coordinates. *Science* 285: 257–260, 1999.
- Buneo CA, Jarvis MR, Batista AP, Andersen RA. Direct visuomotor transformations for reaching. *Nature* 416: 632–636, 2002.
- Carlton LG. Processing visual feedback information for movement control. *J Exp Psychol Hum Percept Perform* 7: 1019–1030, 1981.

- Cashaback JGA, Cluff T, Potvin JR. Muscle fatigue and contraction intensity modulates the complexity of surface electromyography. *J Electromyogr Kinesiol* 23: 78–83, 2013.
- Chapman BB, Corneil BD. Neuromuscular recruitment related to stimulus presentation and task instruction during the anti-saccade task. *Eur J Neurosci* 33: 349–360, 2011.
- Cisek P, Kalaska JF. Neural Correlates of Reaching Decisions in Dorsal Premotor Cortex: Specification of Multiple Direction Choices and Final Selection of Action. *Neuron* 45: 801–814, 2005.
- Confais J, Kilavik BE, Ponce-Alvarez A, Riehle A. On the anticipatory precue activity in motor cortex. *J Neurosci* 32: 15359–15368, 2012.
- Corneil BD, Munoz DP. Overt Responses during Covert Orienting. *Neuron* 82: 1230–1243, 2014.
- Corneil BD, Munoz DP, Chapman BB, Admans T, Cushing SL. Neuromuscular consequences of reflexive covert orienting. *Nat Neurosci* 11: 13–15, 2008.
- Corneil BD, Olivier E, Munoz DP. Visual responses on neck muscles reveal selective gating that prevents express saccades. *Neuron* 42: 831–841, 2004.
- Crawford JD, Medendorp WP, Marotta JJ. Spatial transformations for eye-hand coordination. *J Neurophysiol* 92: 10–19, 2004.
- Day BL, Brown P. Evidence for subcortical involvement in the visual control of human reaching. *Brain* 124: 1832–1840, 2001.
- Day BL, Lyon IN. Voluntary modification of automatic arm movements evoked by motion of a visual target. *Exp Brain Res* 130: 159–168, 2000.
- Desmurget M, Epstein CM, Turner RS, Prablanc C, Alexander GE, Grafton ST. Role of the posterior parietal cortex in updating reaching movements to a visual target. *Nat Neurosci* 2: 563–567, 1999.
- Diedrichsen J, Nambisan R, Kennerley SW, Ivry RB. Independent on-line control of the two hands during bimanual reaching. *Eur J Neurosci* 19: 1643–1652, 2004.

- Distler C, Hoffmann K-P. Direct projections from the dorsal premotor cortex to the superior colliculus in the macaque (*macaca mulatta*). *J Comp Neurol* 523: 2390–2408, 2015.
- Donders FC. On the speed of mental processes. *Acta Psychol (Amst)* 30: 412–31, 1969.
- Fautrelle L, Prablanc C, Berret B, Ballay Y, Bonnetblanc F. Pointing to double-step visual stimuli from a standing position: very short latency (express) corrections are observed in upper and lower limbs and may not require cortical involvement. *Neuroscience* 169: 697–705, 2010.
- Franklin DW, Reichenbach A, Franklin S, Diedrichsen J. Temporal Evolution of Spatial Computations for Visuomotor Control. *J Neurosci* 36: 2329–2341, 2016.
- Fries W. Cortical projections to the superior colliculus in the macaque monkey: a retrograde study using horseradish peroxidase. *J Comp Neurol* 230: 55–76, 1984.
- Fries W. Inputs from motor and premotor cortex to the superior colliculus of the macaque monkey. *Behav Brain Sci*.
- Gandhi NJ, Katnani HA. Motor functions of the superior colliculus. *Annu Rev Neurosci* 34: 205–231, 2011.
- Gaveau V, Pisella L, Priot A-E, Fukui T, Rossetti Y, Pélisson D, Prablanc C. Automatic online control of motor adjustments in reaching and grasping. *Neuropsychologia* 55: 25–40, 2014.
- Goonetilleke SC, Katz L, Wood DK, Gu C, Huk AC, Corneil BD. Cross-species comparison of anticipatory and stimulus-driven neck muscle activity well before saccadic gaze shifts in humans and nonhuman primates. *J Neurophysiol* 114: 902–913, 2015.
- Gu C, Wood DK, Gribble PL, Corneil BD. A Trial-by-Trial Window into Sensorimotor Transformations in the Human Motor Periphery. *J Neurosci* 36: 8273–8282, 2016.

- Himmelbach M, Linzenbold W, Ilg UJ. Dissociation of reach-related and visual signals in the human superior colliculus. *Neuroimage* 82: 61–67, 2013.
- Klaes C, Westendorff S, Chakrabarti S, Gail A. Choosing Goals, Not Rules: Deciding among Rule-Based Action Plans. *Neuron* 70: 536–548, 2011.
- Kwan HC, MacKay WA, Murphy JT, Wong YC. Distribution of responses to visual cues for movement in precentral cortex of awake primates. *Neurosci Lett* 24: 123–128, 1981.
- Linzenbold W, Himmelbach M. Signals from the deep: reach-related activity in the human superior colliculus. *J Neurosci* 32: 13881–13888, 2012.
- Luce RD. *Their Role in Inferring Elementary Mental Organization*. New York: Oxford University Press, 1986.
- Lünenburger L, Kleiser R, Stuphorn V, Miller LE, Hoffmann KP. A possible role of the superior colliculus in eye-hand coordination. *Prog Brain Res* 134: 109–125, 2001.
- MacKay WA, Crammond DJ. Neuronal correlates in posterior parietal lobe of the expectation of events. *Behav Brain Res* 24: 167–179, 1987.
- Mauritz KH, Wise SP. Premotor cortex of the rhesus monkey: neuronal activity in anticipation of predictable environmental events. *Exp Brain Res* 61: 229–244, 1986.
- Medendorp WP, Goltz HC, Vilis T, Crawford JD. Gaze-centered updating of visual space in human parietal cortex. *J Neurosci* 23: 6209–6214, 2003.
- Norman RW, Komi P V. Electromechanical delay in skeletal muscle under normal movement conditions. *Acta Physiol Scand* 106: 241–248, 1979.
- Oostwoud Wijdenes L, Brenner E, Smeets JBJ. Fast and fine-tuned corrections when the target of a hand movement is displaced. *Exp Brain Res* 214: 453–462, 2011.
- Pesaran B, Nelson MJ, Andersen RA. Dorsal premotor neurons encode the relative position of the hand, eye, and goal during reach planning. *Neuron* 51: 125–134, 2006.

- Philipp R, Hoffmann KP. Arm movements induced by electrical microstimulation in the superior colliculus of the macaque monkey. *J Neurosci* 34: 3350–3363, 2014.
- Pisella L, Gréa H, Tilikete C, Vighetto A, Desmurget M, Rode G, Boisson D, Rossetti Y. An “automatic pilot” for the hand in human posterior parietal cortex: toward reinterpreting optic ataxia. *Nat Neurosci* 3: 729–736, 2000.
- Pruszynski JA, Johansson RS, Flanagan JR. A Rapid Tactile-Motor Reflex Automatically Guides Reaching toward Handheld Objects. *Curr Biol* 26: 788–792, 2016.
- Pruszynski JA, King GL, Boisse L, Scott SH, Flanagan JR, Munoz DP. Stimulus-locked responses on human arm muscles reveal a rapid neural pathway linking visual input to arm motor output. *Eur J Neurosci* 32: 1049–1057, 2010.
- Reynolds RF, Day BL. Direct visuomotor mapping for fast visually-evoked arm movements. *Neuropsychologia* 50: 3169–3173, 2012.
- Rezvani S, Corneil BD. Recruitment of a head-turning synergy by low-frequency activity in the primate superior colliculus. *J Neurophysiol* 100: 397–411, 2008.
- Rodgers CK, Munoz DP, Scott SH, Paré M. Discharge properties of monkey tectoreticular neurons. *J Neurophysiol* 95: 3502–3511, 2006.
- Schiller PH, Malpeli JG, Schein SJ. Composition of geniculostriate input to superior colliculus of the rhesus monkey. *J Neurophysiol* 42: 1124–33, 1979.
- Shen Y, Richards VM. A maximum-likelihood procedure for estimating psychometric functions: thresholds, slopes, and lapses of attention. *J Acoust Soc Am* 132: 957–967, 2012.
- Snyder LH, Batista AP, Andersen RA. Change in motor plan, without a change in the spatial locus of attention, modulates activity in posterior parietal cortex. *J Neurophysiol* 79: 2814–2819, 1998.
- Snyder LH, Dickinson AR, Calton JL. Preparatory Delay Activity in the Monkey Parietal Reach Region Predicts Reach Reaction Times. *J Neurosci* 26: 10091–10099, 2006.

- Soechting JF, Lacquaniti F. Modification of trajectory of a pointing movement in response to a change in target location. *J Neurophysiol* 49: 548–564, 1983.
- Song J-HH, McPeck RM. Neural correlates of target selection for reaching movements in superior colliculus. *J Neurophysiol* 113: 1414–1422, 2015.
- Song J-HH, Rafal RD, McPeck RM. Deficits in reach target selection during inactivation of the midbrain superior colliculus. *Proc Natl Acad Sci* 108: E1433-40, 2011.
- Stavisky SD, Kao JC, Ryu SI, Shenoy K V. Motor Cortical Visuomotor Feedback Activity Is Initially Isolated from Downstream Targets in Output-Null Neural State Space Dimensions. *Neuron*: 6–8, 2017.
- Stewart BM, Gallivan JP, Baugh LA, Flanagan JR. Motor, not visual, encoding of potential reach targets. *Curr Biol* 24: R953-4, 2014.
- Stuphorn V, Bauswein E, Hoffmann KP. Neurons in the primate superior colliculus coding for arm movements in gaze-related coordinates. *J Neurophysiol* 83: 1283–1299, 2000.
- Stuphorn V, Hoffmann KP, Miller LE. Correlation of primate superior colliculus and reticular formation discharge with proximal limb muscle activity. *J Neurophysiol* 81: 1978–1982, 1999.
- Tanji J, Evarts E V. Anticipatory activity of motor cortex neurons in relation to direction of an intended movement. *J Neurophysiol* 39: 1062–1068, 1976.
- Weinrich M, Wise SP. The premotor cortex of the monkey. *J Neurosci* 2: 1329–1345, 1982.
- Welford AT. Choice reaction time: basis concept BT - Reaction times. In: *Reaction times*, edited by Welford AT. New York, NY: Academic Press, 1980, p. 73–128.
- Werner W, Dannenberg S, Hoffmann KP. Arm-movement-related neurons in the primate superior colliculus and underlying reticular formation: comparison of neuronal activity with EMGs of muscles of the shoulder, arm and trunk during reaching. *Exp Brain Res* 115: 191–205, 1997.

Wong AL, Goldsmith J, Krakauer JW. A motor planning stage represents the shape of upcoming movement trajectories. *J Neurophysiol* 116: 296–305, 2016.

Wood DK, Gu C, Corneil BD, Gribble PL, Goodale MA. Transient visual responses reset the phase of low-frequency oscillations in the skeletomotor periphery. *Eur J Neurosci* 42: 1919–1932, 2015.

Wurtz RH, Goldberg ME. Activity of superior colliculus in behaving monkey. 3. Cells discharging before eye movements. *J Neurophysiol* 35: 575–586, 1972.

Chapter 4 – A rapid visuomotor response on the human upper limb is selectively influenced by implicit motor learning

Chao Gu (顾超)^{1,3}, J. Andrew Pruszynski¹⁻⁴, Paul L. Gribble¹⁻³, and Brian D. Corneil¹⁻⁴

Departments of ¹Psychology and ²Physiology & Pharmacology, University of Western Ontario, London, Ontario, Canada N6A 5B7

³Brain and Mind Institute and ⁴Robarts Research Institute, University of Western Ontario, London, Ontario, Canada N6A 5B7

Keywords: Human, reaching movement, EMG, motor learning, visuomotor transformation, error-based learning

Gu, C., Pruszynski, J.A., Gribble, P.L., and Corneil, B.D. (2018) A rapid visuomotor response on the human upper limb is selectively influenced by implicit, but not explicit, motor learning. bioRxiv 354381.

4.1 Abstract

How do humans learn to adapt their motor actions to achieve task success? Recent behavioral and patient studies have challenged the classic notion that motor learning arises solely from the errors produced during a task, suggesting instead that explicit cognitive strategies can act in concert with the implicit, error-based, motor learning component. Here, we show that the earliest wave of directionally-tuned neuromuscular activity that begins within ~100 ms of peripheral visual stimulus onset is selectively influenced by the implicit component of motor learning. In contrast, the voluntary neuromuscular activity associated with reach initiation, which evolves ~100 to 200 ms later is influenced by both the implicit and explicit components of motor learning. The selective influence of the implicit, but not explicit, component of motor learning on the directional tuning of the earliest cascade of neuromuscular activity supports the notion that these components of motor learning can differentially influence descending motor pathways.

4.2 Introduction

Motor learning occurs throughout the human lifespan, from children learning to walk to the aged adjusting to a new set of reading glasses. Motor learning involves establishing and constantly recalibrating the mapping of a desired goal onto the required motor commands (Shadmehr et al. 2010). A predominant theory of motor learning posits that learning arises from an implicit error-based process, in which

the brain learns by computing an error between actual and predicted sensory consequences of the generated motor command (Wolpert et al. 1998; Thoroughman and Shadmehr 2000). Recent behavioral work using a visuomotor rotation task (Krakauer 2009) which systematically rotates the visual cursor denoting hand position around the center of the workspace, has suggested that a second explicit process also contributes to motor learning (Mazzoni and Krakauer 2006; Taylor and Ivry 2011; Taylor et al. 2014). The explicit process is driven by awareness of task errors, which participants exploit to achieve task success. The implicit and explicit components of motor learning appear largely independent, as research with individuals who have brain lesions shows that the implicit and explicit components of motor learning have distinctive neural substrates, relying on the integrity of cerebellar (Taylor et al. 2010; Morehead et al. 2017) and frontal circuits (Slachevsky et al. 2001, 2003), respectively (but see Butcher et al., 2017 for evidence showing that an explicit aiming process is also impaired following cerebellar damage). However, multiple descending pathways originating from the cortex and brainstem contribute to motor control in healthy individuals (Kuypers 1981; Lemon 2008; Alstermark and Isa 2012) and the comparative influence of the implicit and explicit components of motor learning on these pathways is not known.

Our interest here is to examine the comparative effects of implicit and explicit motor learning on the first wave of directionally-tuned upper limb muscle activity that occurs time-locked ~ 100 ms after visual stimulus onset (termed stimulus-locked responses, or SLRs) (Pruszynski et al. 2010). We compared these

learning effects against the changes in muscle activity associated with of reach initiation, occurring roughly 200-300 ms after stimulus onset (Welford 1980). Previous work has shown that the largest SLRs occur when stimuli are presented at locations associated with the largest reach-related responses (Pruszynski et al. 2010; Gu et al. 2018), and SLRs persist even if the ensuing reach movement is withheld (Wood et al. 2015; Atsma et al. 2018) or proceeds in the opposite direction (Gu et al. 2016). These response properties, as well as the fact that SLRs evolve at latencies that preclude extensive cortical processing, have led us to propose that SLRs and later reach-related activity arise from distinct descending motor pathways (Pruszynski et al. 2010; Gu et al. 2016).

Here, we study how the implicit and explicit components of motor learning influence these two waves of EMG activity during the visuomotor rotation task. Success in this task requires that participants learn a new mapping between the location of the visual stimulus and the direction of the reach movement. We quantify the change in directional tuning of the SLR and reach-related activity across three different variants of the visuomotor rotation task that either combine or isolate the implicit and explicit components of motor learning. We show that changes in SLR tuning only occur during tasks that involve implicit motor learning, and that the partial shifts in SLR tuning observed during these experiments (~ 10 - 15° for different rotation sizes) are consistent with previous estimates of implicit learning based on measures of participants' gaze behavior (De Brouwer et al. 2018) or verbal reports of aiming direction (Taylor et al. 2014; Bond and Taylor 2015).

In contrast, the tuning of reach-related activity shifts completely in all tasks, consistent with influences of both implicit and explicit motor learning. Taken together, our results show that the earliest wave of muscle activity following a visual stimulus is selectively influenced by implicit motor learning, whereas later voluntary waves of muscle activity are influenced by both implicit and explicit motor learning.

4.3 Materials and Methods

4.3.1 Participants and Procedures

In total, we had 32 participants (21 males and 11 females, mean \pm SD age: 25 \pm 5 years old) perform at least one of the three experiments. All participants were self-declared right-handed except for one left-handed male and four left-handed females, had normal or corrected-to-normal vision, and reported no current visual, neurological, and/or musculoskeletal disorders. Participants provided written consent, were paid for their participation, and were free to withdraw from any experiment at any time. All procedures were approved by the Health Science Research Ethics Board at the University of Western Ontario.

4.3.2 Method Details

The apparatus, electromyographic (EMG) recording setup, and parts of the data analyses has been previously described (Wood et al. 2015; Gu et al. 2016, 2018).

4.3.3 Apparatus and kinematic acquisition

Briefly, in all three experiments, participants sat at a desk with their right elbow supported by a custom-built air-sled. They performed right-handed horizontal planar reaches while holding the handle of a planar robotic manipulandum (InMotion Technologies, Watertown, MA, USA). The x - and y -positions of the manipulandum were sampled and recorded at 600 Hz. A constant rightward load force of 5 N was applied throughout Experiments 2 and 3 to increase the baseline activity of the muscle of interest, due to the use of surface electrodes. No load was applied in Experiment 1, since we used both surface and intramuscular electrodes. Note that even though we applied a constant load in Experiments 2 and 3, Franklin and colleagues (2012) found that rapid visuomotor responses are not modulated with changes in constant background load. Thus, we assumed that the background load also did not affect any of our results. All visual stimuli were presented onto an upward-facing horizontal mirror, located just below the participant's chin level, which reflected the display of a downward-facing LCD monitor with a refresh rate of 75 Hz. The precise timing of the peripheral visual stimulus onset on the LCD screen was determined by a photodiode. The mirror occluded view of the participant's right arm throughout the experiment and real-time visual feedback of the handle of the manipulandum was given by a small red cursor on a white background.

4.3.4 EMG acquisition

EMG activity from the clavicular head of the right pectoralis major (PEC) muscle was recorded using either intramuscular (Experiment 1) and/or surface recordings (Experiments 1-3). Intramuscular EMG activity was recorded using fine-wire (A-M Systems, Sequim, WA, USA) electrodes inserted into the PEC muscle (see Wood et al., 2015 for insertion procedure). Briefly, for each recording we inserted two monopolar electrodes ~2.5 cm into the belly of the PEC muscle. Insertions were aimed ~1 cm inferior to the inflection point of the clavicle, and staggered by 1 cm along the muscle's fiber direction. All intramuscular EMG activity was recorded with a Myopac Junior System (Run Technologies, Mission Viejo, CA, USA). Surface recordings were made with doubled-differential electrodes (Delsys Inc., Natick, MA, USA) placed at the same location as the intramuscular recordings. EMG activity and the photodiode signal were digitized and recorded at 4 kHz.

4.3.5 Experiment 1: Abrupt visuomotor rotation task

Each trial began with the appearance of a central start position. Participants ($N = 7/8$ with a detectable SLR, SLR+, see below detection criterion) moved the cursor into the start position and after a randomized delay in the start position (1-1.25 sec) a peripheral black circle appeared (10 cm away from the start position at one of eight equidistant locations). The onset of the peripheral visual stimulus coincided with the offset of the start position. Participants were instructed to perform an out-and-back reach movement towards the peripheral stimulus. Additionally, they were

instructed to reach as accurately as possible with the cursor to the peripheral stimulus during the outward phase of the reach movement. A small yellow circle also appeared at the position where the cursor crossed the 10-cm radius of the start position until the start of the next trial (1 sec); this provided additional visual feedback on the accuracy of the outward reach movement.

Each participant performed 11 sub-blocks during the experiment, each sub-block consisted of 20 cycles (Fig. 2a, one cycle consists of eight trials, one trial for each of the eight different stimulus locations). In the first three sub-blocks (Pre-Rotation block, black shade), the cursor veridically represented handle position. During the next four sub-blocks (Peri-Rotation block, red), the cursor representing handle position was rotated by 60° CW around the start position. In the final four sub-blocks (Post-Rotation block, blue) the cursor once again represented handle position.

4.3.6 Experiment 2: Gradual visuomotor rotation task

Like in Experiment 1, participants ($N = 14/14$ SLR+) moved the cursor into the start position and after a randomized delay in the start position (1-1.25 sec) a peripheral black circle appeared at one of eight equidistant locations around the start position. Participants were instructed to perform an out-and-back reach movement towards the peripheral stimulus and reach as accurately as possible with the cursor to the peripheral stimulus during the outward movement. However, during this task no yellow circle was presented after each outward reach movement.

Each participant performed nine sub-blocks, each consisting of 20 cycles (**Fig 3a**). In the first two sub-blocks (Test Block 1), the cursor veridically represented handle position. Afterward, participants performed reaches in both a 20° CW and 20° CCW visuomotor rotations, with gradual transitions between them. A gradual rotation was imposed during the third sub-block, in which the cursor representing handle position was rotated by 1° around the start position after each cycle; over the entire block the total rotation was 19°. Participants were counterbalanced between experiencing either a CW or CCW rotation first ($N = 7$ per group, solid or dashed lines in **Fig. 3a**, respectively). During Test Block 2 (sub-blocks 4 and 5), participants performed reaches while the cursor was constantly rotated by 20°. In the next two sub-blocks (sub-blocks 6 and 7), a gradual rotation was imposed 1° per cycle in the opposite direction as in sub-block 3; thus, by the end of sub-block 7 the total rotation imposed during the two sub-blocks was 39°. During Test Block 3 (sub-blocks 8 and 9), participants reached with a constant 20° rotation, which was in the opposite direction as Test Block 2. Thus, all participants performed visually-guided reaches with veridical feedback (Pre-Rotation), and reaches with both a 20° CW and 20° CCW rotations (black, red, and blue shades in **Fig. 3a**, respectively).

4.3.7 Experiment 3: Mental visuomotor rotation task

Each trial began with the appearance of a start position and black outlines of the eight equidistant locations 10 cm from the start position. Participants ($N = 13/18$

SLR+) moved the cursor into the start position and after a randomized delay in the start position (1-1.25 sec) one of the peripheral stimulus location was filled. Each participant performed six sub-blocks of 20 cycles (**Fig. 4a**). In three of the sub-blocks (VIS block), participants performed out-and-back reach movements to the peripheral stimulus, while in the other three rotation sub-blocks (ROT block), participants were instructed to reach towards the open stimulus location 90° CCW to the filled in peripheral stimulus location. Unlike Experiments 1 and 2, the cursor always veridically represented handle position throughout the experiment. The order of the blocks was counterbalanced between participants ($N = 9$ per group).

4.3.8 Data pre-processing

All analyses were performed with custom-written scripts in Matlab (version R2014b, Mathworks Inc., Natick, MA, USA). To achieve sample matching between the kinematics and EMG data, all kinematic data was up-sampled from 600 Hz to 1000 Hz with a low-pass interpolation algorithm, and then lowpass-filtered with a second-order Butterworth filter with a cutoff at 150 Hz. Reach reaction times (RTs) were calculated as the time from the onset of the peripheral visual stimulus (measured by the photodiode) to the initiation of the reach movement. Reach initiation was identified by first finding the peak tangential movement velocity after stimulus onset, and then moving backwards to the closest time at which the tangential velocity profile surpassed 8% of the peak velocity. All EMG data was rectified and then either bin-integrated into 1 ms bins (intramuscular) or down-

sampled (surface) to 1000 Hz. EMG activity was then normalized relative to each block's mean baseline EMG activity (defined as the mean EMG activity 40 ms prior to the onset of the peripheral visual stimulus). We defined the SLR epoch as 85-125 ms after stimulus onset and the SLR magnitude as the mean EMG activity during the SLR epoch. We also defined the reach-related movement (MOV) epoch as 20 ms before to 20 ms after reach RT. All trials with RTs less than 185 ms were excluded to prevent contamination of the SLR epoch by shorter latency reach-related responses (Wood et al. 2015; Gu et al. 2016).

To determine the normalized movement trajectories, we first determined the movement duration for each trial individually. The movement duration was defined as the time when the handle position surpassed 2 cm from the center of the start position to 50 ms after the time when the handle position surpassed 8 cm from the center of the start position. We then interpolated the movement duration into 101 equally spaced time-samples, and calculated the x - and y -positions at each given time-sample.

4.3.9 SLR Detection

Based on previous studies detecting the presence of the SLR (Corneil et al. 2004; Pruszynski et al. 2010), we also used a receiver-operating characteristic (ROC) analysis to quantitatively detect the presence of a SLR. In all experiments, we examined EMG activity for leftward and rightward reaches during veridical visual feedback, and we performed the following ROC analysis. For every time-sample

(1 ms bin) between 100 ms before to 300 ms after visual stimulus onset, we calculated the area under the ROC curve between the leftward and rightward trials. This metric indicates the probability that an ideal observer could discriminate the side of the stimulus location based solely on EMG activity. A ROC value of 0.5 indicates chance discrimination, whereas a value of 1 or 0 indicates perfectly correct or incorrect discrimination, respectively. We set the thresholds for discrimination at 0.6; these criteria exceed the 95% confidence intervals of data randomly shuffled with a bootstrap procedure (Chapman and Corneil 2011). The earliest discrimination time was defined as the time after stimulus onset at which the ROC was above 0.6 and remained above that threshold for at least 5 out of the next 10 samples. Previous studies have also reported decreased SLR magnitude during an anti-reach task (Gu et al. 2016), thus we lower our threshold to 0.55 for the ROT block in Experiment 3. Based on the ROC analyses we defined the SLR epoch as from 85 to 125 ms after visual stimulus onset and categorized any participant with a discrimination time <125 ms as having a SLR (SLR+ participant). Across the three experiments we could reliably detect a SLR in 29 out of 32 participants.

4.3.10 Tuning curve fit

To determine the tuning curve of EMG activity during both the SLR and MOV epochs, we assumed that the relationship between EMG activity and the peripheral visual stimulus location took the form of a sinusoidal function **Eq. 1**:

$$EMG(x) = A \times \cos(x - \theta) + \gamma \quad (\text{Equation 1})$$

in which x is the angular location of the peripheral visual stimulus in degrees; $EMG(x)$ is the logarithm of the normalized EMG activity for the given stimulus location; A is the amplitude of the sinusoidal fit; θ is the preferred direction (PD) of the sinusoidal fit; and γ is the offset of the sinusoidal fit. We used Matlab's curve fitting toolbox, in which we constricted our parameters so that $A < 0$ and $0 \leq \theta < 360$, and the starting point of the parameters were $A = 1$, $\theta = 180^\circ$, and $\gamma = 0$.

4.3.11 Statistical Analyses

For statistical analyses done on the EMG data from the representative participants of Experiments 1 and 2, we performed a 1-way ANOVA (visuomotor rotation blocks) for both the SLR and MOV epochs separately. For the Experiment 3, we performed a 2-way ANOVA (direction \times visuomotor rotation block) for the SLR epoch. For the group RT data, we performed either a repeated measures 1-way ANOVA (visuomotor rotation blocks; Experiments 1 and 2) or paired t-test (Experiment 3). For the group Δ PD data, we performed either a repeated measures 2-way ANOVA (epochs \times visuomotor rotation blocks) or an one sample t-test to compare against zero. For ANOVA post-hoc test, we performed a Tukey's HSD correction. The statistical significance was set as $P < 0.05$.

4.3.12 Data and Software Availability

All data was analyzed using MATLAB R2014b.

4.4 Results

Figure 4.1a shows the normalized mean \pm SD movement trajectories for both the leftward (180° CCW from straight right) and rightward (0°) stimulus locations from a representative participant, when they had veridical visual feedback of their hand position (i.e., the cursor moved in register with the participant's hand). **Figure 4.1b** shows the corresponding normalized mean \pm SEM (top) and individual (bottom color panels) PEC EMG activity from leftward and rightward trials. EMG activity was aligned to the onset of the peripheral visual stimulus onset (thick black vertical lines), and individual trials were sorted based on reaction time (RT; squares, fastest to slowest from bottom to top). We observed a reliable SLR, which consisted of a brief increase or decrease in EMG activity \sim 100 ms after the presentation of leftward or rightward stimulus locations, respectively (Pruszynski et al. 2010; Wood et al. 2015; Gu et al. 2016). We defined the SLR magnitude for each trial as the mean EMG activity during the SLR epoch (85-125 ms after stimulus onset, shaded regions in mean EMG sub-panels in **Figure 4.1b**).

To determine the directional tuning of the EMG activity during both the SLR and the later reach response (MOV, -20 to 20 ms around RT) epochs, we derived the preferred direction (PD) of each epoch assuming a sinusoidal fit (**Eq. 1**).

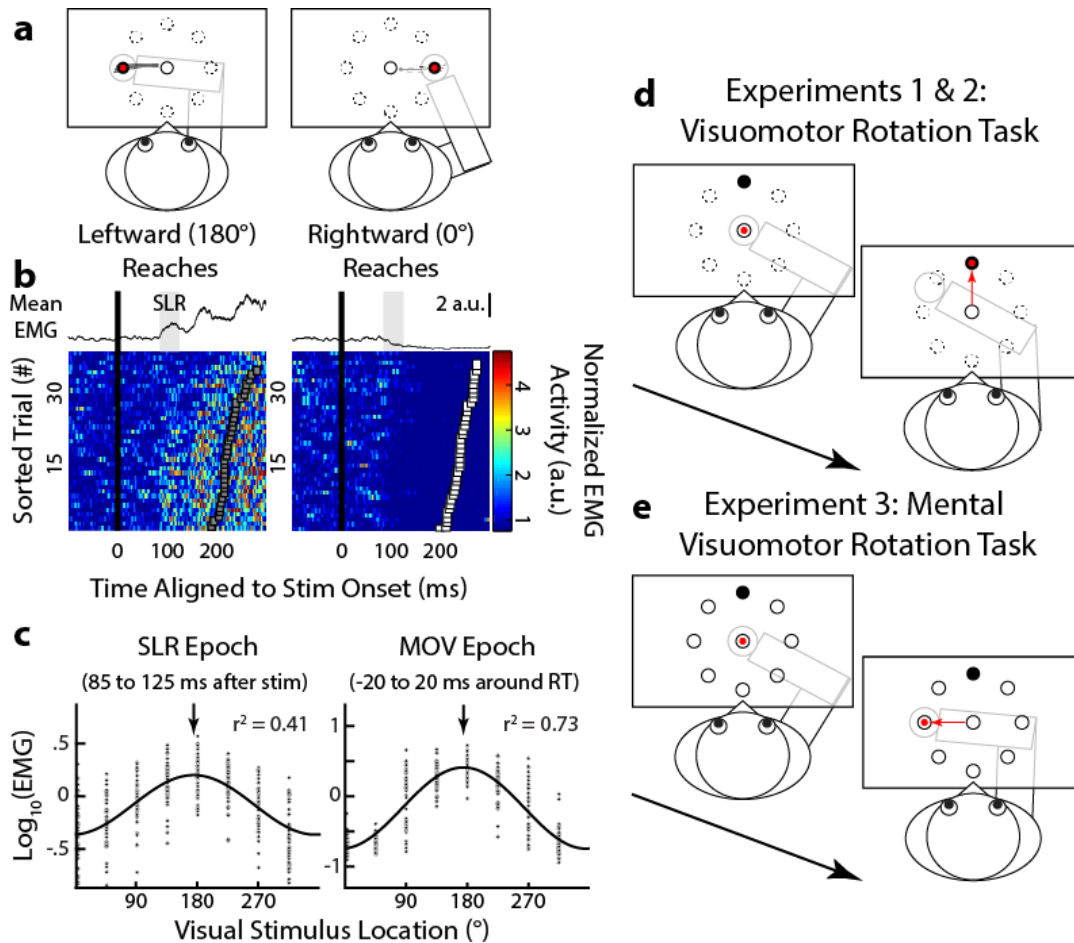


Figure 4.1: Experimental paradigm and spatial tuning of the SLR on human limb muscle during visually-guided reaches

(a) The mean \pm SD normalized movement trajectories for leftward and rightward visually-guided reaches from a representative participant. (b) The corresponding mean \pm SEM (top panels) and individual trials (bottom) of EMG activity from the right pectoralis major muscle aligned to visual stimulus onset (black line). For the colour panels, each row represents EMG activity from a single trial, with trials sorted based on reach RT (squares). EMG activity diverged during the SLR epoch (shaded regions, 85-125 ms after stimulus onset), regardless of the ensuing RT. (c) Sinusoidal relationship between the log-normalized mean EMG activity and visual stimulus location during the SLR (left panel) and MOV (right) epochs for this participant. Arrows indicate the PD of each fit. (d) Experiments 1 and 2: the visuomotor rotation task. Participants generating reach movements to move the cursor (red circle) to the visual stimulus location (black circle). To induce motor learning, the cursor was systematically rotated (60° CW in this case) around the start position. (e) Experiment 3: the mental visuomotor rotation task. During the task, the cursor always gave veridical feedback of the robotic handle but participants were explicitly instructed to reach to the stimulus location 90° CCW to the visual stimulus location.

Figure 4.1c shows the log-normalized EMG activity as a function of visual stimulus location (arrows indicate the PDs of each fit). With veridical feedback, a reliable SLR was detected in 29 out of 32 participants (see *ROC analysis* in **Materials and Methods** for detection criteria). Consistent with a previous study (Pruszynski et al. 2010), we also found a small but reliable difference in PD of EMG activity between the SLR and MOV epochs (mean \pm SEM: $172.5 \pm 1.6^\circ$ and $180.0 \pm 1.2^\circ$, respectively, paired *t*-test, $t_{(36)} = -4.0$, $P = 0.001$). Data from participants who did not exhibit an SLR were excluded from all subsequent analyses (see **Materials and Methods** for exact numbers for each experiment). Having established the tuning of EMG activity during the SLR and MOV epochs with veridical hand position feedback, we next examined how the PDs changed during two different visuomotor rotation tasks (**Figure 4.1d**) and a mental visuomotor rotation task (**Figure 4.1e**).

4.4.1 Partial adaptation of the SLR during an abrupt 60° CW visuomotor rotation

In Experiment 1, we used an abrupt visuomotor rotation task which has been previously shown to engage both implicit and explicit motor learning components (Mazzoni and Krakauer 2006; Taylor et al. 2014). During both the Pre- and Post-Rotation blocks (**Figure 4.2a**, black and blue shades, respectively), participants ($N = 7$) performed 60 and 80 cycles (a cycle consists of 8 reaches, 1 reach per direction) of visually-guided reaches under veridical visual feedback, respectively.

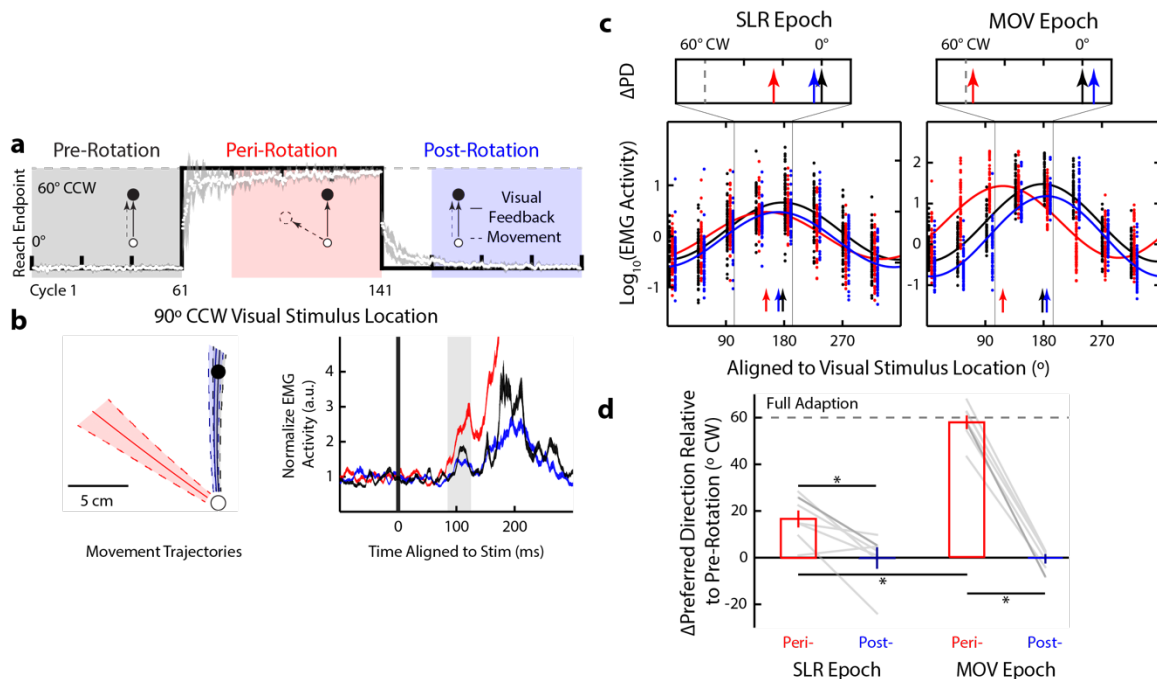


Figure 4.2: Partial adaptation of the SLR tuning during the abrupt visuomotor rotation task (a) Timeline and behavioural performance during an 60° CW abrupt visuomotor rotation. The group mean \pm SEM (white circles and gray shade) reach endpoint per cycle relative to the stimulus location is plotted against perfect task performance (black line). Veridical visual feedback was provided during Pre- (black shade) and Post-Rotation (blue) blocks. During the Peri-Rotation (red) block, the virtual cursor feedback was rotated around the start position by 60° CW. (b) Mean \pm SD normalized movement trajectories and mean \pm SEM PEC EMG activity for the outward visual stimulus location (90° CCW from straight right) of a representative participant. The EGM activity is aligned to stimulus onset, and the SLR epoch (85-125 ms after stimulus onset is highlighted). (c) Sinusoidal tuning curve fits (Equation 4-1) between visual stimulus location the log-normalized mean EMG activity during the SLR (left panel) and MOV epochs (right). Each dot indicates data from single trial, while the solid lines show the best fit for each block; vertical arrows indicate the PD for each fit. Note for illustration purposes only, we have staggered the individual trial data. Top inserts show the shifts in PD (ΔPD) during the Peri- and Post-Rotation blocks relative to the Pre-Rotation block. Vertical dashed gray line represents full adaptation to the 60° CW visuomotor rotation. (d) Group mean \pm SEM of ΔPD for both Peri- (red bars) and Post-Rotation blocks (blue) during both the SLR and MOV epochs across participants. A $\Delta PD = 0^{\circ}$ or 60° CW would indicate either no adaptation or a complete adaptation to the imposed rotation, respectively. Each gray line represents data from an individual participant, with the darker line indicating data from the participant in c. * $P < 0.05$.

During the Peri-Rotation block (red, 80 cycles), we imposed a 60° CW rotation on the visual cursor around the start position. **Figure 4.2a** also shows the group mean \pm SEM reach endpoint (white dot and shade) plotted relative to the stimulus location, while the solid black line indicates perfect task performance. Consistent with previous experiments (Pine et al. 1996; Krakauer et al. 2005), our participants rapidly adapted their endpoint reach direction during the beginning of the Peri-Rotation block and exhibited signs of motor learning as seen by the aftereffect during the beginning of the Post-Rotation block (Mazzoni and Krakauer 2006). We excluded the first 20 cycles of both the Peri- and Post-Rotation blocks to ensure that participants' behavioral performance had plateaued. We observed an increase in median RTs during the Peri-Rotation block (**Figure 4.5a**, group mean \pm SEM = 301 ± 17 ms) compared to both Pre- and Post-Rotation blocks (246 ± 14 ms and 254 ± 13 ms, respectively, repeated measures 1-way ANOVA, $F_{(2,12)} = 11.99$, $P = 0.001$, post-hoc Tukey's HSD, both $P < 0.01$). Prolonged RTs during the visuomotor rotation task have been associated with explicit motor learning as participants employ an aiming strategy (Fernandez-Ruiz et al. 2011; Haith et al. 2015). Thus, participants' behavior provided evidence for the engagement of both implicit and explicit motor learning components during this task.

Figure 4.2b shows mean movement trajectories and PEC EMG activity for the outward visual stimulus location (90° CCW) across the three different blocks, for one participant. As seen from the mean movement trajectories, during Peri-Rotation (red) the participant learned that the imposed 60° CW visuomotor rotation

required them to generate a left-outward reach movement $\sim 60^\circ$ CCW to the stimulus location. These left-outward movements during the Peri-Rotation block required more PEC recruitment compared to straight outward movements during both Pre- and Post-Rotation blocks. As expected, during the MOV epoch we observed reliable modulation in PEC EMG activity across blocks (1-way ANOVA, main effect, $F_{(2,176)} = 486.4$, $P < 10^{-71}$), with greater EMG activity during Peri- compared to both Pre- and Post-Rotation blocks (post-hoc Tukey's HSD, both $P < 10^{-9}$).

For the outward stimulus location, we also observed a similar pattern of modulation during the SLR epoch (1-way ANOVA, main effect, $F_{(2,176)} = 7.97$, $P = 0.001$), with greater EMG activity during the SLR epoch for Peri- compared to both Pre- and Post-Rotation blocks (post-hoc Tukey's HSD, $P = 0.006$ and $P = 0.001$, respectively). Thus, even though the same visual stimulus location was presented across all three blocks, the magnitude of the SLR changed during motor learning.

To quantify the influence of motor learning on directional tuning, we derived the PDs of EMG activity during the two different epochs for all three blocks (colored arrows in **Figure 4.2c**). We normalized the results across participants by using each participant's PD during the Pre-Rotation block as a baseline and quantified the shifts in PD (Δ PD) for both Peri- and Post-Rotation blocks (top panels in **Figure 4.2c**). Across participants (**Figure 4.2d**), we found that Δ PD for the MOV epoch adapted almost completely during the Peri-Rotation block (Δ PD mean \pm SEM = $57.7 \pm 2.9^\circ$ CW, one sample t -test, $t_{(6)} = 19.61$, $P < 10^{-5}$) to the imposed 60° CW

visuomotor rotation (gray dashed line). Note this is expected as we aligned the tuning curves relative to visual stimulus location rather than the reach direction. We also found that Δ PD returned to baseline during the Post-Rotation block (Δ PD = $0.7 \pm 1.6^\circ$ CW, one sample t -test, $t_{(6)} = 0.46$, $P = 0.66$), and a reliable difference in Δ PD between the Peri- and Post-Rotation blocks (repeated measures 2-way ANOVA – epoch and rotation blocks, interaction effect, $F_{(1,6)} = 74.15$, $P < 10^{-6}$, post-hoc Tukey's HSD, $P = 0.0001$). Thus, we observed nearly complete adaptation (Δ PD $\approx 60^\circ$ CW) and de-adaptation (Δ PD $\approx 0^\circ$ CW) during the MOV epoch for the Peri- and Post-Rotation blocks, respectively.

We next examined the change in the directional tuning of EMG activity during the SLR epoch. Like the later MOV epoch, we also observed reliable adaptation during the Peri-Rotation block (Δ PD = $16.7 \pm 3.6^\circ$ CW, one-sample t -test, $t_{(6)} = 4.6$, $P = 0.004$), and de-adaptation during the Post-Rotation block (Δ PD = $0.0 \pm 4.2^\circ$ CW, one-sample t -test, $t_{(6)} = 0.01$, $P = 0.99$). However, the extent of adaptation during Peri-Rotation for the SLR epoch was reliably smaller than that during the later MOV epoch (repeated measures 2-way ANOVA, post-hoc Tukey's HSD, Peri-Rotation – SLR vs MOV epoch, $P = 0.0001$).

To summarize the results from Experiment 1, motor learning induced via an abrupt 60° CW visuomotor rotation systematically altered the tuning of the SLR, despite its short-latency. However, unlike the full adaptation of EMG in the later MOV epoch, we observed only partial adaptation of EMG during the SLR interval. The abrupt visuomotor rotation task is thought to engage both implicit and explicit

motor learning components. In Experiment 2 we tested whether the shift in SLR tuning is still present when the explicit component of motor learning is minimized.

4.4.2 SLR adaptation occurs despite a lack of explicit awareness of a visuomotor rotation

In Experiment 2, participants ($N = 14$) performed a gradual visuomotor rotation task (**Figure 4.3a**). A previous imaging study has suggested that abrupt and gradual visuomotor rotation tasks engage different neural substrates (Werner et al. 2014), and behavioral studies have shown that gradual visuomotor rotations produced larger aftereffects (Kagerer et al. 1997) and longer-lasting retention (Klassen et al. 2005) compared to abrupt visuomotor rotations. Here, we imposed a visuomotor rotation gradually (1° per cycle). Once again, participants initially performed visually-guided reaches to one of eight equidistant visual stimuli with veridical feedback (**Figure 4.3a**, Test Block 1, Pre-Rotation) for 40 cycles. Then for the next 20 cycles, the visual feedback of the cursor was rotated either 1° CW or CCW per cycle (solid or dashed lines), counterbalanced between participants. Over the next 40 cycles, the visual feedback remained rotated at 20° CW or CCW (Test Block 2). Afterwards, the feedback was rotated 1° per cycle in the opposite direction to the initial imposed rotation for 40 cycles. Finally, the feedback remained constantly rotated at 20° CCW or CW (Test Block 3). We found no reliable differences in endpoint reach direction between the three Test Blocks based on the order of imposed rotation (2-way ANOVA – Test Blocks and group,

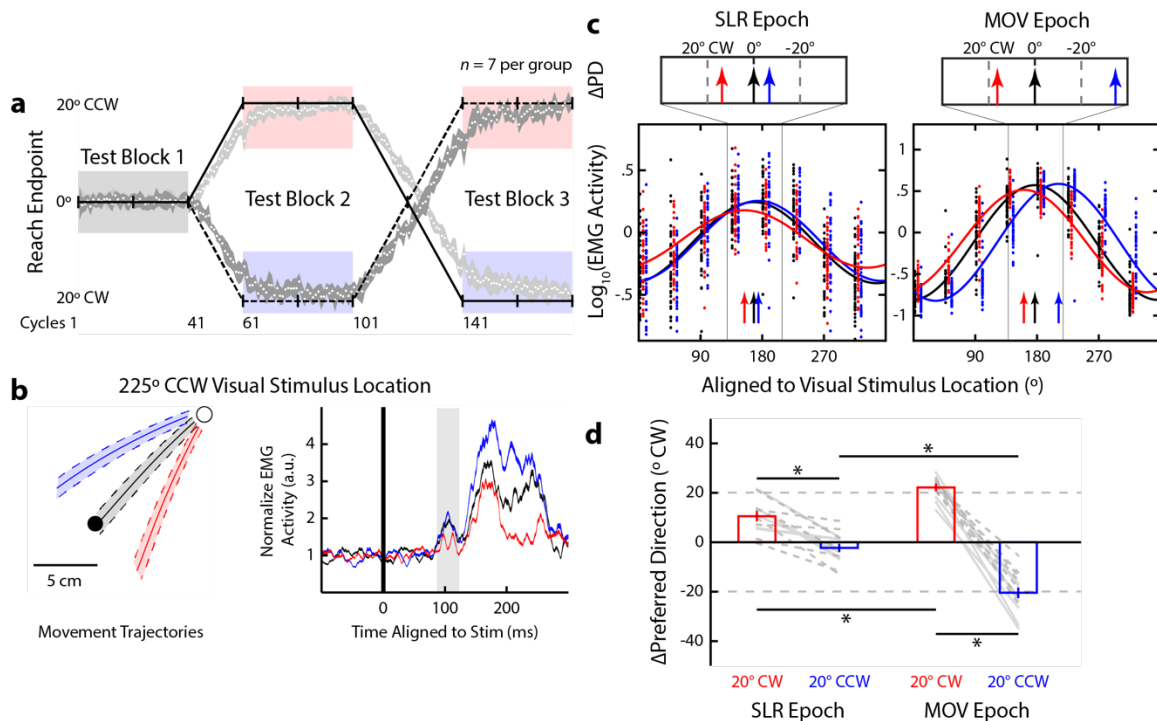


Figure 4.3: Partial adaptation of the SLR tuning during the gradual visuomotor rotation task
 Same layout as **Figure 4.2**. **(a)** Timeline and behavioural performance during a gradual visuomotor rotation task. After the first 40 cycles of reaches (Test Block 1) with veridical cursor feedback, the cursor was gradually rotated 1° per cycle to 20° CW (black solid line) or CCW (dashed line). After participants performed 40 cycles with the cursor constantly rotated 20° CW or CCW (Test Block 2), the cursor was rotated in the opposite direction for 40 cycles. Finally, participants performed 40 cycles with the cursor constantly rotate 20° CCW or CW (Test Block 3). Both groups performed reaches with veridical (Pre-Rotation, black), 20° CW (red), and 20° CCW (blue) visual feedback blocks. **(b)** Mean \pm SD movement trajectories and mean \pm SEM EMG activity for the left-inward visual stimulus location (225° CCW) during the three blocks from a participant who experienced the CW rotation first. **(c)** PD for each of the Test Blocks during the SLR and MOV epochs (vertical arrows). **(d)** Mean \pm SEM of the Δ PD for CW and CCW blocks compared to Pre-Rotation block for both the SLR and MOV epochs across all participants. Dashed or solid lines indicate participants who first experienced CW or CCW rotation, respectively. * $P < 0.05$.

interaction effect, $F_{(1,24)} = 7.14$, $P = 0.01$, post-hoc Tukey's HSD, both $P > 0.21$). Thus, we pooled data from all participants together for the subsequent analyses.

The size of the imposed visuomotor rotation, 1° per cycle, during Experiment 2 is less than the trial-by-trial variance of the participants' reach endpoint during the Pre-Rotation block (Gaussian fit, mean \pm SD, $\mu = 0.4 \pm 0.1$, $\sigma^2 = 5.0 \pm 0.2$, adjusted $r^2 = 0.94 \pm 0.01$). Consistent with previous studies (Galea et al. 2010; Honda et al. 2012), participants reported no explicit awareness of changes in the underlying sensorimotor mapping at any point during the experiment. Further, unlike Experiment 1, we found no difference in median RTs between veridical feedback (**Figure 4.5b**, Pre-Rotation, mean \pm SEM = 232 ± 5 ms) and the two rotation blocks (CW and CCW, 233 ± 5 ms and 236 ± 5 ms, repeated measures 1-way ANOVA, $F_{(2,26)} = 1.79$, $P = 0.19$). This lack of RT increase during the gradual visuomotor rotation is also consistent with a minimal influence of explicit aiming during the experiment.

Figure 4.3b shows mean movement trajectories and PEC EMG activity from one participant for the left-inward stimulus location (225° CCW) across the three Test Blocks: Pre-Rotation, 20° CW, and 20° CCW (black, red, and blue traces, respectively). Like in Experiment 1, we found reliable differences in normalized EMG activity across the three blocks for both the SLR and MOV epochs for this stimulus location (1-way ANOVA, main effect, $F_{(2,109)} = 5.74$ and 57.6 , $P = 0.004$ and $P < 10^{-17}$, respectively). For example, during the 20° CW rotation block, the participant generated reaches away from the PD of the PEC

muscle, hence there was a decrease in mean EMG activity both during the MOV epoch (red trace in **Figure 4.3b**, starting ~150 ms after stimulus onset, post-hoc Tukey's HSD, $P < 10^{-5}$) and during the SLR epoch (shaded region, post-hoc Tukey's HSD, $P = 0.01$). **Figure 4.3c** shows the tuning curve fits during both the SLR and MOV epochs across the three different blocks for this participant, demonstrating the changes in the PD in both the SLR and MOV epochs.

When we examined the shifts in PD across our sample, as expected we observed full Δ PD adaptations of $22.2 \pm 1.1^\circ$ CW and $20.4 \pm 2.1^\circ$ CCW during the MOV epoch for the 20° CW and 20° CCW rotation blocks relative to the Pre-Rotation block, respectively (**Figure 4.3d**, right panel, repeated measures 2-way ANOVA – epoch and rotation, interaction effect, $F_{(1,13)} = 122.08$, $P < 10^{-10}$, post-hoc Tukey's HSD, $P < 10^{-8}$). When we performed the same analysis during the SLR epoch (**Figure 4.3d**, left panel), we found that the SLR Δ PD rotated $10.5 \pm 1.7^\circ$ CW and $2.3 \pm 1.6^\circ$ CCW for the 20° CW and CCW rotations, respectively (post-hoc Tukey's HSD, $P < 10^{-4}$). Similar to the reach direction error, we found no difference between the Δ PD of the SLR based on the order of visuomotor rotation for both the 20° CW and CCW blocks (2-way ANOVA, order and block, main effect of order, $F_{(1,24)} = 0.31$, $P = 0.59$). Although there is an asymmetry in how much the tuning of the SLR changed for CW and CCW rotations, the main contrast that the experiment was designed to examine was the difference in PDs between the 20° CW and CCW blocks. As in Experiment 1, we observed a reliable smaller overall change in Δ PD during the SLR versus MOV epoch when collapsing these changes

across the 20° CW and 20° CCW rotation blocks ($12.8 \pm 1.9^\circ$ and $42.6 \pm 2.1^\circ$, paired t -test, $t_{(13)} = 11.0$, $P < 10^{-7}$).

Thus, as with an abrupt visuomotor rotation, motor learning induced by a gradual visuomotor rotation systematically altered the tuning of the SLR. Experiment 2 also demonstrated that explicit awareness of changes in the underlying visuomotor mapping is not required for the tuning of the SLR to change. However, the extent of adaptation during the SLR epoch was still reliably less than that observed in the later MOV epoch. This finding is consistent with literature suggesting that another cognitive strategy, such as reward-based learning, could still be engaged in the gradual visuomotor rotation task, despite the lack of explicit awareness (Galea et al. 2010).

4.4.3 Changes in the explicit aiming strategy do not alter the PD of the SLR

In Experiment 3, participants ($N = 13$) performed a mental visuomotor rotation task (Georgopoulos and Massey 1987; Mazzoni and Krakauer 2006; Taylor and Ivry 2011). Unlike in the first two experiments, participants received veridical visual feedback of their hand position throughout the experiment. It has been proposed that this eliminates implicit motor learning, since such learning is thought to occur only when there is a mismatch between the visual location of the virtual cursor and the participant's hand position (Mazzoni and Krakauer 2006; Morehead et al. 2017). Instead, participants were explicitly instructed to reach either directly to the

stimulus location (VIS block, **Figure 4.4a**, black) or 90° CCW relative to the stimulus location (Rotation [ROT] block, red). The order of the blocks was counterbalanced between participants. To assist participants, all eight stimulus locations were presented as open circles throughout the whole experiment, and the peripheral stimulus onset occurred when one of the open circles filled in. Like in Experiment 1, we found an increase in median RTs during the ROT (**Figure 4.5c**, mean \pm SEM = 398 \pm 15 ms) compared to VIS block (243 \pm 7 ms, paired *t*-test, $t_{(12)}$

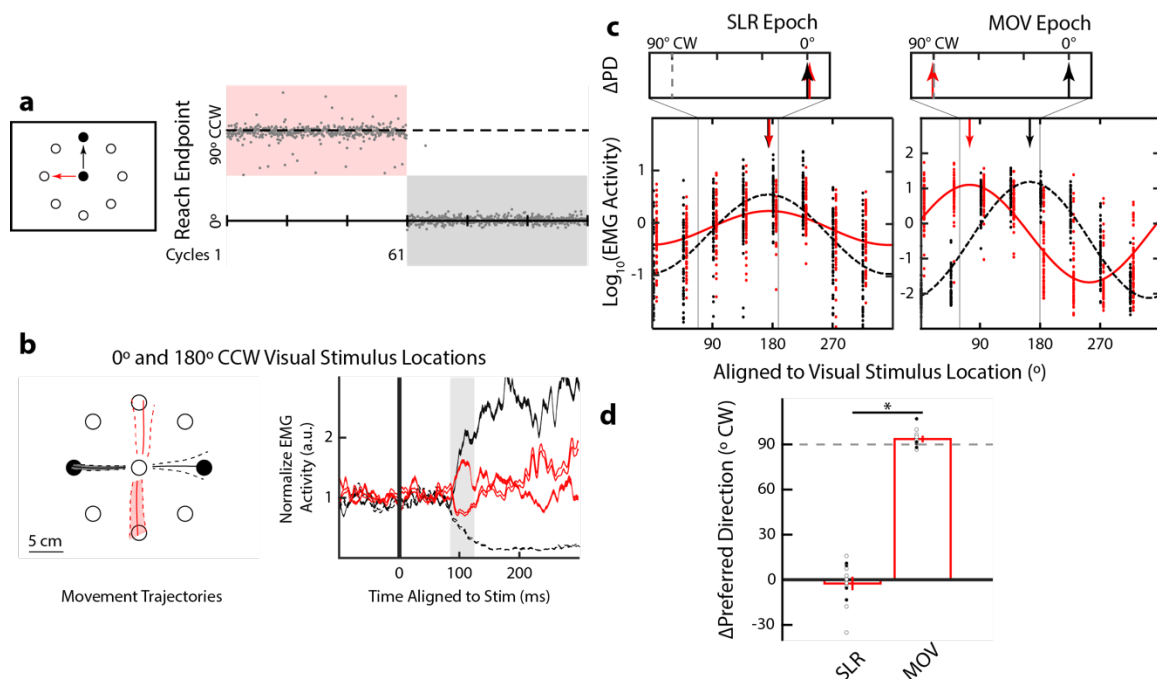


Figure 4.4: SLR tuning did not adapt during a mental visuomotor rotation task.

Same layout as **Figure 4.2**. (a) Task schematic, timeline, and behavioural performance for a representative participant during the mental visuomotor rotation task. Veridical visual feedback was given throughout the whole experiment. Participants were instructed to reach directly (VIS, black) or 90° CCW (ROT, red) to the stimulus location, with the order counterbalanced across participants. (b) Mean \pm SD movement trajectory and mean \pm SEM EMG activity for both the leftward and rightward stimulus locations. (c) PD for both the VIS and ROT blocks during the SLR and MOV epochs (vertical arrows). (d) Mean \pm SEM of the Δ PD between VIS and ROT blocks across all participants. Open and filled dots indicate participants who first performed the VIS and ROT block first, respectively. * $P < 0.05$.

$= -17.8$, $P < 10^{-9}$), supporting the idea that participants used an aiming strategy during the ROT block.

Figure 4.4a shows the endpoint reach direction from a participant who performed the ROT block first. There was no aftereffect during the initial few cycles after the end of the ROT block, which is consistent with the absence of implicit motor learning. **Figure 4.4b** shows a participant's mean movement trajectories and PEC EMG activity for leftward and rightward stimulus locations (180° and 0° locations, filled and open lines, respectively). Note that regardless of the voluntary movement direction, we observed greater EMG activity after leftward compared to rightward stimulus presentation during the SLR epoch in both the VIS (**Figure 4.4b**, black lines, 2-way ANOVA – direction and block, interaction effect, $F_{(1,225)} = 12.57$, $P = 0.0005$, post-hoc Tukey's HSD, $P < 10^{-8}$) and ROT blocks (red lines, post-hoc Tukey's HSD, $P < 10^{-7}$). Like the previous two experiments, we derived the PD of EMG activity during both the SLR and MOV epochs (**Figure 4.4c**).

Across our sample, we observed a reliable shift in PD between the VIS and ROT blocks during the MOV epoch (**Figure 4.44d**, $\Delta PD = 93.6 \pm 1.5^\circ$ CW, one sample t -test, $t_{(12)} = 63.0$, $P < 10^{-15}$). In contrast, the SLR tuning did not reliably differ between the two blocks ($\Delta PD = -2.5 \pm 3.8^\circ$ CW, one sample t -test, $t_{(12)} = -0.7$, $P = 0.52$). Although there was a significant attenuation in the amplitude of the SLR tuning curve between the VIS and ROT blocks (paired t -test, $t_{(12)} = 5.96$, $P < 10^{-4}$), this attenuation could be related to the corresponding increase in RT during the ROT block, as SLR magnitude is known to decrease when preceding

movements with longer RTs (Pruszynski et al. 2010; Gu et al. 2016). This decrease in amplitude was also observed during the Peri-Rotation block in Experiment 1, when there was also an increase in median RTs, but a decrease in amplitude was not seen in Experiment 2, when there was no reliable increase in median RTs (see **Figure 4.5** for the relationship between SLR amplitude fits and median RTs in all three experiments). Thus, in Experiment 3, learning induced during a mental visuomotor rotation task did not systematically alter the tuning of the SLR.

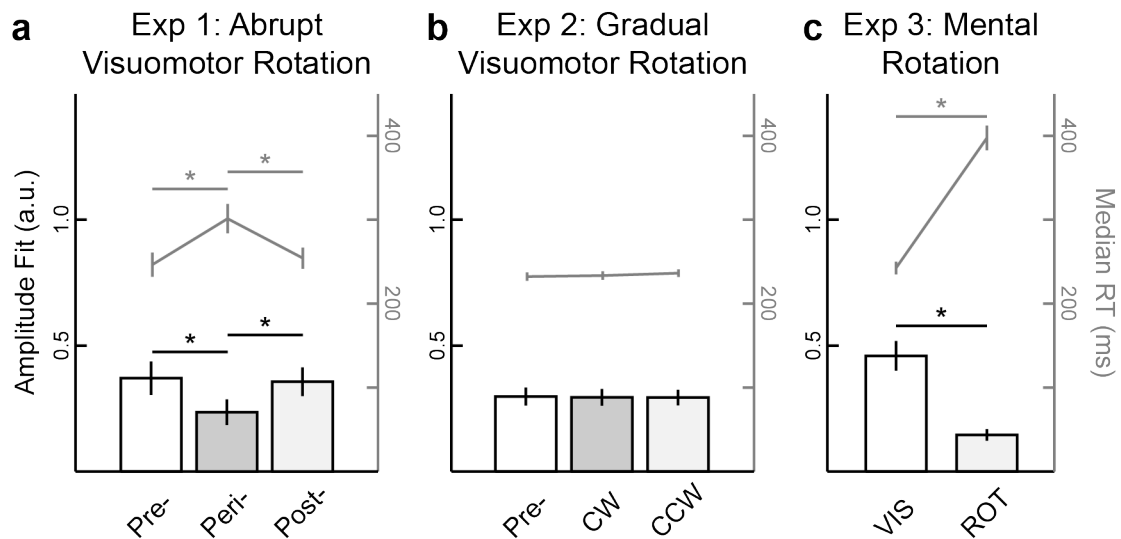


Figure 4.5: An explicit aiming strategy attenuated SLR magnitude and increased RTs.

(a-c) Group mean \pm SEM of both the amplitude parameter for the sinusoidal fits during the SLR epoch (bars, left axis) and median RTs (lines, right axis) across the three different experiments.

* $P < 0.05$.

4.5 Discussion

Recent studies have suggested that motor learning can be driven by multiple learning components: an implicit learning component related to the mismatch between the actual and predicted sensory consequences of a generated motor

command (Mazzoni and Krakauer 2006; Morehead et al. 2017), and an explicit learning component that involves changes to aiming strategy (Taylor and Ivry 2011; Taylor et al. 2014). What has not been clear from this literature is how such components engage various descending motor pathways. Here, we measured the changes in the directional tuning of EMG activity on the human pectoralis muscle during three variations of the visuomotor rotation task. We found both the implicit and explicit components of motor learning modulated the tuning of voluntary reach-related EMG activity. In contrast, we found that only the implicit motor learning component modulated the tuning of the earliest wave of muscle activity that is time-locked to the onset of a peripheral visual stimulus.

4.5.1 Implicit motor learning drives the partial adaptation of SLR tuning during visuomotor rotations

Our central result is that implicit motor learning altered the directional tuning during the SLR epoch (85-125 ms after stimulus onset), while both implicit and explicit motor learning altered the tuning of reach-related MOV activity (-20 to 20 ms around RT, ~200-300 ms after stimulus onset). Thus, implicit motor learning can induce adaptation in the fastest, essentially reflexive, visuomotor pathway. The amount of adaptation was considerably less than either of our imposed visuomotor rotations: SLR tuning changed by $16.7 \pm 3.6^\circ$ for a 60° visuomotor rotation in Experiment 1, and by $12.8 \pm 1.9^\circ$ for an overall 40° visuomotor rotation in Experiment 2. These observations match well with previous behavioral estimates

of implicit learning component of $\sim 10^\circ$ - 15° from both the initial aftereffect (Taylor and Ivry 2011) and during the visuomotor rotation regardless of the magnitude of the imposed visuomotor rotation (Taylor et al. 2014; Bond and Taylor 2015). The latter estimates are based on a subtraction logic, wherein the implicit component is estimated as the difference between the actual reach direction and the verbal reporting of the participant's aiming direction. Recent work has also shown that gaze behavior in a subset of subjects correlates with their explicit aiming strategy (De Brouwer et al. 2018).

The gradual visuomotor rotation used in Experiment 2 attempted to minimize the explicit aiming component of motor learning. Evidence that participants learned the new visuomotor mapping without using an explicit aiming strategy is found in the lack of difference in RTs between the veridical and rotation blocks (**Figure 4.5**), and post-experiment confirmation that our participants were unaware of any changes in the visuomotor mapping during the experiment (Galea et al. 2010; Honda et al. 2012). However, a previous study has reported impaired learning rates during a similar gradual visuomotor task when participants concurrently performed a cognitively demanding task (Galea et al. 2010), suggesting a distinction between explicit awareness and contribution of other forms of learning. This may explain why we only observed a partial adaptation of SLR tuning ($\sim 13^\circ$) compared to a full adaptation during the MOV epoch ($\sim 40^\circ$). Our paradigm was designed to test the influence of error-based learning, but may have also engaged reinforcement-based learning (Lee et al. 2012).

Reinforcement-based learning was likely engaged in all three experiments, as participants gauged their success in hitting the target. Previous studies have shown that changes in sensorimotor mapping can be driven purely by reinforcement learning (Izawa and Shadmehr 2011; Shmuelof et al. 2012; Therrien et al. 2016), which can occur without awareness (Alamia et al. 2016). Further, recent studies have shown that reward signals can modulate the extent of implicit motor learning (Reichenthal et al. 2016; Kim et al. 2018; Leow et al. 2018). At the current time, whether modulation of reward can alter the tuning of the SLR is not known.

4.5.2 Distinct neural substrates for the implicit and explicit components of motor learning

To our knowledge, no previous animal neurophysiological or human imaging studies have described a neural correlate for partial adaptation during either a gradual or an abrupt visuomotor rotation task. Previous fMRI studies have shown that BOLD activity within the posterior parietal cortex (PPC) faithfully encodes visual stimulus location during the visuomotor rotation task, regardless of the ensuing reach direction (Fernandez-Ruiz et al. 2007; Haar et al. 2015). Similarly, during saccadic adaptation, neurons within the lateral intraparietal cortex also encode visual stimulus location rather than saccadic endpoint (Steenrod et al. 2013). Conversely, both fMRI and neurophysiological studies have shown that both premotor and primary motor cortices encode the final movement direction,

regardless of the visual stimulus location (Shen and Alexander 1997a, 1997b; Paz et al. 2003; Haar et al. 2015; Perich et al. 2017). Thus, the pattern of the modulation of SLR tuning is distinct from signals observed in either the PPC or motor cortices, which would presumably be relayed via corticospinal projections.

Previous clinical studies suggest that implicit and explicit components of motor learning have distinct underlying neural substrates. For example, even though patients with prefrontal lesions lacked any explicit awareness of changes during an abrupt visuomotor rotation task, they still partially adapted their reaching movements (Slachevsky et al. 2001, 2003). This result suggested that while the explicit aiming component is impaired, the implicit motor learning component is spared in such patients. Conversely, patients with cerebellar damage show impairment when adapting to novel environments (Morton and Bastian 2004; Tseng et al. 2007; Rabe et al. 2009), regardless of the size or how the perturbation is imposed (Gibo et al. 2013; Schlerf et al. 2013). While these patients can still compensate for the sensorimotor perturbations through either reinforcement learning (Izawa and Shadmehr 2011; Therrien et al. 2016) or the use of an explicit aiming strategy (Taylor et al. 2010), they still had impaired implicit error-based learning (Taylor et al. 2010; Therrien et al. 2016; Morehead et al. 2017) and displayed much smaller aftereffects after motor learning (Werner et al. 2010).

4.5.3 A cerebellar influence on the tectoreticulospinal pathway

Given that the cerebellum has been strongly implicated in implicit motor learning, we surmise that the changes in SLR tuning observed in Experiments 1 and 2 are modulated via the cerebellum. How then could the cerebellum be altering this visuomotor mapping? We have speculated that the SLR is mediated by a tectoreticulospinal pathway (Pruszynski et al. 2010; Wood et al. 2015; Gu et al. 2016), and there is substantial evidence for interaction between the cerebellum and the reticular formation. Consistent with cerebellar projections to the reticular formation (Cohen et al. 1958; Bantli and Bloedel 1975a; Gonzalo-Ruiz et al. 1988), electrical stimulation to both human (Mottolese et al. 2013) and non-human primate (Bantli and Bloedel 1975b; Soteropoulos and Baker 2008) cerebellum evokes short-latency EMG response on upper limb muscles. These responses are still intact even after the inactivation of the contralateral primary motor cortex (Bantli and Bloedel 1975b). Further, the cerebellum receives an internal copy of the descending reticulospinal command from propriospinal neurons via the lateral reticular nucleus (Azim et al. 2014).

The (tecto)-reticulospinal pathway has also been implicated in other rapid motor responses such as the startReact effect (Valls-Solé et al. 1995; Carlsen et al. 2004; Oude Nijhuis et al. 2007; Honeycutt et al. 2013), forced-RT paradigms (Haith et al. 2015, 2016), or corrective reach movements (Carlton 1981; Day and Brown 2001; Reynolds and Day 2012). Our results, which demonstrate a selective influence of implicit motor learning on this descending pathway, may also explain

the adaptation of these responses during various motor learning paradigms. For example, both startReact and corrective reach movements are modulated during motor learning induced by a force field (Franklin et al. 2012; Wright et al. 2015) or, as studied here, a visuomotor rotation (Telgen et al. 2014; Hayashi et al. 2016). However, the contribution of implicit versus explicit components of motor learning was not considered in these paradigms. Here, by isolating EMG activity attributable to the tectoreticulospinal pathway and segregating the implicit and explicit components of motor learning, we can directly quantify the influence of different components of motor learning via the changes in the tuning of the SLR. Such an approach may be particularly useful for future work on motor learning in animal models to directly quantify both the implicit and the explicit components via the SLR and eye tracking (De Brouwer et al. 2018), as these objective measures could serve as benchmarks for comparison with simultaneously recorded neural activity.

4.6 References

- Alamia A, Orban de Xivry J-J, San Anton E, Olivier E, Cleeremans A, Zenon A. Unconscious associative learning with conscious cues. *Neurosci Conscious* 2016: niw016, 2016.
- Alstermark B, Isa T. Circuits for skilled reaching and grasping. *Annu Rev Neurosci* 35: 559–578, 2012.
- Atsma J, Maij F, Gu C, Medendorp WP, Corneil BD. Active braking of whole-arm reaching movements provides single-trial neuromuscular measures of movement cancellation. *J Neurosci* 38: 1745–17, 2018.
- Azim E, Jiang J, Alstermark B, Jessell TM. Skilled reaching relies on a V2a propriospinal internal copy circuit. *Nature* 508: 357–363, 2014.
- Bantli H, Bloedel JR. Monosynaptic activation of a direct reticulo-spinal pathway by the dentate nucleus. *Pflugers Arch* 357: 237–242, 1975a.
- Bantli H, Bloedel JR. The action of the dentate nucleus on the excitability of spinal motoneurons via pathways which do not involve the primary sensorimotor cortex. *Brain Res* 88: 86–90, 1975b.
- Bond KM, Taylor JA. Flexible explicit but rigid implicit learning in a visuomotor adaptation task. *J Neurophysiol* 113: 3836–3849, 2015.
- De Brouwer AJ, Albaghdadi M, Flanagan JR, Gallivan JP. Using Gaze Behavior to Parcellate the Explicit and Implicit Contributions to Visuomotor Learning. *J Neurophysiol* (July 11, 2018). doi: 10.1152/jn.00113.2018.
- Butcher PA, Ivry RB, Kuo S-H, Rydz D, Krakauer JW, Taylor JA. The cerebellum does more than sensory-prediction-error-based learning in sensorimotor adaptation tasks. *J Neurophysiol* 118: jn.00451.2017, 2017.
- Carlsen AN, Chua R, Inglis JT, Sanderson DJ, Franks IM. Prepared movements are elicited early by startle. *J Mot Behav* 36: 253–264, 2004.
- Carlton LG. Processing visual feedback information for movement control. *J Exp Psychol Hum Percept Perform* 7: 1019–1030, 1981.

- Chapman BB, Corneil BD. Neuromuscular recruitment related to stimulus presentation and task instruction during the anti-saccade task. *Eur J Neurosci* 33: 349–360, 2011.
- Cohen D, Chambers WW, Sprague JM. Experimental study of the efferent projections from the cerebellar nuclei to the brainstem of the cat. *J Comp Neurol* 109: 233–259, 1958.
- Corneil BD, Olivier E, Munoz DP. Visual responses on neck muscles reveal selective gating that prevents express saccades. *Neuron* 42: 831–841, 2004.
- Day BL, Brown P. Evidence for subcortical involvement in the visual control of human reaching. *Brain* 124: 1832–1840, 2001.
- Fernandez-Ruiz J, Goltz HC, DeSouza JFX, Vilis T, Crawford JD. Human parietal “reach region” primarily encodes intrinsic visual direction, not extrinsic movement direction, in a visual motor dissociation task. *Cereb Cortex* 17: 2283–2292, 2007.
- Fernandez-Ruiz J, Wong W, Armstrong IT, Flanagan JR. Relation between reaction time and reach errors during visuomotor adaptation. *Behav Brain Res* 219: 8–14, 2011.
- Franklin S, Wolpert DM, Franklin DW. Visuomotor feedback gains upregulate during the learning of novel dynamics. *J Neurophysiol* 108: 467–478, 2012.
- Galea JM, Sami SA, Albert NB, Miall RC. Secondary tasks impair adaptation to step- and gradual-visual displacements. *Exp Brain Res* 202: 473–484, 2010.
- Georgopoulos AP, Massey JT. Cognitive spatial-motor processes - 1. The making of movements at various angles from a stimulus direction. *Exp Brain Res* 65: 361–370, 1987.
- Gibo TL, Criscimagna-Hemminger SE, Okamura AM, Bastian AJ. Cerebellar motor learning: are environment dynamics more important than error size? *J Neurophysiol* 110: 322–333, 2013.
- Gonzalo-Ruiz A, Leichnetz GR, Smith DJ. Origin of cerebellar projections to the region of the oculomotor complex, medial pontine reticular formation, and

- superior colliculus in new world monkeys: A retrograde horseradish peroxidase study. *J Comp Neurol* 268: 508–526, 1988.
- Gu C, Pruszynski JA, Gribble PL, Corneil BD. Done in 100 ms: path-dependent visuomotor transformation in the human upper limb. *J Neurophysiol* 119: 1319–1328, 2018.
- Gu C, Wood DK, Gribble PL, Corneil BD. A Trial-by-Trial Window into Sensorimotor Transformations in the Human Motor Periphery. *J Neurosci* 36: 8273–8282, 2016.
- Haar S, Donchin O, Dinstein I. Dissociating visual and motor directional selectivity using visuomotor adaptation. *J Neurosci* 35: 6813–6821, 2015.
- Haith AM, Huberdeau DM, Krakauer JW. The Influence of Movement Preparation Time on the Expression of Visuomotor Learning and Savings. *J Neurosci* 35: 5109–5117, 2015.
- Haith AM, Pakpoor J, Krakauer JW. Independence of Movement Preparation and Movement Initiation. *J Neurosci* 36: 3007–3015, 2016.
- Hayashi T, Yokoi A, Hirashima M, Nozaki D. Visuomotor Map Determines How Visually Guided Reaching Movements are Corrected Within and Across Trials. *eNeuro* 3, 2016.
- Honda T, Hirashima M, Nozaki D. Adaptation to visual feedback delay influences visuomotor learning. *PLoS One* 7: e37900, 2012.
- Honeycutt CF, Kharouta M, Perreault EJ. Evidence for reticulospinal contributions to coordinated finger movements in humans. *J Neurophysiol* 110: 1476–83, 2013.
- Izawa J, Shadmehr R. Learning from sensory and reward prediction errors during motor adaptation. *PLoS Comput Biol* 7: e1002012, 2011.
- Kagerer FA, Contreras-Vidal JL, Stelmach GE. Adaptation to gradual as compared with sudden visuo-motor distortions. *Exp Brain Res* 115: 557–561, 1997.
- Kim HE, Parvin DE, Ivry RB. Intrinsic rewards modulate sensorimotor adaptation. *bioRxiv* (July 6, 2018). doi: 10.1101/363606.

- Klassen J, Tong C, Flanagan JR. Learning and recall of incremental kinematic and dynamic sensorimotor transformations. *Exp Brain Res* 164: 250–259, 2005.
- Krakauer JW. Motor learning and consolidation: the case of visuomotor rotation. *Adv Exp Med Biol* 629: 405–421, 2009.
- Krakauer JW, Ghez C, Ghilardi MF. Adaptation to visuomotor transformations: consolidation, interference, and forgetting. *J Neurosci* 25: 473–478, 2005.
- Kuypers HGJM. Anatomy of the descending pathways. In: *Handbook of Physiology - The Nervous System II.*, edited by Brookhart JM, Mountcastle VB. Bethesda, MD: Am. Physiol. Soc., 1981, p. 597–666.
- Lee D, Seo H, Jung MW. Neural Basis of Reinforcement Learning and Decision Making. *Annu Rev Neurosci* 35: 287–308, 2012.
- Lemon RN. Descending pathways in motor control. *Annu Rev Neurosci* 31: 195–218, 2008.
- Leow L-A, Marinovic W, rugy A de, Carroll T. Task errors contribute to implicit remapping in sensorimotor adaptation. *bioRxiv* (February 28, 2018). doi: 10.1101/263988.
- Mazzoni P, Krakauer JW. An implicit plan overrides an explicit strategy during visuomotor adaptation. *J Neurosci* 26: 3642–3645, 2006.
- Morehead JR, Taylor JA, Parvin D, Ivry RB. Characteristics of Implicit Sensorimotor Adaptation Revealed by Task-irrelevant Clamped Feedback. *J Cogn Neurosci* 25: 1–14, 2017.
- Morton SM, Bastian AJ. Prism adaptation during walking generalizes to reaching and requires the cerebellum. *J Neurophysiol* 92: 2497–2509, 2004.
- Mottolese C, Richard N, Harquel S, Szathmari A, Sirigu A, Desmurget M. Mapping motor representations in the human cerebellum. *Brain* 136: 330–342, 2013.
- Oude Nijhuis LB, Janssen L, Bloem BR, van Dijk JG, Gielen SC, Borm GF, Overeem S. Choice reaction times for human head rotations are shortened by startling acoustic stimuli, irrespective of stimulus direction. *J Physiol* 584: 97–109, 2007.

- Paz R, Boraud T, Natan C, Bergman H, Vaadia E. Preparatory activity in motor cortex reflects learning of local visuomotor skills. *Nat Neurosci* 6: 882–890, 2003.
- Perich MG, Gallego JA, Miller LE. A neural population mechanism for rapid learning. *bioRxiv preprint*: 1–24, 2017.
- Pine ZM, Krakauer JW, Gordon J, Ghez C. Learning of scaling factors and reference axes for reaching movements. *Neuroreport* 7: 2357–2361, 1996.
- Pruszynski JA, King GL, Boisse L, Scott SH, Flanagan JR, Munoz DP. Stimulus-locked responses on human arm muscles reveal a rapid neural pathway linking visual input to arm motor output. *Eur J Neurosci* 32: 1049–1057, 2010.
- Rabe K, Livne O, Gizewski ER, Aurich V, Beck A, Timmann D, Donchin O. Adaptation to visuomotor rotation and force field perturbation is correlated to different brain areas in patients with cerebellar degeneration. *J Neurophysiol* 101: 1961–1971, 2009.
- Reichenthal M, Avraham G, Karniel A, Shmuelof L. Target size matters: target errors contribute to the generalization of implicit visuomotor learning. *J Neurophysiol* 116: 411–424, 2016.
- Reynolds RF, Day BL. Direct visuomotor mapping for fast visually-evoked arm movements. *Neuropsychologia* 50: 3169–3173, 2012.
- Schlerf JE, Xu J, Klemfuss NM, Griffiths TL, Ivry RB. Individuals with cerebellar degeneration show similar adaptation deficits with large and small visuomotor errors. *J Neurophysiol* 109: 1164–1173, 2013.
- Shadmehr R, Smith MA, Krakauer JW. Error correction, sensory prediction, and adaptation in motor control. *Annu Rev Neurosci* 33: 89–108, 2010.
- Shen L, Alexander GE. Neural correlates of a spatial sensory-to-motor transformation in primary motor cortex. *J Neurophysiol* 77: 1171–1194, 1997a.
- Shen L, Alexander GE. Preferential representation of instructed target location versus limb trajectory in dorsal premotor area. *J Neurophysiol* 77: 1195–1212, 1997b.

- Shmuelof L, Huang VS, Haith AM, Delnicki RJ, Mazzoni P, Krakauer JW. Overcoming Motor “Forgetting” Through Reinforcement Of Learned Actions. *J Neurosci* 32: 14617–14621a, 2012.
- Slachevsky A, Pillon B, Fourneret P, Pradat-Diehl P, Jeannerod M, Dubois B. Preserved Adjustment but Impaired Awareness in a Sensory-Motor Conflict following Prefrontal Lesions. *J Cogn Neurosci* 13: 332–340, 2001.
- Slachevsky A, Pillon B, Fourneret P, Renié L, Levy R, Jeannerod M, Dubois B. The prefrontal cortex and conscious monitoring of action: An experimental study. *Neuropsychologia* 41: 655–665, 2003.
- Soteropoulos DS, Baker SN. Bilateral representation in the deep cerebellar nuclei. *J Physiol* 586: 1117–1136, 2008.
- Steenrod SC, Phillips MH, Goldberg ME. The lateral intraparietal area codes the location of saccade targets and not the dimension of the saccades that will be made to acquire them. *J Neurophysiol* 109: 2596–2605, 2013.
- Taylor JA, Ivry RB. Flexible cognitive strategies during motor learning. *PLoS Comput Biol* 7: e1001096, 2011.
- Taylor JA, Klemfuss NM, Ivry RB. An explicit strategy prevails when the cerebellum fails to compute movement errors. *The Cerebellum* 9: 580–586, 2010.
- Taylor JA, Krakauer JW, Ivry RB. Explicit and implicit contributions to learning in a sensorimotor adaptation task. *J Neurosci* 34: 3023–3032, 2014.
- Telgen S, Parvin D, Diedrichsen J. Mirror reversal and visual rotation are learned and consolidated via separate mechanisms: recalibrating or learning de novo? *J Neurosci* 34: 13768–13779, 2014.
- Therrien AS, Wolpert DM, Bastian AJ. Effective reinforcement learning following cerebellar damage requires a balance between exploration and motor noise. *Brain* 139: 101–114, 2016.
- Thoroughman KA, Shadmehr R. Learning of action through adaptive combination of motor primitives. *Nature* 407: 742–747, 2000.

- Tseng Y-W, Diedrichsen J, Krakauer JW, Shadmehr R, Bastian AJ. Sensory prediction errors drive cerebellum-dependent adaptation of reaching. *J Neurophysiol* 98: 54–62, 2007.
- Valls-Solé J, Solé A, Valldeoriola F, Muñoz E, Gonzalez LE, Tolosa ES. Reaction time and acoustic startle in normal human subjects. *Neurosci Lett* 195: 97–100, 1995.
- Welford AT. Choice reaction time: basis concepts. In: *Reaction times*, edited by Welford AT. New York, NY: Academic Press, 1980, p. 73–128.
- Werner S, Bock O, Gizewski ER, Schoch B, Timmann D. Visuomotor adaptive improvement and aftereffects are impaired differentially following cerebellar lesions in SCA and PICA territory. *Exp Brain Res* 201: 429–439, 2010.
- Werner S, Schorn CF, Bock O, Theysohn N, Timmann D. Neural correlates of adaptation to gradual and to sudden visuomotor distortions in humans. *Exp Brain Res* 232: 1145–1156, 2014.
- Wolpert DM, Miall RC, Kawato M. Internal models in the cerebellum. *Trends Cogn Sci* 2: 338–347, 1998.
- Wood DK, Gu C, Corneil BD, Gribble PL, Goodale MA. Transient visual responses reset the phase of low-frequency oscillations in the skeletomotor periphery. *Eur J Neurosci* 42: 1919–1932, 2015.
- Wright ZA, Carlsen AN, MacKinnon CD, Patton JL. Degraded expression of learned feedforward control in movements released by startle. *Exp Brain Res* 233: 2291–2300, 2015.

Chapter 5 – General Discussion

In this thesis, I have attempted to characterize the sensorimotor properties of a rapid visuomotor response in humans. To do this, I recorded neuromuscular activity from an upper limb muscle while healthy human participants performed visually-mediated reach movements from a static starting posture to different novel visual stimuli. I specifically examined the initial stimulus-locked response (*SLR*), which is the earliest wave of directionally-tuned EMG activity that occurs ~100 ms after the onset of a novel visual stimulus (Pruszynski et al., 2010; Wood et al., 2015). These SLRs precede the larger and temporally stochastic wave of neuromuscular activity associated with volitional control, which occurs ~200-300 ms after stimulus onset (Welford, 1980). Despite the short-latency of these SLRs, the results of this thesis demonstrated that the neural circuit that mediates the SLR has a level of sophistication classically associated with volitional control (**Figure 5.1**). Below, I will summarize the key findings from each chapter and highlight the sensorimotor properties of the SLR. Afterwards, I will detail the limitations of the current experiments and suggest some potential avenues for future experiments. Finally, in the last section, I will speculate on the possible roles of these descending motor commands for healthy human motor control.

5.1 Summary of results

A prior study, using a delayed visually-guided reach task, showed that the SLR could be temporally dissociated from the ensuing volitional reach movement (Wood et al., 2015). However, coming out of that study, it was still unknown if the

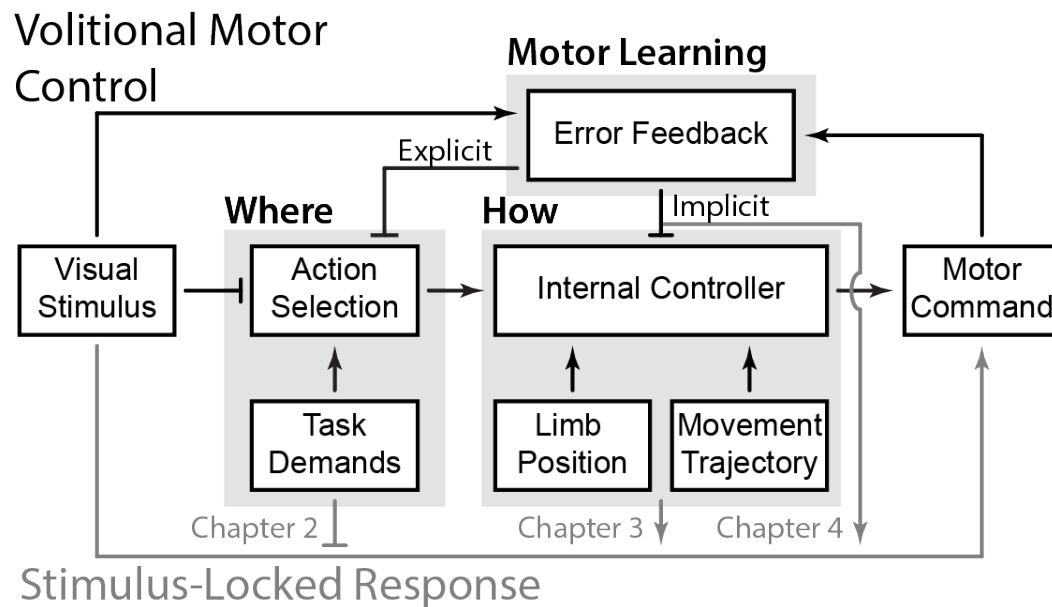


Figure 5.1: Summary of results from all experiments.

In **Chapter 2**, by using the pro-/anti-task, I showed that while the SLR still encodes the visual location, the magnitude of the SLR is modulated by task demands. In **Chapter 3**, I showed the pathway mediating SLR integrates visual input with both the current limb position and the planned movement trajectory. Finally in **Chapter 4**, I showed that the SLR is selectively influenced by the implicit, but not the explicit, motor learning process.

SLR was either a reflexive motor command towards the visual stimulus or a preparatory response for the delayed reach movement. In Chapter 2, I directly tested these two different possibilities by examining the SLR during a pro-/anti-reach task (Munoz and Everling, 2004; Gail and Andersen, 2006). Participants performed intermixed reaching movements either towards (pro-reach) or in the diametrically opposite direction (anti-reach) of the stimulus location. This task spatially dissociated the visual stimulus from the ensuing reach movement. I found two main differences between the SLR and volitional control during the task. First, the SLR was a directionally-tuned motor command towards the spatial location of the visual stimulus, not the ensuing goal-direction movement. Second, the

increase in task demand (i.e. anti- compared to pro-reach trials) prolonged mean RTs for volitional control but only altered the magnitude of the SLR, not its latency. Thus, the SLR is a rapid visuomotor reflex towards the visual stimulus location, but changes in task demand can influence the SLR magnitude (**Figure 5.1**). The sensorimotor properties of the SLR from Chapter 2 are consistent with previous studies of both online reach corrective movements during a pro-/anti-point task (Day and Lyon, 2000) and express saccades during a pro-/anti-saccade task (Hallett, 1978). Further, the attenuation of the SLR magnitude during anti-reach trials was similar to that previously observed with visual responses in the SCi during the pro-/anti-task (Everling et al., 1998, 1999).

Since the SLR is a visuomotor reflex towards the visual stimulus location, in Chapter 3, I next examined the underlying reference frame of the SLR. For any given visually-guided volitional reach movements, there must be a non-trivial coordinate transformation from the visual stimulus location that is in an eye-centric reference frame to a motor command that is in a hand-centric reference frame (Buneo and Andersen, 2006). The first experiment in Chapter 3 examined if the pathway mediating the SLR could also perform this visual-to-motor transformation. To do this, participants started in three different eye and hand configurations and they generated coordinated eye-hand movements towards novel visual stimulus locations (**Figure 3.1**). I found that the pathway mediating the SLR rapidly integrated visual and proprioceptive information and transformed the eye-centric visual input into a proper hand-centric motor output (**Figure 5.1**). The hand-centric

reference frame of the SLR is distinct from the neural responses previously observed in both the PPC and PMd, as neurophysiological studies have reported either an eye-centric or a mixture of both eye and hand-centric references in both PPC (Batista et al., 1999; Bremner and Andersen, 2012, 2014) and PMd (Pesaran et al., 2006; Batista et al., 2007), respectively.

In the second part of Chapter 3, I examined whether different pre-planned movement trajectory altered the magnitude of the SLR to the same visual stimulus location. Up to this point, participants in the previous experiments examining the SLR have generated stereotypically straight point-to-point reach movements (Flash and Hogan, 1985), even though there are an infinite number of possible reach trajectories for any two-dimensional horizontal reach movement. To elicit different reach trajectories, participants were instructed to reach either around or through different obstacles to the same visual stimulus location (**Figure 3.2** and **Figure 3.3**). The obstacles were presented ahead of time so that participants had time to pre-plan their volitional reach trajectory. I found that the SLR magnitude was systematically altered based on the initial direction of the participant's pre-planned reach trajectory, even though the same visual stimulus appeared. Further, the changes in SLR magnitude correlated with the later involvement of the muscle during the volitional reach movement (**Figure 5.1**).

Given that the pathway mediating the SLR could integrate visual and proprioceptive inputs, in Chapter 4, I examined how the SLR altered after participants learned a novel visual-to-motor mapping. Predominant theories of

motor control have suggested that the brain maintains an internal model and predicts sensory consequences of motor actions (Wolpert et al., 1998). Further, the brain recalibrates its internal model by learning from an error signal computed from the difference between the predicted and actual sensory inputs. Experimentally, a simple way to elicit motor learning is by systematically altering the visual representation of the participant's hand, via a visuomotor rotation task (Krakauer, 2009; **Figure 1.2a**). This task requires participants to learn a new motor command for the exact same visual stimulus location.

Recent behavioral studies have suggested that two distinct components of motor learning are engaged during this task; an implicit error-based process and an explicit cognitive aim strategy (Mazzoni and Krakauer, 2006; Taylor et al., 2014). To dissociate between the implicit and explicit motor learning components, I examined the changes in SLR magnitude and the directional tuning of the SLR during three variations of the visuomotor rotation task. I found that the directional tuning of the SLR systematically altered during tasks with an implicit motor learning component (i.e. a mismatch between the visual feedback and the participant's actual hand position), while both the implicit and explicit components influenced the tuning of the later volitional control (**Figure 5.1**). However, the extent of SLR adaptation were significantly smaller compared to the full adaptation during volitional control. This partial adaptation was consistent with previous indirect estimates of the implicit motor learning component in similar tasks (Taylor et al., 2014; Bond and Taylor, 2015; Morehead et al., 2017). In contrast, SLR tuning did

not systematically alter during a task that only engaged in the explicit motor learning component.

5.2 Future Directions

5.2.1 Neural substrate that mediates the SLR

The current experiments in this thesis and previous studies examining the SLR (Pruszynski et al., 2010; Wood et al., 2015) have all hypothesized that the SLR is mediated via a tecto-reticulospinal pathway rather than the classical corticospinal pathway (Alstermark and Isa, 2012) associated with volitional control. However, all the current experiments examining the SLR have used healthy human participants, and causal animal experiments are necessary to test if a tecto-reticulospinal pathway truly mediates the SLR.

A specific region of interest along this possible tecto-reticulospinal pathway is the SCi within the brainstem. As mentioned in the General Introduction, previous neurophysiological and imaging studies have shown an increase in SCi activity prior to contralateral reach movements (Werner, 1993; Stuphorn et al., 2000; Linzenbold and Himmelbach, 2012; Himmelbach et al., 2013). Further, neural activity in SCi correlated with EMG activity on upper limb muscles (Werner et al., 1997; Stuphorn et al., 1999), and electrical stimulation of SCi can evoke contralateral arm movements in both NHPs (Philipp and Hoffmann, 2014) and cats (Courjon et al., 2004). Additionally, the SLR results from the pro-/anti-reach task in

Chapter 2 are highly reminiscent of visuomotor neurons previously described in the SCi (Everling et al., 1998, 1999).

The anatomical layout of the SCi is also ideal for this potential causal experiment. Due to its well-defined retinotopic organization (Robinson, 1972; Ottes et al., 1986; Hafed and Chen, 2016), pharmacological inactivation via muscimol infusion can selectively alter both saccadic eye movements (Hikosaka and Wurtz, 1985; Aizawa and Wurtz, 1998; Quaia et al., 1998) and covert attention (Robinson and Kertzman, 1995; Lovejoy and Krauzlis, 2010; Zénon and Krauzlis, 2012) towards a specific portion of the contralateral visual hemifield. Additionally, a previous study has shown that inactivation of the SCi can cause reach selection deficits to the contralateral visual hemifield, but does not affect the actual reach kinematics associated with the volitional reach movements (Song et al., 2011).

If the SCi is truly mediating the SLR, then I predict that inactivation of the SCi will selectively abolish the SLR to the contralateral visual hemifield, while sparing the ensuing volitional reach movement. Furthermore, if the tecto-reticulospinal pathway plays an even broader role and mediates other types of rapid visuomotor responses, then inactivation of the SCi will also selectively abolish the initial portion of online reach corrections (Day and Brown, 2001; Day, 2014) and will alter task performance in forced-RT paradigms (Stanford et al., 2010; Haith et al., 2016).

5.2.2 Inter-limb coordination of human rapid visuomotor responses

In addition to the causal animal experiments required to determine the underlying neural substrates mediating the SLR, more human behavioral studies that are also required to test other sensory and motor properties of the SLR.

Previous studies have also shown that anticipatory postural adjustments (APAs) are generated to counteract the forces from the ensuing voluntary movement (Marsden et al., 1981; Bouisset and Zattara, 1987). APAs occur throughout different axial and lower limb muscles, even when they are not directly involved in movement, and these APAs are altered when participant learn novel environment (Ahmed and Wolpert, 2009). Physiological recordings in the cat have suggested that neural activity in the pontomedullary reticular formation correlated with APAs (Prentice and Drew, 2001; Schepens and Drew, 2004; Schepens et al., 2008).

Since the SLR is an active motor command towards the stimulus location, are APAs also generated to counteract the SLR? Previous work has shown that the SLR on the right PEC muscle persist even when the ensuing reach is delay (Wood et al., 2015; Atsma et al., 2018). So, does the profile of the SLR on the right PEC muscle change when the participants perform a left-handed reach movement and the right PEC muscle becomes a stabilizing muscle rather than an agonist muscle? Further, if APAs do occur for the SLR, there should also be changes in EMG activity during the SLR epoch in various axial/trunk muscles to stabilize the SLR observed on the upper limb muscles.

5.2.3 Sensory properties of human rapid visuomotor responses

In this thesis, I have only examined how the SLR magnitude altered when participant adjusted their motor output for the same visual stimulus. In all the previous experiments, I used the onset of a small stationary black punctate dot on a white LCD screen to elicit the SLR. However, little is known about the optimal visual parameters that can best elicit these rapid visuomotor responses. A previous study demonstrated that both SLR magnitude and latency modulated as a function of the overall contrast (i.e. the darkness) of the visual stimulus (Wood et al., 2015), but nothing else is known about the best parameters to elicit the SLR. Below, I detail two possible visual properties of the SLR to test in the future.

First, the optimal eccentricity and size of the visual stimulus to best elicit the SLR is still unknown. A previous study demonstrated that the magnitude of online reach corrections saturated when the stimulus jumped greater than 2 cm (Franklin et al., 2016). Similarly for the SLR, Pruszynski and colleagues (2010) found no reliable differences in SLR magnitude between a stimulus located either at 10 or 15 cm from the start position. Here, I replicated this result when the stimulus was either 10 or 20 cm from the start position during the Experiment 1 of Chapter 3. However, in all these experiments the size of the stimulus did not change. This creates a potential confound as more eccentric visual stimuli have a smaller retinotopic representation compared to more foveal stimuli. A better controlled experiment is required to determine the optimal combination of size and eccentricity of the visual stimulus to elicit the SLR.

Second, visual stimuli can also be quantified along a spatial frequency domain. Broadly speaking, visual information enters the brain via two distinct pathways: a faster magnocellular (M) pathway that transmits low-spatial frequency information and a slower parvocellular (P) pathway that transmits high-spatial frequency information (Merigan and Maunsell, 1993). By using a punctate black dot, I have completely ignored which of these visual pathways may mediate the SLR. A current ongoing project in the lab has been trying to dissociate between the M and P pathways by using visual stimuli with different spatial frequencies. Previous animal studies have suggested that SCs receives direct retinotectal projections from M, but not P, pathway (Hoffmann, 1973; Marrocco and Li, 1977). Further inactivation of the M pathway selectively abolishes visual responses in SCi (Schiller et al., 1979). Thus, if the SLR is mediated through the SCi, then low spatial frequency visual stimuli should evoke a larger SLR compared to a high spatial frequency stimuli when controlled for overall contrast.

5.3 The role of the rapid visuomotor responses

Classically, motor control has generally categorized motor commands into either low-level reflexes that response to external perturbations (such as the classic H-reflex) or sophisticated deliberate motor actions (such as volitional control). However, recent experiments examining reflexive-like movements to both visual and mechanical perturbations (Pruszynski and Scott, 2012; Scott, 2016) have argued instead for a continuum. Consistent with this notion, the results of this

thesis have demonstrated that the sensorimotor properties of the SLR lies on that continuum, somewhere in between low-level reflexes and volitional control. The logic follow-up question becomes why do humans have these intermediate rapid visuomotor responses?

One possible explanation may be that the tecto-reticulospinal pathway mediating the SLR is a remnant of a phylogenetically older visuomotor system. The superior colliculus, or the optic tectum in non-mammals, is highly conserved as are general orienting behaviours across a variety of different species (Land, 2011). Additionally, seminal lesion experiments from Lawrence and Kyupers (1968a, 1968b) demonstrated that the reticulospinal descending motor pathway is critical for gross overt movements and postural control. In contrast, the phylogenetically newer corticospinal pathway seems to contribute primarily for fine dexterous movements. Consistent with the functions of the reticulospinal pathway, the SLR generates an overt orienting movement towards the novel stimulus. And as seen in Chapters 2 and 4, the pathway mediating the SLR is incapable of generating novel motor commands away from the stimulus location based on different task demands. The presences of a more flexible and sophisticated corticospinal pathway may have diminished the role of this older reflexive reticulospinal pathway during visually-guided movements. However, the trade-off of this additional cortical processing comes at a cost of increased latency, thus allowing us to temporal dissociate these two pathways (Scott, 2016). While this increase in latency is generally advantageous for healthy motor control, there are

specific cases where this rapid sub-cortical pathway can still be beneficial (i.e. express saccades and online reach control).

However, not all orienting movements towards novel visual stimulus are advantageous. For example, it is known that the SCi in rodents mediates two diametrically opposite types of motor commands in response to novel visual stimuli: (1) the general orienting responses towards the stimulus mentioned throughout this thesis and (2) an avoidance or defense-like responses away from the stimulus (Dean et al., 1989). Behaviorally, a “looming” stimulus, where the visual stimulus expands symmetrically towards the viewer, can also elicit avoidance behaviour in both humans and NHPs (Schiff et al., 1962; King et al., 1992). Further ablation of primary visual cortex does not abolish these defensive responses (King and Cowey, 1992), while over-excitation of the primate SCi can produce similar defensive responses (DesJardin et al., 2013). The logical question becomes is how does the human brain determine if the novel stimulus is one of interest (i.e. to orient towards) or one of danger (i.e. to avoid) to generate the proper motor command?

5.4 Reference

- Ahmed AA, Wolpert DM (2009) Transfer of Dynamic Learning Across Postures. *J Neurophysiol* 102:2816–2824.
- Aizawa H, Wurtz RH (1998) Reversible inactivation of monkey superior colliculus. I. Curvature of saccadic trajectory. *J Neurophysiol* 79:2082–2096.

- Alstermark B, Isa T (2012) Circuits for skilled reaching and grasping. *Annu Rev Neurosci* 35:559–578.
- Atsma J, Majij F, Gu C, Medendorp WP, Corneil BD (2018) Active braking of whole-arm reaching movements provides single-trial neuromuscular measures of movement cancellation. *J Neurosci* 38:1745–17.
- Batista AP, Buneo CA, Snyder LH, Andersen RA (1999) Reach plans in eye-centered coordinates. *Science* 285:257–260.
- Batista AP, Santhanam G, Yu BM, Ryu SI, Afshar A, Shenoy K V (2007) Reference frames for reach planning in macaque dorsal premotor cortex. *J Neurophysiol* 98:966–983.
- Bond KM, Taylor JA (2015) Flexible explicit but rigid implicit learning in a visuomotor adaptation task. *J Neurophysiol* 113:3836–3849.
- Bouisset S, Zattara M (1987) Biomechanical study of the programming of anticipatory postural adjustments associated with voluntary movement. *J Biomech* 20:735–742.
- Bremner LR, Andersen RA (2012) Coding of the reach vector in parietal area 5d. *Neuron* 75:342–351.
- Bremner LR, Andersen RA (2014) Temporal analysis of reference frames in parietal cortex area 5d during reach planning. *J Neurosci* 34:5273–5284.
- Buneo CA, Andersen RA (2006) The posterior parietal cortex: sensorimotor interface for the planning and online control of visually guided movements. *Neuropsychologia* 44:2594–2606.
- Courjon JH, Olivier E, Pelisson D (2004) Direct evidence for the contribution of the superior colliculus in the control of visually guided reaching movements in the cat. *J Physiol* 556:675–681.
- Day BL (2014) Subcortical visuomotor control of human limb movement. *Adv Exp Med Biol* 826:55–68.
- Day BL, Brown P (2001) Evidence for subcortical involvement in the visual control of human reaching. *Brain* 124:1832–1840.

- Day BL, Lyon IN (2000) Voluntary modification of automatic arm movements evoked by motion of a visual target. *Exp Brain Res* 130:159–168.
- de Brouwer AJ, Jarvis T, Gallivan JP, Flanagan JR (2017) Parallel Specification of Visuomotor Feedback Gains during Bimanual Reaching to Independent Goals. *eNeuro* 4:ENEURO.0026-17.2017.
- Dean P, Redgrave P, Westby GWM (1989) Event or emergency? Two response systems in the mammalian superior colliculus. *Trends Neurosci* 12:137–147.
- DesJardin JT, Holmes AL, Forcelli PA, Cole CE, Gale JT, Wellman LL, Gale K, Malkova L (2013) Defense-Like Behaviors Evoked by Pharmacological Disinhibition of the Superior Colliculus in the Primate. *J Neurosci* 33:150–155.
- Diedrichsen J, Nambisan R, Kennerley SW, Ivry RB (2004) Independent on-line control of the two hands during bimanual reaching. *Eur J Neurosci* 19:1643–1652.
- Everling S, Dorris MC, Klein RM, Munoz DP (1999) Role of primate superior colliculus in preparation and execution of anti-saccades and pro-saccades. *J Neurosci* 19:2740–2754.
- Everling S, Dorris MC, Munoz DP (1998) Reflex suppression in the anti-saccade task is dependent on prestimulus neural processes. *J Neurophysiol* 80:1584–1589.
- Flash T, Hogan N (1985) The coordination of arm movements: an experimentally confirmed mathematical model. *J Neurosci* 5:1688–1703.
- Franklin DW, Reichenbach A, Franklin S, Diedrichsen J (2016) Temporal Evolution of Spatial Computations for Visuomotor Control. *J Neurosci* 36:2329–2341.
- Gail A, Andersen RA (2006) Neural dynamics in monkey parietal reach region reflect context-specific sensorimotor transformations. *J Neurosci* 26:9376–9384.
- Hafed ZM, Chen C-Y (2016) Sharper, Stronger, Faster Upper Visual Field Representation in Primate Superior Colliculus. *Curr Biol* 26:1647–1658.

- Haith AM, Pakpoor J, Krakauer JW (2016) Independence of Movement Preparation and Movement Initiation. *J Neurosci* 36:3007–3015.
- Hallett PE (1978) Primary and secondary saccades to goals defined by instructions. *Vision Res* 18:1279–1296.
- Hikosaka O, Wurtz RH (1985) Modification of saccadic eye movements by GABA-related substances. I. Effect of muscimol and bicuculline in monkey superior colliculus. *J Neurophysiol* 53:266–291.
- Himmelbach M, Linzenbold W, Ilg UJ (2013) Dissociation of reach-related and visual signals in the human superior colliculus. *Neuroimage* 82:61–67.
- Hoffmann K-P (1973) Conduction velocity in pathways from retina to superior colliculus in the cat: a correlation with receptive-field properties. *J Neurophysiol* 36:409–24.
- King SM, Cowey A (1992) Defensive responses to looming visual stimuli in monkeys with unilateral striate cortex ablation. *Neuropsychologia* 30:1017–1024.
- King SM, Dykeman C, Redgrave P, Dean P (1992) Use of a distracting task to obtain defensive head movements to looming visual stimuli by human adults in a laboratory setting. *Perception* 21:245–259.
- Krakauer JW (2009) Motor learning and consolidation: the case of visuomotor rotation. *Adv Exp Med Biol* 629:405–421.
- Land MF (2011) Oculomotor behaviour in vertebrates and invertebrates. In: *The Oxford Handbook of Eye Movements* (Liversedge SP, Gilchrist I, Everling S, eds). Oxford University Press.
- Lawrence DG, Kuypers HG (1968a) The functional organization of the motor system in the monkey. I. The effects of bilateral pyramidal lesions. *Brain* 91:1–14.
- Lawrence DG, Kuypers HG (1968b) The functional organization of the motor system in the monkey. II. The effects of lesions of the descending brain-stem pathways. *Brain* 91:15–36.

- Linzenbold W, Himmelbach M (2012) Signals from the deep: reach-related activity in the human superior colliculus. *J Neurosci* 32:13881–13888.
- Lovejoy LP, Krauzlis RJ (2010) Inactivation of primate superior colliculus impairs covert selection of signals for perceptual judgments. *Nat Neurosci* 13:261–266.
- Marrocco RT, Li RH (1977) Monkey superior colliculus: properties of single cells and their afferent inputs. *J Neurophysiol* 40:844–60.
- Marsden CD, Merton PA, Morton HB (1981) Human postural responses. *Brain* 104:513–534.
- Mazzoni P, Krakauer JW (2006) An implicit plan overrides an explicit strategy during visuomotor adaptation. *J Neurosci* 26:3642–3645.
- Merigan WH, Maunsell JH (1993) How parallel are the primate visual pathways? *Annu Rev Neurosci* 16:369–402.
- Morehead JR, Taylor JA, Parvin D, Ivry RB (2017) Characteristics of Implicit Sensorimotor Adaptation Revealed by Task-irrelevant Clamped Feedback. *J Cogn Neurosci* 25:1–14.
- Munoz DP, Everling S (2004) Look away: the anti-saccade task and the voluntary control of eye movement. *Nat Rev Neurosci* 5:218–228.
- Ottes FP, Van Gisbergen JAM, Eggermont JJ (1986) Visuomotor fields of the superior colliculus: A quantitative model. *Vision Res* 26:857–873.
- Pesaran B, Nelson MJ, Andersen RA (2006) Dorsal premotor neurons encode the relative position of the hand, eye, and goal during reach planning. *Neuron* 51:125–134.
- Philipp R, Hoffmann KP (2014) Arm movements induced by electrical microstimulation in the superior colliculus of the macaque monkey. *J Neurosci* 34:3350–3363.
- Prentice SD, Drew T (2001) Contributions of the reticulospinal system to the postural adjustments occurring during voluntary gait modifications. *J Neurophysiol* 85:679–698.

- Pruszynski JA, King GL, Boisse L, Scott SH, Flanagan JR, Munoz DP (2010) Stimulus-locked responses on human arm muscles reveal a rapid neural pathway linking visual input to arm motor output. *Eur J Neurosci* 32:1049–1057.
- Pruszynski JA, Scott SH (2012) Optimal feedback control and the long-latency stretch response. *Exp Brain Res* 218:341–359.
- Quaia C, Aizawa H, Optican LM, Wurtz RH (1998) Reversible inactivation of monkey superior colliculus. II. Maps of saccadic deficits. *J Neurophysiol* 79:2097–2110.
- Reichenbach A, Franklin DW, Zatka-Haas P, Diedrichsen J (2014) A dedicated binding mechanism for the visual control of movement. *Curr Biol* 24:780–785.
- Robinson DA (1972) Eye movements evoked by collicular stimulation in the alert monkey. *Vision Res* 12:1795–1808.
- Robinson DL, Kertzman C (1995) Covert orienting of attention in macaques. III. Contributions of the superior colliculus. *J Neurophysiol* 74:713–721.
- Schepens B, Stapley P, Drew T (2008) Neurons in the pontomedullary reticular formation signal posture and movement both as an integrated behavior and independently. *J Neurophysiol* 100:2235–2253.
- Schepens BB, Drew T (2004) Independent and convergent signals from the pontomedullary reticular formation contribute to the control of posture and movement during reaching in the cat. *J Neurophysiol* 92:2217–2238.
- Schiff W, Caviness JA, Gibson JJ (1962) Persistent fear responses in rhesus monkeys to the optical stimulus of “looming.” *Science* 136:982–983.
- Schiller PH, Malpeli JG, Schein SJ (1979) Composition of geniculostriate input to superior colliculus of the rhesus monkey. *J Neurophysiol* 42:1124–33.
- Scott SH (2016) A Functional Taxonomy of Bottom-Up Sensory Feedback Processing for Motor Actions. *Trends Neurosci* 39:512–526.

- Song J-HH, Rafal RD, McPeck RM (2011) Deficits in reach target selection during inactivation of the midbrain superior colliculus. *Proc Natl Acad Sci* 108:E1433-40.
- Stanford TR, Shankar S, Massoglia DP, Costello MG, Salinas E (2010) Perceptual decision making in less than 30 milliseconds. *Nat Neurosci* 13:379–385.
- Stuphorn V, Bauswein E, Hoffmann KP (2000) Neurons in the primate superior colliculus coding for arm movements in gaze-related coordinates. *J Neurophysiol* 83:1283–1299.
- Stuphorn V, Hoffmann KP, Miller LE (1999) Correlation of primate superior colliculus and reticular formation discharge with proximal limb muscle activity. *J Neurophysiol* 81:1978–1982.
- Taylor JA, Krakauer JW, Ivry RB (2014) Explicit and implicit contributions to learning in a sensorimotor adaptation task. *J Neurosci* 34:3023–3032.
- Welford AT (1980) Choice reaction time: basis concepts. In: *Reaction times* (Welford AT, ed), pp 73–128. New York, NY: Academic Press.
- Werner W (1993) Neurons in the primate superior colliculus are active before and during arm movements to visual targets. *Eur J Neurosci* 5:335–340.
- Werner W, Dannenberg S, Hoffmann KP (1997) Arm-movement-related neurons in the primate superior colliculus and underlying reticular formation: comparison of neuronal activity with EMGs of muscles of the shoulder, arm and trunk during reaching. *Exp Brain Res* 115:191–205.
- Wolpert DM, Miall RC, Kawato M (1998) Internal models in the cerebellum. *Trends Cogn Sci* 2:338–347.
- Wood DK, Gu C, Corneil BD, Gribble PL, Goodale MA (2015) Transient visual responses reset the phase of low-frequency oscillations in the skeletomotor periphery. *Eur J Neurosci* 42:1919–1932.
- Zénon A, Krauzlis RJ (2012) Attention deficits without cortical neuronal deficits. *Nature* 489:434–437.

Appendix A: Documentation of Ethics Approval



Date: 12 January 2018

To: Brian Corneil

Project ID: 103341

Study Title: Saliency responses in human arm muscles during reaching

Application Type: Continuing Ethics Review (CER) Form

Review Type: Delegated

Meeting Date: 23/Jan/2018

Date Approval Issued: 12/Jan/2018

REB Approval Expiry Date: 08/Jan/2019

LAPSE IN REB APPROVAL: 09/Jan/2018 - 11/Jan/2018

Dear Brian Corneil ,

The Western University Research Ethics Board has reviewed the application. This study, including all currently approved documents, has been re-approved until the expiry date noted above.

REB members involved in the research project do not participate in the review, discussion or decision.

Western University REB operates in compliance with, and is constituted in accordance with, the requirements of the TriCouncil Policy Statement: Ethical Conduct for Research Involving Humans (TCPS 2); the International Conference on Harmonisation Good Clinical Practice Consolidated Guideline (ICH GCP); Part C, Division 5 of the Food and Drug Regulations; Part 4 of the Natural Health Products Regulations; Part 3 of the Medical Devices Regulations and the provisions of the Ontario Personal Health Information Protection Act (PHIPA 2004) and its applicable regulations. The REB is registered with the U.S. Department of Health & Human Services under the IRB registration number IRB 00000940.

Please do not hesitate to contact us if you have any questions.

Sincerely,

Erika Basile, Director, Office of Human Research Ethics, on behalf of Dr. Joseph Gilbert, HSREB Chair

Note: *This correspondence includes an electronic signature (validation and approval via an online system that is compliant with all regulations).*

Curriculum Vitae

Training and Education

- 2014-2018 **Ph.D. Candidate in Psychology**
University of Western Ontario, London, ON, Canada
Supervisor: Dr. Brian D. Corneil
- 2012-2014 **M.Sc. in Neuroscience**
University of Western Ontario, London, ON, Canada
Thesis: Spatial and state-dependent effects of transcranial magnetic
Stimulation of pre-frontal cortex in non-human primates
Supervisor: Dr. Brian D. Corneil
- 2008-2012 **B.Sc. (Honours) Life Science**
Queen's University, Kingston, ON, Canada

Awards

- 2018 Society for the Neural Control of Movement – Trainee Scholarship
- 2017 NSERC CGS – Michael Smith Foreign Study Supplement
- 2017 Donders and Brain and Mind Institute Exchange Trainee Programme
(Declined)
- 2016-2018 NSERC Alexander Graham Bell Canada Graduate Doctoral
Scholarship (CGS-D)
- 2016-2018 Doctoral Excellence Research Award – University of Western
Ontario
- 2016 Norman E. Nixon Mari Rämö Nixon Award – University of Western
Ontario
- 2015-2016 Ontario Graduate Scholarship – University of Western Ontario
- 2015 Brain Star Award – CIHR institute of Neurosciences, Mental Health
and Addiction
- 2013/2015 Gordon Research Conference on Eye Movement – Trainee
Scholarship
- 2008-2012 Queen's University Dean's List
- 2008-2012 Queen's Elizabeth II Aiming for the Top Scholarship – Queen's
University
- 2008 Queen's University Admission Award

Publications

- Gu, C.**, Pruszynski, J.A., Gribble, P.L., and Corneil, B.D. (2018) A rapid visuomotor response on the human upper limb is selectively influenced by implicit, but not explicit, motor learning. *bioRxiv* 354381.
- Atsma, J.S., Majj, F., **Gu, C.**, W. P. Medendorp, and Corneil, B.D. (2018) Active braking of whole-arm reaching movements provides single-trial neuromuscular measures of movement cancellation. *J Neurosci* 38(18):4367-82.
- Gu, C.**, Pruszynski, J.A., Gribble, P.L., and Corneil, B.D. (2018) Done in 100 ms: Path-dependent visuomotor transformation in the human upper limb. *J. Neurophysiol* 119(4):1319-1328.
- Camp, A.J., **Gu, C.**, Cushing, L.S., Gordon, K., and Corneil, B.D. (2017) Splenius capitis is a reliable target for measurement of the cVEMP in a simple standing posture. *Eur J Neurosci* 45(9):1212-23.
- Gu, C.**, Wood, D.K., Gribble, P.L., and Corneil, B.D. (2016) A trial-by-trial window into sensorimotor transformations in the human motor periphery. *J Neurosci* 36(31):8273-82.
- Goonetilleke, S.A., Katz, L., Wood, D.K., **Gu, C.**, Huk, A.C., and Corneil, B.D. (2015) Cross-species comparison of anticipatory and stimulus-driven neck muscle activity well before saccadic gaze shifts in humans and non-human primates. *J Neurophysiol* 114(2):902-13.
- Wood, D.K., **Gu, C.**, Corneil, B.D., Gribble, P.L., and Goodale, M.A. (2015) Transient visual responses reset the phase of low-frequency oscillations in the skeletomotor periphery. *Eur J Neurosci* 42(3):1919-32.
- Gu, C.** and Corneil, B.D. (2014) Transcranial magnetic stimulation of the prefrontal cortex in awake nonhuman primates evokes a polysynaptic neck muscle response that reflects oculomotor activity at the time of stimulation. *J Neurosci* 34(44):14803-15.

Conference Activities

Oral Presentations

- Corneil, B.D., **Gu, C.**, Faubert K., Bulter B., Cushing, L.S., and Camp, A.J. (2018) Development of a non-human primate model for the cervical vestibular evoked myogenic potential. XXX Bárány Society Meeting, Uppsala, Sweden
- Corneil, B.D., Atsma, J.S., Majj, F., **Gu, C.**, and Medendorp, W.P. (2018) Active braking of whole-arm reaching movements provides single-trial

neuromuscular measures of movement cancellation. International Society for Electrophysiology and Kinesiology, Dublin, Ireland

- Gu, C.**, Pruszynski, J.A., Gribble, P.L., and Corneil, B.D. (2018) Direct readout of implicit motor learning using a fast visuomotor re ex. Neural Control of Movement, Santa Fe, NM, USA
- Selen, J.P.L., **Gu, C.**, Medendorp, W.P., and Corneil, B.D. (2018) Competition between reach targets within the fast visuomotor pathway. TeaP (Tagung Experimentell Arbeitender Psychologen), Marburg, Germany
- Gu, C.**, Park, D.K., Gribble, P.L., and Corneil, B.D. (2015) Ultra-rapid integration of proprioceptive information with visual stimulus on human limb muscle. Gordon Research Seminar on Eye Movements, Boston, MA, USA

Poster Presentations

- Kozak, R.A., **Gu, C.**, Johnston, K., and Corneil, B.D. (2017) Short-latency stimulus-locked responses on human upper limb muscles are preferentially evoked by low spatial frequency stimuli. Society for Neuroscience, Washington, DC, USA
- Gu, C.**, Selen L.P.J., Medendorp W.P., and Corneil B.D. (2017) Spatio-temporal competition between visual stimuli within the fast visuomotor pathway. Gordon Research Conference on Eye Movements, Lewiston, ME, USA
- Kozak, R.A., **Gu, C.**, Johnston, K., and Corneil, B.D. (2017) Stimulus locked visual responses on human upper limb muscles are preferentially sensitive to low spatial frequencies. CAPnet-CPS CAN- ACN Satellite Symposium, Montreal, Canada
- Sengupta, S., Selen, L.P.J., Medendorp, W.P., **Gu, C.**, Corneil, B.D., and Praamstra, P. (2017) High- density surface EMG recording of the SLR. Neural Control of Movement, Dublin, Ireland
- Gu, C.**, Pruszynski, J.A., Gribble, P.L., and Corneil, B.D. (2017) Visuomotor properties of the reticulospinal contribution during human visually-guided reach movements. Neural Control of Movement, Dublin, Ireland
- Gu, C.**, Pruszynski, J.A., Gribble, P.L., and Corneil, B.D. (2016) Visual stimulus-locked responses on upper limb muscle are modulated by the upcoming reach trajectory. Society for Neuroscience, San Diego, CA, USA
- Gu, C.**, Wood, D.K, Pruszynski, J.A., Gribble, P.L., and Corneil, B.D. (2016) The sensorimotor properties of the fast visuomotor system. Neural Control of Movement, Montego Bay, Jamaica
- Gu, C.**, Pruszynski, J.A., Gribble, P.L., and Corneil, B.D. (2015) Adaptation of ultra-rapid visual responses on a human upper limb muscle during visuomotor rotation. Society for Neuroscience, Chicago, IL, USA
- Camp, A.J., **Gu, C.**, Cushing, L.S., Gordon, K., and Corneil, B.D. (2015) Splenius Capitis is a reliable target for measurement of the cVEMP in a simple standing posture. Gordon Research Conference on Eye Movements,

Boston, MA, USA

- Gu, C.**, Park, D.K., Gribble, P.L., and Corneil, B.D. (2015) Ultra-rapid integration of proprioceptive information with visual stimulus on human limb muscle. Gordon Research Conference on Eye Movements, Boston, MA, USA
- Gu, C.**, Wood, D.K., Gribble, P.L., Doherty T.J., and Corneil, B.D. (2014) Visual responses on upper limb muscles during pro- and anti-reach movement implicate the superior colliculus. Society for Neuroscience, Washington D.C., USA
- Gu, C.**, Wood, D.K., Gribble, P.L., Doherty T.J., and Corneil, B.D. (2014) Visual responses on human upper limb muscles can be independent of the ensuing reach movement. Neural Control of Movement, Amsterdam, Netherland
- Gu, C.**, Stevens, T., Thielscher, A., Bell, A.H., and Corneil, B.D. (2013) Spatial and state-dependent effects of transcranial magnetic stimulation of the frontal eye fields in non-human primates. Society for Neuroscience, San Diego, CA, USA
- Gu, C.**, Stevens, T., Thielscher, A., Bell, A.H., and Corneil, B.D. (2013) Development of an animal model for the effects of transcranial magnetic stimulation on the primate oculomotor system. Gordon Research Conference on Eye Movements, Boston, MA, USA